NASA TECHNICAL TRANSLATION NASA TT F-15766

TECHNOLOGY FOR THE PRODUCTION OF SPACE EQUIPMENT

A. V. Breslavets

Translation of "Tekhnologiya Proizvodstva Kosmicheskoy Apparatury", "Nauka" Press, Moscow, 1974, pp. 1-134.

(NASA-TT-F-15766) TECHNOLOGY FOR THE PRODUCTION OF SPACE EQUIPMENT (Joint Publications Research Service) 146 p HC CSCL 13H

N74-33976
THRU
N74-33996
Unclas
G3/15 47547

NATIONAL AERONAUTICS AND SPACE ADMINISTRATION
WASHINGTON, DC 20546 SEPTEMBER 1974

STANDARD TITLE PAGE

1. Report No. NASA TT F-15766	2. Government Accession No.	3. Recipient's Catalog No.
4. Title and Subtitle TECHNOLOGY FOR THE PRODUCTION OF SPACE EQUIPMENT		5. Report Date September 1974
		6. Performing Organization Code
7. Author(s) A. V. Breslavets, et al		8. Performing Organization Report No.
		10. Work Unit No.
9. Performing Organization Name and Address U.S. Joint Publications Research Service 1000 N. Glebe Road Arlington, VA 22201		11. Contract or Grant No. W13,183
		13. Type of Report and Period Covered Translation
12. Sponsoring Agency Name and Address NASA Washington, DC 20546		14. Sponsoring Agency Code

15. Supplementary Notes

Translation of "Tekhnologiya Proizvodstva Kosmicheskoy Apparatury", "Nauka" Press, Moscow, 1974, pp. 1-134.

16. Abstract

17. Key Words (Selected by Author(s))	18. Distribution Statement Unclassified - Unlimited		
19. Security Classif. (of this report) Unclassified	20. Security Classif. (of this page) Unclassified	21. No. of Pages	22. Price

NASA-HQ

SPACE EQUIPMENT PRODUCTION TECHNOLOGY

Moscow TEKHNOLOGIYA PROIZVODSTVA KOSMICHESKOY APPARATURY [Space Equipment Production Technology] in Russian 1974 pp 1-134

[Book edited by A. V. Breslavets, B. N. Pyak, V. V. Shcherbakov, D. G. Gryunvald', Izdatel'stvo Nauka, signed to press 6 February 1974, 1,500 copies]

CONTENTS PAGE

CONTENTS (Continued) Page

UDC 658.562.3:629.78

SPACE EQUIPMENT PRODUCTION TECHNOLOGY

Moscow TEKHNOLOGIYA PROIZVODSTVA KOSMICHESKOY APPARATURY [Space Equipment Production Technology] in Russian 1974 pp 1-134

[Book edited by A. V. Breslavets, B. N. Pyak, V. V. Shcherbakov, D. G. Gryunval'd, Izdatel'stvo Nauka, signed to press 6 February 1974, 1,500 copies]

[Text] This collection is devoted to the specific nature of the experimental design work, organization, planning and manufacturing processes for space research equipment and instruments. The PERT simulation principle is presented.The characteristic features of building pulse stabilizers, pumping generators, electric converters, transistorized elements, low-peak transmissions, mirror coatings and slit collimators are illustrated. Material on production quality control is included.

The book is designed for scientific and engineering-technical workers.

INTRODUCTION

[by A. V. Breslavets, B. N. Pyak, V. V. Shcherbakov, D. G. Gryunval'd]

[Text] Scientific space instrument making is a new, young field of instrument making which has been in existence a little more than 10 years. The stormy development of space engineering in recent years has made it possible to carry out experimental studies of outer space directly in a broad scientific range. This has given rise to the necessity for the development and manufacture of experimental scientific space instruments and equipment, and it has led to the creation of a new field of instrument making -- space instrument making.

This area of instrument making is characterized by specific peculiarities which, above all, include insurance of stable fitness of the equipment under the conditions of space irradiation, low vacuum, a broad temperature range and other factors not taken into account when developing ground-based scientific equipment.

The individual experimental programs impose rigid requirements on insuring continuous operation of the space equipment for a prolonged period. And the high cost of each space experiment makes it necessary that the space equipment have high reliability.

All of these factors require a specific approach when planning and organizing the scientific research and experimental design work and when selecting the schematic and structural designs for the assemblies and modules of the equipment. They impose the basic process requirements for manufacturing, monitoring and testing the equipment.

Unfortunately, in practice there is no literature which generalizes the indicated peculiarities of the scientific space instrument making as a whole.

The proposed collection contains articles of an applied nature pertaining to various aspects of the planning of scientific research and planning and design work, the manufacturing technology and the testing of scientific instruments and equipment for use in outer space. The collection does not claim to be an exhaustive theoretical generalization of the problems touched on but is of a practical engineering nature. It is addressed to a wide circle of engineering-technical workers connected with planning, design and the manufacturing process for scientific space equipment.

N74-33977

UDC 629.785.002.2

OPERATIONS PLANNING AND ORGANIZATION

CHARACTERISTIC FEATURES OF DETERMINING THE LABOR INPUT AND ESTIMATED COST OF THE DEVELOPMENT AND MANUFACTURE OF EQUIPMENT

[by T. I. Kurmanaliyev, A. V. Breslavets]

[Text] The difficulties in obtaining exact calculation data for the labor input and estimated cost are noted. The method of calculating the labor cost of the design work using the provisional normative indexes with respect to individual forms of operations is proposed. Values of certain coefficients recommended for use in the practical calculations of the labor input for the development of new scientific equipment for space research are presented. There are 6 references.

The scientific and technical progress in the field of mastering outer space requires a constant increase in the list of scientific instruments being manufactured for space research with a simultaneous reduction in the times for their planning, design and mastery in production. Therefore, the proper determination of the labor consumption of the experimental design work and the estimated cost of manufacturing the experimental models of the instruments is one of the main problems facing the enterprise.

The enterprises occupied with the development and manufacture of scientific equipment for space research do, as a rule, put out a small-nomenclature low-series product. This leads to the fact that the composition and volume of operations of the enterprise in time are undergoing significant fluctuations which will increase the accuracy requirements when determining the composition of the labor consumption and the total estimated cost of the new developments.

The total estimated cost of the industrial model of the instrument comprises two basic parts: 1) the estimated cost of the scientific research work and the estimated cost of the planning and design work determined basically by the labor involved in developing the technical documentation; 2) the estimated cost of manufacturing the industrial model in experimental production determined by the production expenses.

In the process of the scientific research work and planning and design, the technical problems are closely intertwined with economic problems which complicates the scientific basis for the given part of the estimated cost. This is explained primarily by the absence of prototypes and analogs of the developed instruments and, consequently, also the statistical or scientifically based normative base with respect to labor consumption and estimated cost. The application of the normatives permits specific definition of the volume and steps in the performance of the operations, matching the operations in time between the interrelated subdivisions and the individual executors, determination of the actual load and the required number of subdivisions and also more efficient control of the expenditure of the appropriations allocated for scientific research and experimental design work. Thus, the normatives are the basis for the organization and planning of operations for instrument development.

However, in connection with the fact that the scientific instruments for space research with respect to structural-technological characteristics, operating conditions and tactical-technical requirements differ theoretically from each other and have no analogs in other branches, it is impossible to use the experimental-statistical normatives for scientific research work and planning and design work borrowed from other branches. The opinion exists that it is possible to establish the dependence of the expenditures on the instrument development as a whole on the tactical-technical requirements imposed on it. The degree of effect of the basic tactical-technical requirements on the development cost is assumed to be established by performing a correlation analysis of the accumulated statistical materials. The given method, however, can not be used when developing the space scientific instruments since it requires prolonged accumulation of comparative initial data on the expenditures for numerous instruments of the same type.

The normatives for the development of scientific space instruments must correspond to the following requirements:

Encompassing consolidated units of normalization of expenditures (the block, subblock, the functional assembly, and so on);

Consideration of modern achievements in the field of space research and the organization of labor and production at the advanced Soviet and foreign scientific research institutes and experimental design offices;

Consideration of the developed organizational-technical conditions and qualifications of the executors in the given enterprise and promotion of further improvement of the productivity of labor;

Insurance of sufficient accuracy of the calculations with respect to determining the expenditures;

Calculations with respect to determining the estimated cost of the labor consumption for the development of new instruments should not be complicated and awkward.

Beginning with the listed requirements imposed on the normatives for the development of new instruments, the expenditures on experimental design work are assumed determined by the method of provisional normatives. The initial data here are the actual expenditures on the previously performed experimental design work when developing the same type of equipment, the instruments or modules at a defined enterprise. In this case, differentiation is carried out on the newly developed instrument for individual functional nodes and the structural-technological setup assemblies which are easily subjected to classification.

As a rule, all of the experimental design work for the development of scientific instruments comprises three steps: the drawings, the development of the technical plan and the development of the working documents.

As a result of developing the individual funtional nodes and the structural-technological subassemblies it is possible with a sufficient degree of accuracy to determine the coefficients of labor consumption of all three steps in the development with respect to total labor consumption:

$$K_{\text{э}} + K_{\text{т}} + K_{\text{р}} = 1.$$

Here $K_{\text{э}}$, $K_{\text{т}}$ and $K_{\text{р}}$ are the labor consumption coefficients for the drawings, the technical and operating designs respectively defined by the formulas

$$K_{\text{э}} = \frac{\sum_{i=1}^{n} A_{\text{э}i}}{\sum_{i=1}^{n} A_{\text{ОКР}i}}; \qquad K_{\text{т}} = \frac{\sum_{i=1}^{n} A_{\text{т}i}}{\sum_{i=1}^{n} A_{\text{ОКР}i}}; \qquad K_{\text{р}} = \frac{\sum_{i=1}^{n} A_{\text{р}i}}{\sum_{i=1}^{n} A_{\text{ОКР}i}}, \qquad (1)$$

Key: 1. experimental design work

where $A_{\text{э}}$, $A_{\text{т}}$, $A_{\text{р}}$ are the labor consumption for the drawings, the technical and operating designs of the corresponding functional node or the structural-technological subassembly of the instrument; $A_{\text{ОКР}}$ is the labor consumption of the development of the functional node or the structural-technological subassembly of the instrument in all three steps.

Knowing the labor consumption coefficients it is possible easily to determine the labor consumption of all the experimental design work.

In connection with the fact that in the drawing in technical design steps the search is made for the most optimal version of the schematic and structural solutions of the instrument, these steps are characterized by instability of the labor consumption, and depending on the number of previously developed versions, their labor consumption can vary within a quite broad range. Therefore, it turns out to be expedient to take the step of development of the working design as the initial base for gathering data on the actual expenditures. The labor consumption of this step is analyzed by the following components:

A_{dev} -- the expenditures of the developers on developing the schematic documentation;

A_{des} -- the expenditures of the designers on developing the design documentation;

A_t -- the expenditures of the technologists on developing the technological documentation;

A_{man} -- the experimental production expenditures on manufacturing the mockups and the experimental model;

A_{op} -- the expenditures on developing the accompanying operations and maintenance documents and agreement on these documents with the customer.

In this case the total actual labor expenditure on developing the functional node of the instrument in the operating design step is expressed in the form of the sum

$$A_{tot} = A_{dev} + A_{des} + A_t + A_{man} + A_{op}.$$

All the terms of this sum can be determined from the individual assignments imposed on the executors in the corresponding laboratories and divisions and also by the details generated in the experimental production facility. However, summing the actual labor consumption by the indicated procedure is inconvenient in connection with the fact that it is done over the entire development stage of the working design which sometimes lasts for several quarters.

The provisional-normative labor consumption for the development of the modules insuring the same accuracy can be obtained by simple means using the method of expert-point evaluation of the complexity of the modules. The essence of the given method consists in the fact that after completion of the operating design step all of the modules entering into the instrument or the system are divided into groups with respect to functional assignment. From among the experimental developers the expert is assigned with respect to each group which determines the relative complexity of the development of the modules by means of a point system. The points assigned to the modules are summed with respect to each group, and the actual expenditures of time on the development of the instrument or the system are distributed with respect to modules in accordance with the points.

The provisional-normative labor consumption of the i-th module $t_{p.\ n.\ dev_i}$ with respect to the given subdivision is determined by the following formula:

$$t_{p.n.dev_i} = T_{act}/\Sigma \text{ points},$$

where T_{act} are the actual labor expenditures on developing the working design of the entire instrument or the system in the given division or laboratory.

If we use the services of other subdivisions not directly developing the module but participating in the development (scientific-theoretical, patent-information, technical and other divisions), these additional expenditures are separated proportionally to the established points, multiplying the provisional-normative labor expenditure times the corresponding coefficient. Considering these additional expenditures, the provisional-normative labor consumption of developing the i-th module with respect to developing divisions is determined by the formula

$$t_{p.n.dev_i} = (T_{act}/\Sigma \text{ points})\eta_1,$$

where η_1 is the coefficient taking into account the degree of participation of the auxiliary subdivisions not directly occupied with the development of the modules. In practice the value of the coefficient η_1 is within the limits of 1-1.3.

The expenditures on developing the design documentation of the i-th module $t'_{p.n.des_i}$ are defined by the UKRUPNENNYY NORMY NA KONSTRUKTORSKIYE RABOTY [Consolidated Norms for Structural Design Work]. When determining the labor consumption of the development of the design documentation it is necessary to consider the form of the device and the degree of its novelty, that is, the complexity group of the device; the expected number of drawings; the list of borrowed and standardized drawings.

The actual expenditures of time in the operating design step, as a rule, are below the expenditures arising from the norms since part of the design documentation goes from the technical design step without complete development. Therefore, the time expenditures $t'_{p.n.des_i}$ defined by the norms for the development of the modules must be corrected using the corresponding coefficient found from the ratio of the actual expenditures to the planned expenditures. The provisional normative labor consumption of the design operations will be defined in the following way:

$$t_{p.n.des_i} = t'_{p.n.des_i}\eta_2,$$

where η_2 is the coefficient taking into account the decrease in labor consumption by the design divisions as a result of the transition without complete development of part of the design documentation from the technical design step. In practice this coefficient is within the limits of 0.5-1.

Analogously, by using the UKRUPNENNYYE NORMY NA TEKHNOLOGICHESKIYE RABOTY [Consolidated Norms for Technological Operations], the provisional-normative labor consumption of the technological development of the working design of the i-th module $t_{p.n.t_i}$ is determined.

The labor consumption for manufacturing the mockups and the experimental model in production is determined by normalization of the drawings for the modules by the calculated time norms developed for the enterprises considering the level of technology and organization of labor. The actual expenditures on manufacturing the mockups and the experimental model are determined by the monthly reports of the experimental production facility. Here, as a rule, the actual expenditures on experimental production exceed the planned (calculated) expenditures as a result of the large number of modifications of the assemblies and modules. The planned labor consumption of manufacturing each module $t_{p.man_i}$ must also be corrected by the corresponding coefficient reflecting the ratio of the actual labor consumption of manufacturing the device to the planned expenditures. The provisional-normative consumption of the manufacturing process $t_{p.n.man_i}$ is defined by the formula

$$t_{p.n.man_i} = t_{plan.man_i}\eta_3,$$

where η_3 is the coefficient reflecting the ratio of the actual expenditures for the manufacturing of the instrument to the planned expenditures. On the basis of developing the statistical data it is established that the value of the coefficient η_3 lies in the range of 1.1-1.6.

The provisional-normative labor consumption of developing the text of the accompanying operation and maintenance documentation and agreement on it with the customer can be determined with sufficient accuracy in terms of the provisional-normative labor consumption of developing the schematic documentation by multiplying it times the corresponding coefficient:

$$t_{p.n.op_i} = t_{p.n.dev_i}\eta_4$$

where η_4 is the coefficient taking into account the operating and maintenance requirements of the customer on the given group of functional nodes and assemblies. By the statistical data the value of the coefficient η_4 as a function of the type and purpose of the instrument lies in the range of 0.1-0.25.

Knowing all the components of the provisional-normative labor consumption with respect to forms of operations, it is easy to determine the total provisional-normative labor consumption of the entire cycle of development of the working design of the i-th module with respect to all subdivisions

$$A_{dev_i} = t_{p.n.dev_i} + t_{p.n.des_i} + t_{p.n.t_i} + t_{p.n.man_i} + t_{p.n.op_i}.$$

The generalizing tables are compared with respect to each group of modules, and the mean provisional-normative labor consumption is derived for the planning, design and manufacture of one module or functional assembly of the given group. The mean values obtained for the labor consumption per module with respect to each group are the planned labor consumption for the development and manufacture of the modules. It is understood that the more modules in the given group taken for analysis, the more precisely the mean magnitude of the labor consumption can be determined.

When determining the labor consumption for the development of new instruments in the stage of comparison and approval of the technical assignments it is necessary to compile an approximate block diagram of the instrument and, using the corresponding classifier, to determine the planned labor consumption for the development of the operating design of each module A_{dev_i}.

The total labor consumption for the development of the module in all stages of the experimental design work is defined by the formula

$$A_{EDW_i} = A_{dev_i}/K_{dev},$$

where K_{dev} is the labor consumption coefficient of the working design.

The total labor consumption for the development of the entire instrument or module is defined by the formula

$$\overset{0}{A}_{OKP} = \sum_{i=1}^{n} A_{OKPi}.$$

Knowing the labor consumption for the development of a new module or instrument, it is easy to determine its estimated cost. For the new module it is defined by the formula:

$$C_{OKPi} = \overset{\circ}{A}_{OKPi}\, З_{cp}(K_1 + K_2 + K_3) + C_{к},$$

where $З_{cp}$ is the mean wages for the enterprise in a month; K_1 is the overhead coefficient for the enterprise; K_2 is the material consumption coefficient (the planned magnitude of material consumption per ruble of wages); K_3 is the consumption coefficient of the component products (the planned magnitude of the consumption of component products per ruble of wages); C_k is the cost of the operations performed as a cooperative effort.

The estimated cost of developing the entire device C_{EDW} or the system is determined by summing the estimated cost of all the modules making up the device or system:

$$C_{OKP} = \sum_{i=1}^{n} C_{OKPi}.$$

In connection with the fact that in the development stage and the stage of agreement on the technical assignments it is not always possible exactly to define the modular composition of the equipment; when calculating the estimated cost the defined inaccuracies can unconditionally be assumed. However, when accumulating a sufficient quantity of statistical data and with a defined amount of experience it is possible to establish the estimated cost of a new development with an accuracy of ± 20–30 percent.

In the step of the development of the drawing or the technical design, it appears expedient and possible to more precisely define the estimated cost with an accuracy of ± 5-10 percent. The more precisely defined estimated cost in this step of the operations can be the stable price of the development.

Determination of the estimated cost of the manufacturing the single industrial models of the devices or small series production with the presence of working documentation presents no special difficulties and is carried out according to the generally accepted procedure.

BIBLIOGRAPHY

1. METODIKA RAZRABOTKI UKRUPNENNYKH NORMATIVOV NA VYPOLNENIYE OKR (Procedure for Developing Consolidated Norms for Experimental Design Work), Second Edition, NIIEIR, 1968.

2. Bobkov, S. A., "Determining the Labor Consumption and the Estimated Cost of Experimental Design Work," OBMEN OPYTOM V RADIOPROMYSHLENNOSTI (Exchange of Experience in the Radio Industry), NIIEIR, No 6, 1970.

3. Znamenskiy, A. Ye., "Normalization of the Labor of Radio Equipment Developers," OBMEN OPYTOM V RADIOPROMYSHLENNOSTI (Exchange of Experience in the Radio Industry), NIIEIR, No 2, 1969.

4. Bashin, M. L., PLANIROVANIYE NAUCHNO-ISSLEDOVATEL'SKIKH I OPYTNO-KONSTRUKTORSKIKH RABOT (Planning of Scientific Research and Experimental Design Work), Moscow, Ekonomika, 1969.

5. Beklashov, V. K., METODY UKRUPNENNOGO OPREDELENIYA TRUDOYEMKOSTI OKR V OTRASLEVYKH NII I KB ELEKTROPRIBOROSTROITEL'NOY PROMYSHLENNOSTI (Methods of Consolidated Determination of the Labor Consumption of Experimental Design Work in the Branch Scientific Research Institutes and Design Offices for Electric Instrument Making Industry), Izd. Leningradskogo Doma nauchno-tekhnicheskoy propagandy, 1969.

6. Puzynya, K. F., METODIKA RAZRABOTKI I VNEDRENIYA SISTEMY NORMATIVOV TRUDOYEMKOSTI DLYA PLANIROVANIYA OPYTNO-KONSTRUKTORSKIKH RAZRABOTOK (Procedure for the development and Introduction of the System of Labor Consumption Normatives for Planning Experimental Design Developments), Izd. Leningradskogo Doma nauchno-tekhnicheskoy propagandy, 1968.

N74-33979

UDC 658.51

PERT SIMULATION OF EXPERIMENTAL DESIGN WORK

[by T. I. Kurmanaliyev, A. S. Pishchulin]

[Text] The basic principles of constructing the models and rules for their application in the development of PERT charts are discussed. There are 2 illustrations.

The search for new methods of planning and control in scientific research and experimental design organizations is acquiring highly urgent significance. The modern planning and design has become so complicated that it is becoming more and more difficult to control this process by means of simple intuitive decisions. The planning of the scientific research and experimental design work realized at the present time on the basis of ordinary linear drafts does not correspond to modern requirements.

One of the most progressive methods of planning and control is the method of PERT planning and control. On the basis of the experience in the introduction of PERT planning in the design office it is possible to note the primary conditions of its effective application:

1. Encompassing the entire complex of operations performed in the organization by PERT planning.

2. The development of optimal models of PERT charts.

In this article a study is made of the methods of PERT simulation of experimental design work developed at the design office.

The structure of PERT models was determined by the possibility of performing the following operations:

1. The processing of PERT charts manually without using a computer.

2. The creation of the complete models for individual steps in the operations.

3. Fast introduction of the changes occurring in a situation without rearranging the chart structure.

In order to implement these conditions as much as possible the excess details were excluded in the structure of the chart. Only the basic relations were stated which could seriously affect the success of performing the experimental design work. The model only included those operations for the execution of which no less than three days were required. In connection with the great duration of the experimental design work with respect to a number of products, the necessity has arisen for the simulation of individual steps in the planning and design work: drawing, technical and operational planning. These steps are characteristic for all the products developed in the design office, and their models have sufficient stability with respect to structure.

The developed models offer the possibility of applying them on a calendar time scale which permits easy, depending on the developed situation, movement of the operations with respect to the time scale to the right or left without distorting the topology of the chart.

The model of the PERT chart is shown in the figure. As is obvious from the figure, the model of the PERT chart (the drawing) is divided into substeps.

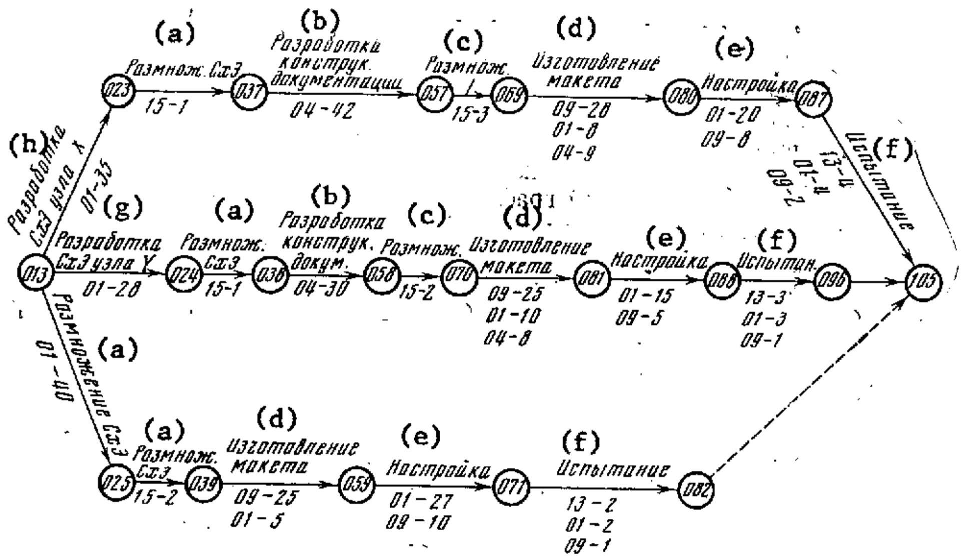

Example of a model of a PERT chart

Key:
- a. multiplication circuit 3
- b. development of the structural documentation
- c. multiplication
- d. manufacture of the mockup
- e. checkout and adjustment
- f. testing
- g. development circuit 3 of assembly Y
- h. development circuit 3 of assembly X

The first substep includes determination of the possibility of the development and manufacture of the instrument in the organization. It ends with the compilation of the PERT chart on the level of the leading designer with respect to the product.

The second substep is the basic substep. It includes the development of the electronic part, the construction, the manufacture of the nodal mockups, the assembly of the product mockup, the checking and testing, and it ends with defense of the drawing.

In a PERT model the basic standard operations which are encountered during planning and design are demonstrated. The possibility of using it for the development of PERT charts depends on the structure of the product. If the product contains a lower number of assemblies by comparison with the model, then in the chart the free events and operations are omitted; if it is necessary to demonstrate a specific part of the instrument absent in the model, then additional events and operations are included.

The basic rules for the construction of PERT charts have been sufficiently well explained in technical periodicals and in specialized literature; therefore they are not considered here.

The proposed model of the PERT charts has been created on the basis of analyzing the developments at the design office and the practical experience of the leading engineers of the organization. Its introduction has permitted a 5-6 fold reduction in duration of development of the PERT charts and, the main thing, insurance of high accuracy of the structure of the PERT chart which has excluded such significant errors as breaking the logical chain of the chart (improperly extended relations of the operations, failure to include the nodal operations, and so on).

The leading designer of the product having a PERT model and a functional schematic of the product (the structure of the product) can easily develop a PERT chart of any phase of the planning and design operations. When formalizing PERT charts on the basis of the model it is necessary to perform the following operations:

1. Omit the unnecessary operations in the PERT model.

2. Include the newly introduced operations.

3. Exclude the unnecessary operations from a description of the PERT model.

4. Include the newly introduced operations in the description.

5. Extend the numbers of the participating subdivisions in the description.

6. Extend the duration of the operations.

7. Plot the model on a time scale.

8. Note the names of the operations above the graphs.

In addition to evaluating the duration of the operations in the PERT chart their labor consumption is extended. This arises from the fact that the PERT charts can be used to develop the cost accounting plans of the subdivisions.

N74-33979

UDC 658.512.6

MULTITOPIC LOAD CHART FOR THE DESIGN OFFICE SUBDIVISIONS

[by A. S. Pishchulin]

[Text] A study is made of the methods of development, designation and application of the charts under multitopic conditions. There is one table and one illustration.

In the case of simultaneous performance of the experimental design work with respect to several products it is necessary to match the PERT charts by them. The tool for the execution of this operation is the multitopic load chart.

The simultaneous execution of operations with respect to different products can be limited by various factors: the presence of a work force, the means and capacities of the equipment, the development times, the manufacturing times, and so on. For the experimental design operations the primary limiting factors are the presence of the necessary number of specialists in the subdivisions and the times for the performance of operations dictated by the schematic plan. Therefore, the multitopic load charts at the design offices are developed considering the labor consumption of the types of operations.

Inasmuch as certain forms of operations in the PERT charts with respect to products can be superposed on each other in the same planning period, the necessity arises for deconcentrating the operations with respect to time and, consequently, correcting the PERT charts.

The basic procedure for the development of multitopic load charts is the selection of operations of the same type from all the PERT charts and superposition of them on each other in a time scale.

Inasmuch as in the design office the technological specialization of the subdivisions has been adopted (schematic, structural, technological, production and other divisions), the multitopic load PERT charts are developed by the indicated subdivisions. Thus, the multitopic load chart will become the basic planning document of the subdivision determining a detailed nomenclature of the planned operations.

The time estimates of the PERT charts permit determination with high accuracy of the labor consumption of the operations, their cost expression and the number of employed co-workers. In addition, the multitopic load chart permits the subdivision manager to distribute the operations considering the capacity and the level of qualification of the executors, realize the in practice automatic execution of the PERT charts with respect to products, having only the multitopic PERT chart available.

The formalization of the multitopic load charts for the subdivisions proceeds as follows:

1. The ordinary PERT chart with the operations distributions with respect to subdivisions is compiled for each product.

2. For all the operations the number of employed workers is defined.

3. The multitopic load chart is compiled for each subdivision participating in the execution of the operations.

4. If it is impossible to execute the operations by the subdivision at the times established by the PERT chart, these operations are carried over to the later periods with the corresponding correction of the PERT charts.

5. The measures are being developed with respect to execution of the critical and subcritical operations.

6. On lack of execution of any events, the PERT and multitopic charts are corrected, the calculations of which must be repeated.

A large number of various data during the multitopic developments requires maximum simplification (within the limits of what is possible) of all elements of the PERT system. The multitopic load chart must carry only the following information:

1. The name and number of the executor subdivision.

2. The name of the product, the modules and assemblies.

3. The number of the product.

4. The number of products (for subdivisions manufacturing experimental models).

5. The planning period (months, weeks).

6. The technological sequence of events.

7. The time estimate in man-days.

8. The number of employee executives.

The multitopic load charts can be calculated for an entire period of development and manufacture of an experimental model, but practice shows that it is more

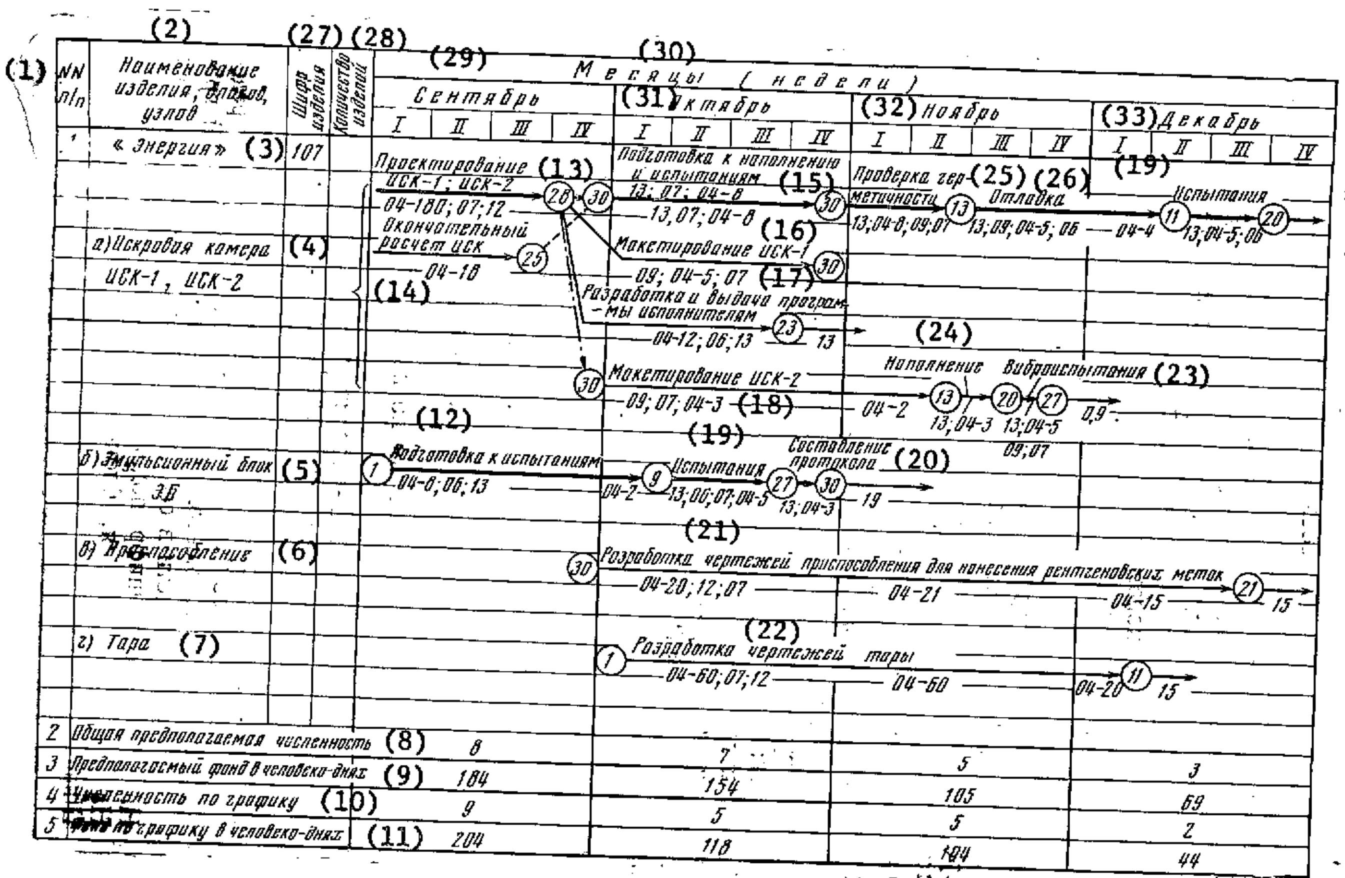

1. Item number
2. name of product, modules, assemblies
3. Energiya [energy]
4. a) spark chamber ISK-1, ISK-2
5. b) emulsion module EB
6. c) attachment
7. d) packaging
8. total proposed number
9. proposed pool in man-days
10. number by the chart
11. pool by the chart in man-days
12. preparation for the tests
13. design ISK-1; ISK-2
14. final calculation of the ISK
15. preparation for filling and testing
16. simulation of the ISK-1
17. development and output of the program to the executors
18. simulation of the ISK-2
19. tests
20. preparing the certificate
21. development of drawings of the attachment for superposing the x-ray marks
22. development of drawings of the packaging
23. vibration testing
24. filling
25. checking the seal
26. checkout and adjustment
27. product number
28. product quantity
29. September
30. months (weeks)
31. October
32. November
33. December

expedient to construct them only for the planned quarter since in this time usually great changes take place and the charts for longer periods require basic reworking.

The multitopic charts developed for four months appear to be the most expedient. The first month is the month of operations converting from one planned period to another. By each month the total number of workers that must be employed in all operations and the labor consumption of the operations performed by the subdivision are calculated.

On the multitopic load chart (see the figure) the circles denote the events with the dates of completion of the operations; the solid lines denote the duration of the operations; the dotted lines denote the time reserve; the bold face lines denote the operations on the critical path. Above the lines depicting the duration of the operations, the name of the operation from the PERT chart is indicated, and under the line the number of the executor, the labor consumption (in man-days) and the number of employed workers are layed out. If several executors participate in a given operation, then the numbers of all the participants are layed out respectively under the line.

At the end of the multitopic load chart the total proposed number of people, the time pool (in man-days) with respect to regular schedule considering holidays and the number of people obtained by the PERT chart with the labor consumption of the operations (in man-days) are noted. Lack of correspondence of the number by the chart and the proposed number during the month by weeks is regulated inside the subdivision; the lack of correspondence of the number with respect to months requires more careful analysis of the planned labor consumption of the operations or shifting of the chart times to the right.

As has already been pointed out above, the multitopic load chart has become the basic planning document reflecting in practice all aspects of the activity of the subdivision. By the chart the monthly reckoning is done with respect to state for the second date following the accounting month.

The procedure for filling out the report is the following (see the table on page 19).

Column 1 is filled out using the procedure noted on the multitopic chart. Columns 2-6 are filled out in accordance with the reported events taking place in the report period; columns 5 and 6 have the date of beginning and ending of the operation. In column 7 we have the date of actual performance of the operations (day and month). In column 8 opposite each operation name there is a code for the corresponding state of the operation:

Code	Designation of state
1	Operation performed by the deadline
2	Operation not performed on the noncritical path
3	Operation not performed on the critical path

Item no.	Name of product	No. of product	Plan			Report				PERT comments			
			Name of operations	Dates of events		Actual date of completion	Operation state code	Number of the one responsible for the overrun	Cause of deviation from the plan	Actual date of completion	Operation state code	Number of the one responsible for the overrun	Comments
				Initial	Final								
1	2	3	4	5	6	7	8	9	10	11	12	13	14
1	Energiya	107	Development and issue of the program to the executors	28 Sept	23 Oct	23 Oct	1	--		23 Oct	1	--	
			Preparation for tests	1 Sept	9 Oct	15 Oct	2	13	Test unit not ready	15 Oct	3	13	Operation on the critical path
2	Vremya	002	Development of commutator drawings	5 Oct	25 Oct	23 Oct	1	--		23 Oct	1	--	
			Development of the commutator test program	15 Oct	28 Oct	--	2	04	Absence of executor	2 Nov	2	04	Operation on the non-critical path

Columns 9 and 10 are filled out in the case of deviation of the state of the operations from the plan. Columns 11-14 are filled out in the PERT subdivision, and after approval of the report by the design office manager they are defining for evaluating the activity of the subdivision.

The introduction of multitopic load charts permitted the design office to improve the operation of the subdivisions significantly in a short time, to provide a report on their activities and compare indexes.

N74-33980

UDC 658.514

ORGANIZATION OF OPERATIONS WITH RESPECT TO CHECKING DRAWINGS (DRAWING CHECKING PROCEDURE)

[by L. M. Greys, S. G. Namestnik]

[Text] A procedure is described for organizing the design check of the drawings.

One of the basic conditions of high-quality manufacture of instruments is the error-free developed design documentation. The design documentation supplied the production facility with undiscovered and uncorrected errors leads to an increase in cost and prolonging the time for manufacturing the devices.

In connection with the fact that the development of the design documentation and, in particular, the drawings is a complex creative process in which the designer must solve a large class of problems (the expediency and technological nature of the structural design, the correctness of the designation of dimensions and tolerances, the selection of materials, and so on), errors can be made even by experienced workers. Therefore, checking the drawings is a mandatory process in the development of the documentation.

The process of checking the drawings includes the design check and the normalization control. In this article we shall discuss only the design check of the drawings. This process can be organized by two procedures depending on the structure of the subdivision. In the cases where in the large design subdivisions there are individual specialized structural subdivisions (the checking office), the drawings are checked by the subject principle. In the small design subdivisions where the work is not specialized, the drawings are checked in the design subdivisions by each of the designers.

In the majority of cases, the work of checking the drawings is organized with respect to the second procedure. Considering that here the drawings must be checked by each designer, it is necessary to create a check procedure, the application of which will permit reduction of the number of errors in the drawings to a minimum. This check procedure is the list of steps proposed below which must be carried out in sequential order when checking drawings of general views (assemblies) or detailed drawings.

Checking the General View (Assembly) Drawings

I. Checking the Structural Design:

1) The design solution of the general view (the assembly); the fitness of the design for satisfaction of the requirements of the technical assignment;

2) Expediency of the adopted structural construction;

3) Possibility of assembly using a standard tool;

4) Possibility of adjustments during the operation and maintenance process;

5) Possibility of dismantling for technical inspection and repair;

6) Possibility of observing all the required modes of operation (cooling, lubrication, and so on) in the maintenance process.

II. Checking the Graphical Section:

1) Necessity and sufficiency of the number of views, cross sections, sections and dimensions giving an exhaustive representation of the mutual arrangement and interaction of all of the component parts;

2) Overall dimensions, adjustable dimensions and coupling dimensions;

3) Dimensions of mutual arrangement of the component parts;

4) Dimensions of mutual arrangement of moving parts;

5) Dimensions of the elements developed by the given drawing;

6) Presence of limiting deviations of the dimensions;

7) Correctness of filling out the data in the stamps of the basic endorsement.

III. Checking the Presence of Component Parts:

1) The presence of the drawings for all the original assemblies and parts entering into the general view (assembly) and also their proper designations and notation in accordance with the angular specifications;

2) Introduction of all of the component parts into the angular specifications;

3) Correctness of the arrangement of all of the component parts relative to each other in the angular specifications;

4) Correctness of the notation in the angular specifications of all of the component parts;

5) Correspondence of the kit parts in the angular specifications to the electrical, schematic or assembly diagrams;

6) Correctness of arranging the position numbers with respect to each other on the cutaway lines and their placement on the drawing field.

IV. Checking the Release Endorsements:

1) Presence and correctness of all endorsements and notation defining the execution of unsplittable joints;

2) Correctness of the endorsements defining the operations performed with respect to each drawing (galvanizing, painting, polishing, and so on);

3) Correctness of designating the finish classes at the machining points.

V. Checking the Text:

Sufficiency and correctness of recording all of the technical requirements (including their technological process sequence) insuring implementation of the planned operating principle of the structural design.

VI. Checking the Electrical Specifications:

Correspondence of the functional node in the assembly of its electric circuit diagram.

Checking the Detail Drawings

I. Checking the Structural Design:

The structural solution of a detail or part, that is, the possibility of performance of all functions planned for it in the assembly.

II. Checking the Graphical Section:

Necessity and sufficiency of the number of views, cross sections and sections giving an exhaustive representation of the shape of the part or detail.

III. Checking the Dimensions:

Reliability and correctness of all dimensions insuring the most efficient possibility of correct manufacture of the part from the technological point of view.

IV. Checking the Limiting Deviations:

The presence of limiting deviations of all dimensions; correspondence of the seating points of contact parts; error in counting the dimensional chains of the dimensions which must provide for the joining of articulated elements of the given part with other parts.

V. Checking the Remaining Elements:

1) Selection of the material and correctness of its designation; the presence and expedience of all the notations for the finish classes of the surface; notation for heat treatment, coatings and other technical specifications characterizing the structural design of the part;

2) Checking the weight.

In conclusion, it is necessary to note that as practice has demonstrated, the use of the described system permits reduction of the number of errors in the drawings to a minimum and significant economy of the time for checking them.

N74-33991

UDC 621.373

DEVELOPMENT AND PLANNING AND DESIGN OF EQUIPMENT

PUMPING GENERATOR OF SEMICONDUCTOR LASERS

[by A. V. Popkov]

[Text] A study is made of the schematic of a multidimensional current pulse generator. A MTKh-90 cold cathode thyratron is used as the current commutator. In the autooscillation mode on a frequency of 380 hertz the generator creates a current to 100 amps per pulse in a control resistance of 1 ohm. The pulse duration is regulated within the limits from 0.1 to 3.0 microseconds. There are two tables, three illustrations and a four-entry bibliography.

One of the basic methods of exciting stimulated radiation in semiconductor materials is the injection of nonequilibrium current carriers through the p-n-junction by application of an external voltage to the specimen. The magnitude of the threshold current through the diode on achievement of which stimulated (laser) radiation occurs, depends on many factors. In particular, for temperatures of the p-n-junction above 20°K the threshold current is proportional to T^3 [1]. Consequently, in order to obtain a laser effect at room temperature it is necessary to pass a current which reaches several tens and even hundreds of amperes through the diode.

Inasmuch as the essential part of the pumping energy fed to the laser diode goes to heat it and the removal of heat from the domain of the p-n-junction presents significant difficulties, the semiconductor injection lasers at the present time operate predominately in the pulse mode with a pulse duration on the order of several microseconds and less.

In order to excite the semiconductor injection lasers, special current pulse generators are used called pumping generators which on a sufficiently low-resistance load (0.1 ohm and less), such as a laser diode must develop a current reaching several tens or hundreds of amperes per pulse.

On performance of certain research work with semiconductor lasers and also for demonstration of their operation, the demand arises for the simplest pumping generator with respect to structure and manufacture. These goals can be served by the simple current pulse oscillator investigated in this paper which is based on a thyratron with a cold cathode type MTKh-90. The schematic of the oscillator is presented in Figure 1. The control electrode of the thyratron is connected through a high-resistance (94 megohms) to the plus side of the power supply. With this inclusion, a weak current of about 3-6 microamperes flows between the grid and the cathode. This insures the creation of a clear ionized gas channel and promotes an increase in the thyratron ignition stability.

The oscillator operates in the autooscillation mode. At the initial point in time the thyratron is extinguished, and the capacitor C is charged through the resistor R1 from the power supply. As soon as the voltage on the capacitor reaches the ignition voltage U_{ignit}, the thyratron is ignited, and a current flows through the laser diode D1 and the control resistance R3. Here, the capacitor C is discharged, and the voltage on the thyratron anode decreases. When the voltage on the capacitor decreases to U_{ex} equal to the extinguishing voltage of the thyratron, the current ceases to flow through the thyratron and the diode. The capacitor C again begins to charge, and the process repeats periodically.

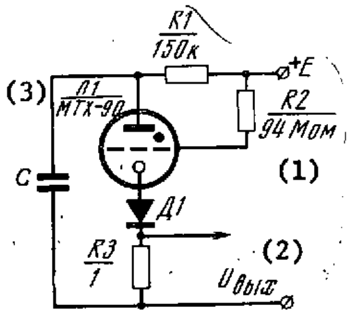

Figure 1. Schematic of the current pulse oscillator

Key: 1. 94 megohms
2. U_{out}
3. L1/MTKh-90

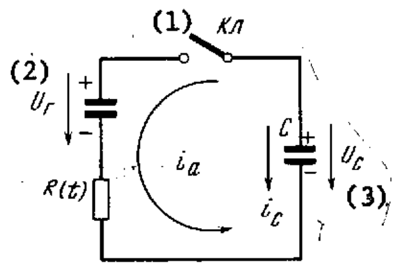

Figure 2. Circuit diagram of the oscillator

Key: 1. switch
2. U_{arc}
3. U_c

The MTKh-90 cold cathode thyratrons usually are used in a weak-current circuit; however, the presence of an activating coating on the cathode permits their use to commutate pulse currents of hundreds and even thousands of amperes [2]. As the studies demonstrated [3], an increase in current amplitude to tens of amperes does not disrupt the normal glow discharge mode in the thyratron and does not cause the appearance of arc discharge. Even for such large currents the magnitude of the voltage drop on the thyratron remains constant and equal to the arcing voltage U_{arc}, just as for currents on the order of milliamperes. Of course, in this operating mode of the thyratron the power dissipated on the cathode must not exceed the admissible amount.

The volt-ampere characteristic of the thyratron with a cold cathode is nonlinear [4], and it has two sections: decreasing on which the voltage on the thyratron decreases with an increase in current and horizontal on which the anode voltage is constant within broad limits of variation of the anode current. The decreasing section has great steepness and becomes horizontal even for currents on the order of 10^{-4} amps.

In order to estimate the parameters of the generated pulses, let us consider the equivalent diagram presented in Figure 2. The thyratron here is replaced by a series-connected equivalent generator of the voltage U_{arc} and a variable resistance R(t). At the initial point in time $U_c = U_{ignit}$, and at the end of the process $U_c = U_{arc}$.

The thyratron resistance varies exponentially after ignition; here it is possible to write the following functional dependence of R (t) on time:

$$R(t) = \frac{R3}{1 - \exp(-t/\tau_1)}, \tag{1}$$

where τ_1 is the time constant characterizing the current buildup process in the thyratron during its ignition.

The instantaneous value of the current in the circuit is

$$i_a = \frac{U_c - U_r^{(1)}}{R3}\left[1 - \exp(-t/\tau_1)\right]. \tag{2}$$

Key: 1. U_{arc}

Let us introduce the following notation:

$$\Delta U_a = U_a^{(1)} - U_r^{(2)} \tag{3}$$

Key: 1. U_{ignit}
2. U_{arc}

and

$$\tau_2 = CR3. \tag{4}$$

After the transformation (2), considering the notation introduced we obtain the following expression for the instantaneous value of the anode current:

$$i_a = \frac{\Delta U_a}{R3}\left[1 - \exp\left(-\frac{t}{\tau_1}\right)\right]\exp\left\{-\frac{t - \tau_1\left[1 - \exp(-t/\tau_1)\right]}{\tau_2}\right\}; \tag{5}$$

The maximum value of the current is

$$i_{a\,max} = \frac{\Delta U_a}{R3}\frac{1}{\sqrt{k}}\exp\left[-\frac{t_{max}}{2\tau_1} - \frac{t_{max}}{\tau_2} + \sqrt{k}\exp\left(-\frac{t_{max}}{2\tau_1}\right)\right], \tag{6}$$

where

$$k = \tau_1/\tau_2 \tag{7}$$

and

$$t_{max} = -\tau_1 \ln\left[1 + \frac{1}{2k}\left(1 - \left|\sqrt{1+4k}\right|\right)\right]. \tag{8}$$

The duration of the generated pulse is found from (5) as the difference of two values of the time for which the current in the circuit is half the maximum. The results of calculating the pulse duration are presented in Table 1.

The duration of the pulse front is found from the equations

$$i_a(t_{0,1}) = 0,1 i_a(t_{max}), \tag{9}$$

$$i_a(t_{0,9}) = 0,9 i_a(t_{max}), \tag{10}$$

where $t_{0.1}$ and $t_{0.9}$ are the time values for which the current reaches 0.1 and 0.9 of the maximum value respectively. The front duration is

$$t_\Phi = t_{0,9} - t_{0,1}$$

or after solution of equations (9) and (10)

$$t_\Phi = t_{max} - \tau_1\left\{\left|\sqrt{\frac{0,2}{k\,[1+\exp(-t_{max}/\tau_1)]}}\right| + 0,1 i_{a\,max}\frac{R3}{\Delta U_a}\right\}. \tag{11}$$

Table 1
Experimental and calculated values of the duration of the pulse and its front (microseconds)

τ_1	$t_{\Phi.э}$	$t_{\Phi.р}$	$\tau_{и.э}$	$\tau_{и.р}$	τ_2	$t_{\Phi.э}$	$t_{\Phi.р}$	$\tau_{и.э}$	$\tau_{и.р}$
0,025	0,08	0,061	0,17	0,168	0,03	0,20	0,186	0,70	0,679
0,05	0,10	0,077	0,24	0 237	0,04	0,20	0,209	0,90	0,832
0,01	0,12	0,114	0,32	0,350	0,05	0,20	0,231	1,05	0,952
0,02	0,18	0,155	0,55	0,532	0,06	0,20	0,249	1,10	1,015

Let us consider the special case where k = 1. Here the duration of the generated pulse determined by numerical solution of equation (5) with sufficient accuracy for practice is

$$\tau_и \approx 2\tau_1 = 2\tau_2. \tag{12}$$

This case can be used to determine the time constant τ_1 which is a characteristic of the thyratron itself. By varying the capacitance of the capacitor C and measuring the duration of the generated pulse, we achieve satisfaction of the equality

$$\tau_и = 2\tau_2 = 2R3 \cdot C,$$

after which on the basis of (12) we have

$$\tau_1 = \tau_{\text{и}}/2.$$

The calculation of the pulse repetition rate F for such generator circuits is made by formula [3]

$$\frac{1}{F} = R1 \cdot C \ln \frac{E - U_{\Gamma}}{E - U_{з}}, \qquad (13)$$

where R1 is the magnitude of the charge resistance (see Figure 1); E is the voltage of the feed source.

In order to check the correctness of the calculated values, measurements were made of the basic generator parameters. In Table 1 we have the experimental and calculated values of the duration of the generated pulse and its front. For the calculations we assumed τ_1 = 0.377 microseconds which was obtained by the method described above. For the thyratron included by the scheme depicted in Figure 1, U_{ignit} = 240 volts, U_{arc} = 60 volts and ΔU_a = 180 volts. As follows from the data obtained, the calculated and experimental values differ little from each other.

The dependence of the pulse current amplitude on the source voltage E is shown in Figure 3. With an increase in the voltage the current amplitude decreases, but here the frequency of the generated pulses increases.

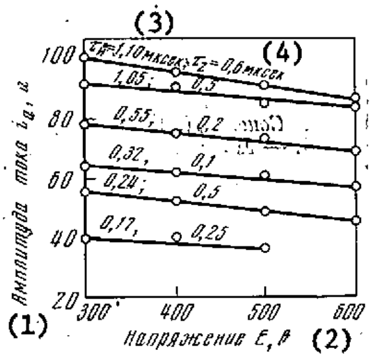

Figure 3. Amplitude of the pulse current as a function of the source voltage (τ_{pulse} is the duration of the generated pulse; τ_2 is the time constant of the discharge circuit)

Key: 1. current amplitude i_a, amps
2. voltage E, volts
3. 1.10 microseconds
4. 0.6 microseconds

For a pulse lasting 1.1 microseconds a maximum amplitude of 100 amps is obtained. The maximum pulse repetition rate for the given circuit was 388 hertz. At higher frequencies there was no self-ignition of the thyratron.

In Table 2 we have the experimental and calculated values of the pulse repetition rate as a function of the time constant of the charge circuit τ_{charge}. The frequency was calculated by formula (13) for U_{ignit} = 240 volts, U_{arc} = 60 volts and R1 = 150 ohms. Quite good comparison of the calculated and experimental values of the frequencies was obtained.

Table 2
Experimental and calculated values of the pulse repetition rate (pulses/sec)

(1) E, в	(2) $\tau_з = R1 \cdot C$ мксек									
	75		30		15		7,5		3,75	
	$F_э$	F_p	$F_э$	F_p	$F_э$	F_p	$F_э$	F_p	$F_э$	F_p
300	9,0	9,6	17,0	24,0	37,1	48,1	62	96	115	192
400	17,5	17,6	36,0	44,1	76,5	88,2	132	176	250	352
500	27,2	25,4	57,7	63,5	112,7	127,1	210	254	388	507
600	34,5	32,9	75,0	75,9	146,0	164,5	273	319	—	658

Key: 1. E, volts
2. τ_{charge} = Rl·C microseconds

Thus, as the experimental test demonstrated, the characteristics of the current pulse generator using a thyratron with a cold cathode are close to the calculated ones and correspond to the required parameters of the pumping sources of the semiconductor lasers. This pumping oscillator is simple with respect to structure and manufacture and has small size and weight.

BIBLIOGRAPHY

1. Barns, Dill, Nathan, "Effect of Temperature on the Properties of a Gallium Arsenide Laser," TRUDY INSTITUTA INZHENEROV PO ELEKTROTEKHNIKE I RADIO-ELEKTRONIKE (Works of the Institute of Electronic Engineering and Radio-electronic Engineering), translated from the English, Vol 51, No 6, 1963.

2. Korablev, L. N., LAMPY S KHOLODNYM KATODOM (Tubes With a Cold Cathode), Moscow, Izd-vo AN SSSR, 1961.

3. Genis, A. A., Gorshteyn, I. L., Pugachev, A. B., PRIBORY TLEYUSHCHEGO RAZRYADA (Glow Discharge Devices), Kiev, GITL UkrSSR, 1963.

4. Akton, D., Swift, D., GAZORAZRYADNYYE LAMPY S KHOLODNYM KATODOM (Gas Discharge Tubes with a Cold Cathode), translated from the English, Moscow-Leningrad, Energiya, 1965.

N74-33992

UDC 621.3

TWO-POSITION DC PULSE VOLTAGE STABILIZER

[by V. I. Osadchiy]

[Text] The advantages of the dc pulse voltage stabilizers over the continuous-action stabilizers are described. These advantages include higher efficiency, low sensitivity to the ambient temperature and insignificant size and weight. A comparison is made between the schematics of the known two-position pulse stabilizer with a Schmitt trigger and that developed by the author. A characteristic feature of the improved system is the increased stabilization coefficient and the possibility of smooth regulation of the output voltage. A practical schematic is presented for the improved two-position pulse stabilizer along with its parameters. There is one table, two illustrations and five references.

The reduction in size and weight, an increase in economy and reliability of the secondary power supplies of special radioelectronic devices and, above all, dc voltage stabilizers are at this time highly urgent problems.

In the widespread series continuous-action voltage stabilizers the regulating element -- a transistor -- operates in the linear mode as a controlled resistance. This regulation mode is characterized by low efficiency (50-60 percent) and the necessity for using awkward heat-removal radiators to improve the cooling of the regulating transistor. Therefore, series pulse dc voltage stabilizers are being used more and more frequently [1-3].

The efficiency of the pulse stabilizer is high (80-90 percent) since the losses in the regulating transistor in the saturation mode are insignificant. Its thermal regime improves correspondingly, and the dimensions of the radiator decrease significantly. The pulse stabilizer systems with a regulating transistor in the switching mode show little sensitivity to the ambient temperature or variation in the transistor parameters. They have the possibility of stabilizing great powers with significant feed voltage fluctuations.

The deficiencies of the pulse stabilizers include the large output voltage pulsations, poor dynamic indexes for pulse variation of the load current and the necessity for protection from the interference created by the stabilizer in a broad frequency range. However, in spite of this the voltage pulse stabilizers are being used successfully to supply static multioutput voltage converters and other devices where the pulsations and dynamic indexes of the structures have secondary significance and the requirements for high economy and reliability, small size and low sensitivity to temperature fluctuations play the primary role.

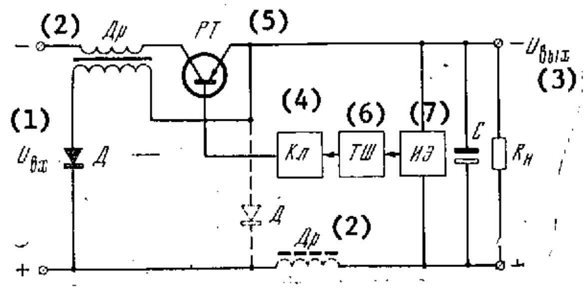

Figure 1. Schematic of a two-position pulse voltage stabilizer with a Schmitt trigger.

Key:
1. U_{inp}
2. choke
3. U_{out}
4. switch
5. regulating transistor
6. Schmitt trigger
7. measuring element

In the literature [4] a series dc voltage pulse stabilizer with a two-position regulator is described in which an asymmetric trigger with an emitter coupling -- a Schmitt trigger -- is used as the threshold modulator. The schematic of this stabilizer is presented in Figure 1. A measuring element -- a parametric stabilizer -- is connected to the output terminals of the stabilizer. The error signal is fed without preamplification to the input of the Schmitt trigger (ST). The parametric stabilizer is used simultaneously as the base divider of the input transistor of the Schmitt trigger; here the ballast resistance of the parametric stabilizer is the lower arm of this divider. On variation of the feed voltage or the load current, the output voltage of the stabilizer fluctuates. Correspondingly, the voltage drop on the ballast resistance becomes greater than or less than the response threshold of the Schmitt trigger, switching it to one of two stable states. For rotation of the phase of the control pulses from the Schmitt trigger there is an auxiliary transistorized switch which controls the regulating transistor. The switching of the Schmitt trigger to one of the two stable states and return to the initial position take place for different voltages of the response threshold and, correspondingly, different values of the control voltage. The interval between the magnitudes of these voltages is the dead zone of the feedback circuit with respect to variation of the output voltage and determines the magnitude of the output pulsations and the stabilization coefficient. Therefore, the two-position voltage pulse stabilizers with the same schematic solution have greater magnitude of the pulsations and a small stabilization coefficient. Another deficiency of this stabilizer is the necessity for an auxiliary transistor switch for rotating the phase of the control pulses from the Schmitt trigger which complicates the circuitry. In addition, smooth regulation of the output voltage is impossible.

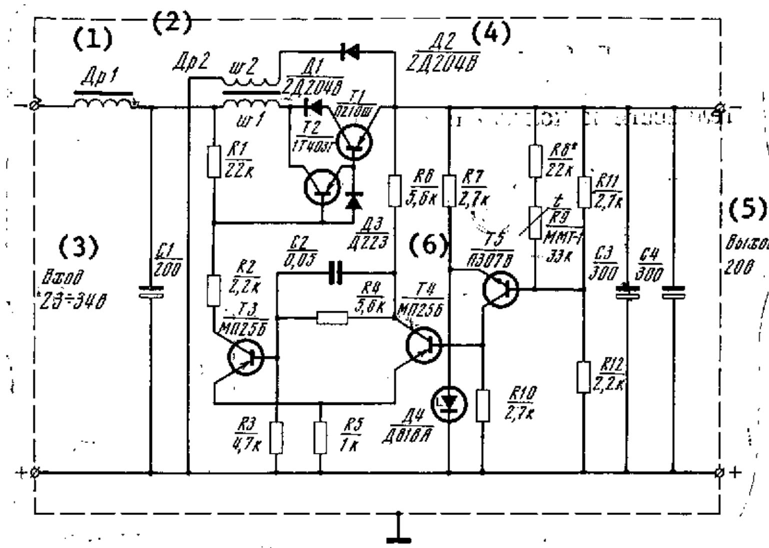

Figure 2. Schematic of the improved two-position pulse voltage stabilizer with a Schmitt trigger

Key: 1. choke 1
2. choke 2
3. input, 23-34 volts
4. D2/2D204V
5. output, 20 volts
6. T4/MP25B

The purpose of developing the two-position pulse voltage stabilizer described in this article was also elimination of the above-indicated deficiencies. The theoretical circuit diagram of the improved pulse stabilizer is presented in Figure 2 [5].

The operating principle of the stabilizer consists in the following. In the pulse mode the series regulating transistor T1 of the stabilizer operates as a switch. The stabilization of the mean value of the output voltage U_{out} is realized as a result of automatic variation of the ratio of the duration of the closed and open states of the regulating transistor, that is, the switching off-duty factor. This is achieved by means of a closed automatic regulation system with a negative feedback circuit comprising a measuring element, a feedback amplifier and a special duration modulator. The duration modulator converts the error signal (the mismatch voltage) into a train of square pulses controlling the regulating transistor of the stabilizer.

In the two-position pulse voltage stabilizers the duration modulator is a threshold device (in the given case the Schmitt trigger) having a relay characteristic.

Depending on the magnitude of the error signal this threshold modulator has two stable states corresponding to the open or closed state of the switching transistor. A comparison of the reference voltage and the output voltage in this stabilizer is made continuously since the threshold modulator switches to one of the two stable states at the time when the error signal becomes greater than or less than the response threshold voltage. Therefore, the two-position stabilizers have higher speed than the pulse-width stabilizers in which the error signal has an effect on the duration modulator -- the master oscillator -- only during part of the switching period.

In contrast to the widespread pulse stabilizer systems, the accumulating choke Дp2) is included at the input of the stabilizer and is connected to the collector of the regulating transistor, to the emitter circuit of which the load is connected. This permits the output voltage of the stabilizer to be used as the blocking voltage of the regulating transistor, and it makes it possible to eliminate the additional bias voltage source characteristic of the other pulse stabilizer circuits. For return of the energy accumulated in the choke during the open state of the regulating transistor to the load, there is a secondary winding of the choke with the commuting diode D2. It is possible to refrain from using the secondary winding if we include the choke in the common conductor of the stabilizer. The introduction of the T5 transistor feedback into the amplifier circuit permitted significant reduction of the dead zone of the feedback circuit of the stabilizer with respect to variation of the output voltage and an increase in the stabilization coefficient.

The measurement element was executed in the form of a nonlinear bridge comprising a parametric stabilizer and a divider in the registers connected to the output terminals and permitting smooth regulation of the output voltage by selecting the magnitudes of the resistances of the divider arms. The input circuit of the T5 transistor of the feedback amplifier is connected to the diagonal of the nonlinear bridge. The collector of the transistor is connected with the base of the input transistor T4 of the Schmitt trigger. The control signal is fed to the base of the input transistor T4 of the Schmitt trigger in phase excluding the use of the phase-rotating transistor switch. Therefore, the collector of the output transistor T3 of the Schmitt trigger is connected to the base of the component regulating transistor using semiconductor triodes T1 and T2.

The improved pulse stabilizer operates in the following way. On connection of the stabilizer to the power supply the voltage at the output is zero; therefore, the output transistor T3 of the Schmitt trigger is closed. Negative voltage is fed through the resistor R1 to the base of the composition regulating transistor insuring inclusion of it, and the charge of the capacitors C3 and C4 begins at the stabilizer output. As soon as the voltage at the output exceeds the upper given level, the voltage drop on the ballast resistor R7 of the parametric stabilizer included to the emitter circuit of the transistor T5 increases. Correspondingly, the collector current of this transistor and the voltage drop on the load resistor R10 decrease. Since the voltage on the load resistor R10 becomes less than the response threshold, the input transistor T4 of the Schmitt trigger is closed, and the output transistor T3 opens. A blocking voltage is applied to the base of the composite regulating transistor equal to part of the output voltage of the stabilizer (it is determined by the divider based on the resistors R1 and R2). The regulating transistor is excluded, and the voltage at the output decreases. As soon as the voltage at the output becomes less than the lower given level, the circuit returns to the initial state in which the regulating transistor is again included. Thus, the autooscillation process is set up in the circuit. The interval between the magnitudes of the voltages of the upper and lower given levels determines the dead zone with respect to the fluctuations of the output voltage. The smoothing of the pulsations of the output voltage is realized by the LC-filter made up of the accumulating choke Др2 and the capacitors C3 and C4. When the regulating transistor is open, a build-up current flows through the choke going to the load and the charging capacitor of the filter. At that time magnetic energy is accumulated in the choke, and the voltage on the choke is equal to the difference in the feed voltage and the output voltage. After blocking the regulating transistor, a self-induction emf of opposite sign arises in the choke, blocking the commuting diode D2. The stored magnetic energy in the choke is spent on supporting the current in the load circuit. When the commuting diode is open, a voltage equal to the feed voltage is applied to the regulating transistor.

In order to decrease the necessity for the spread of spurious inductions created by the stabilizer elements, a complex method of noise suppression is used, that is, the entire volume of the pulse stabilizer is shielded.

For operation of the regulating transistor of the stabilizer in the switching mode the current required by the stabilizer from the primary power supply has a pulse nature. Therefore, at the stabilizer input a constant voltage is observed with a variable component, the amplitude of which is determined by the internal resistance of the power supply. In order to protect the primary power supply from this interference on the stabilizer input side a protection filter is included made up of the choke Др1 and the capacitor C1.

The results of the experimental checking of the improved two-position pulse voltage stabilizer are presented below:

U_{inp}, volts ... 23-24	R_{out}, ohms ... 0.05
U_{out}, volts ... 20	$2U_{max}$, millivolts ... 200
I_H, amps ... 0.8	efficiency (for U_{inp} = 34 volts) ... 0.85
K_{pulse} ... 100	f_{switch} (for U_{inp} = 27 volts), hertz ... 1500

The error in the output voltage on variation of the ambient temperature within the limits from -20 to +50°C does not exceed ± 0.5 percent.

The type of semiconductor devices used, the rated values of the resistors and the capacitors are presented in the schematic (see Figure 2). The choke data are presented in the following table:

Choke	Type of core	Core material	Number of windings	Type of conductor	Conductor diameter, mm
(5) Др1 (1)	ОЛ 12/20-8	Э350×0,08	200	ПЭВ-1	0,31
Др2 (2)	ШЛ 10×10	Э350×0,08 (3)	$w1=200$ $w2=400$	ПЭВ-1 ПЭВ-1 (4)	0,51 0,44

Key: 1. OL12/20-8
2. ShL10 × 10
3. E350 × 0.08
4. PEV-1
5. Dr...

BIBLIOGRAPHY

1. ALEKSANDRIN, V. I., "Transistorized Pulse Voltage Stabilizers," POLUPROVODNIKOVYYE PRIBORY I IKH PRIMENENIYE (Semiconductor Devices and Their Application), No 7, Moscow, Sovetskoye radio, 1961.

2. ISTOCHNIKI ELEKTROPITANIYA NA POLUPROVODNIKOVYKH PRIBORAKH. PROYEKTIROVANIYE I RASCHET (Electric Power Supplies Based on Semiconductor Devices. Planning, Design and Engineering Calculation), edited by S. D. Dodik and Ye. I. Gal'perin, Moscow, Sovetskoye radio, 1969.

3. Vilenkin, A. G., IMPUL'SNYYE TRANZISTORNYYE STABILIZATORY NAPRYAZHENIYA (Transistorized Pulse Voltage Stabilizers), Moscow, Energiya, 1970.

4. EKSPRESS-INFORMATSIYA, SERIYA PRIBORY I ELEMENTY PROMYSHLENNOY AVTOMATIKI (Express Information, Instruments and Elements of Industrial Automation Series), Moscow, VINITI, No 39, abstract No 272, 1962.

5. Osadchiy, V. I., "DC Pulse Voltage Stabilizer," USSR Author's Certificate No 275161, BYULLETEN' IZOBRETENIY (Invention Bulletin), No 22, 1970.

N74-33983

UDC 621.375.4:621.382

SOME CHARACTERISTIC FEATURES OF THE CONSTRUCTION OF THE AMPLIFYING CHANNEL FOR WORKING WITH SEMICONDUCTOR DETECTORS IN THE CHARGED PARTICLE ENERGY SPECTROMETER

[by E. I. Kuzyuta]

[Text] A study was made of a transistorized spectrometric amplifier with a shaper to select the shape of the frequency characteristic of the amplifying channel for which the primary frequency spectrum of the signal will pass, but the noise spectrum is limited to the maximum. A procedure is presented for selecting the shaping circuits and their inclusion principle. There are 3 illustrations and 6 references.

The conversion of the energy lost by a charged particle in a semiconductor detector to an electric signal of the corresponding amplitude takes place with accuracy characterized by the resolution of the detector-amplifier system. The latter depends on many causes [1] and, in particular, the noise characteristics of the amplifying channel. Therefore when constructing the amplifying channels a great deal of attention has been given to obtaining minimum noise present at the input of the preamplifier.

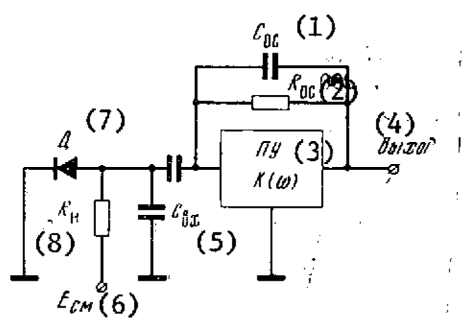

Figure 1. Functional diagram of the detector-amplifier channel.

Key: 1. $C_{feedback}$ 2. $R_{feedback}$ 3. preamplifier 4. output 5. C_{input} 6. E_{bias} 7. detector 8. R_{load}

The load resistance R_{load} of the detector D (Figure 1) is always included in parallel with the capacitance C_{input} which is determined by the equivalent capacitance of the detector C_D, the input capacitance of the preamplifier C_{pre} and the spurious capacitances of the mounting C_{spur}, that is,

$$C_{input} = C_D + C_{pre} + C_{spur}.$$

It is known [2] that the voltage of the thermal resistance noise included at the preamplifier input is defined by the expression

$$\overline{U}_{\text{т}}^2 = \frac{4kTR}{2\pi}\int_0^\infty \frac{d\omega}{1+(\omega C_{\text{вх}} R)^2} = \frac{KT}{C_{\text{вх}}}. \tag{1}$$

(1)

Key: 1. C_{input}

Expression (1) indicates the maximum possible value of the thermal resistance noise voltage at the input to the preamplifier under the condition of an unlimited pass band of the amplifying channel. As is obvious from this expression, the mean square value of the noise voltage depends on C_{input} and not on R which is completely the result of the width of the pass band which this capacitance limits and, as a result, decreases the noise voltage.

The capacitive feedback ($C_{feedback}$ in Figure 1) introduced into the charge-sensitive preamplifiers [3] does not change the signal/noise ratio. However, the introduction of feedback implies a variation in the frequency band as a result of the addition of the dynamic capacitance to the preamplifier input leading to an increase in the input capacitance by $(1 + \beta K_1)$ times.

Considering what has been stated, expression (1) can be rewritten in the following form:

$$\overline{U}_{\text{т}}^2 = \frac{KT}{(C_{\text{вх}} + C_{\text{ос}})(1+\beta K_1)}. \tag{2}$$

(1) (2)

Key: 1. C_{input} 2. $C_{feedback}$

Usually in the amplitude analysis channels the frequency band is still limited as a result of the shaping (differentiating and integrating) circuits which are included for shortening and shaping the pulses coming from the preamplifier output in order to increase the time resolution [1, 3]. They also basically determine the frequency and the transfer characteristics of the entire amplifying channel.

If the time constants of the differentiating and integrating circuits are identical (which is frequently encountered in practice), that is,

$$\tau_{diff} = \tau_{int} = \tau, \qquad \approx 6{,}43 \cdot 10^6 \sqrt{\frac{\tau}{R}}.$$

then the square of the modulus of the transfer coefficient will be

$$|K_\Phi(\omega)|^2 = \frac{\omega^2\tau^2}{(1+\omega^2\tau^2)^2}. \tag{3}$$

Now the effective voltage of the interference acting at the preamplifier input considering the pass band of the shaping circuits will be

$$\bar{U}_\tau^2 = 2KTR/2\pi \int_0^\infty |K_1(\omega)|^2 |K_\Phi(\omega)|^2 d\omega = \frac{KT}{2C}\frac{RC/\tau}{(1+RC/\tau)^2}, \tag{4}$$

where $C = (C_{inp} + C_{feedback})(1 + \beta K_1)$.

The function (4) has a maximum for $R = \tau/C$. In this case

$$\bar{U}_{\tau\,max}^2 = KT/8C. \tag{5}$$

Hence it follows that the maximum noise (5) corresponds to the condition of equality to the time constant of the input (RC) defining the decrease in the detector pulse and the time constant of the shaping circuits.

In order to decrease the magnitude of the noise voltage at the input of the amplifying channel, it is necessary to constrict the pass band. This can be done by decreasing τ. However, the decrease in τ is limited by the magnitude of the front (τ_{fr}) of the detector signal.

When selecting τ_{diff} it is also necessary to consider that the value of τ_{diff} in a real circuit is affected by the spurious circuits (the output resistance R_{out} and the capacitance C_{out} of the cascade after which the shortening circuit is included) and the capacitive component C_{spur} of the load of the differentiating circuit. Taking this into account it is possible to consider the optimal value of τ_{diff}:

$$\tau_{diff.opt} = 4\tau_{spur}/A^2,$$

where $A = \tau_{spur}/\tau_s\,(\gamma_{min} + 1)\,F_s(\gamma_{min}) - 1$; $\tau_{spur} = R_{out}(C_{out} + C_{spur})$ is the time constant of the spurious circuits; τ_s is the signal duration at the output of the differentiating circuit; $\gamma_{min} = 1.8 + 1.72\,\tau_s/\tau_{spur}$.

The function $F_s(\gamma_{min})$ is nonlinear and in certain sections can be approximated by hyperbolas:

$$F_c(\gamma_{min}) \approx \frac{2}{\gamma_{min}} + 0{,}78 \text{ for } 1{,}5 < \gamma_{min} < 20,$$

$$F_c(\gamma_{min}) \approx \frac{3}{\gamma_{min}} + 0{,}7 \text{ for } \gamma_{min} > 20.$$

Key: 1. F_s

It is necessary to note that for normal operation of the shortening circuit it is necessary that the stage of the amplifier to which the differentiating RC-circuit is connected be made with an output impedance less than R_{diff} and its output capacitance and input capacitance of the following stage must be appreciably less than C_{diff}, that is,

$$R_{out} < R_{diff}, \qquad C_{out} + C_{spur} \ll C_{diff};$$

but in any case it is possible to maintain the condition

$$2.4\tau_{fr} \leq \tau_{diff} \ll RC. \tag{6}$$

Then considering condition (6), expression (4) can be written in the form

$$\overline{U_\tau^2} = \frac{KT}{2C^2}\frac{\tau}{R}, \tag{7}$$

which corresponds to the contribution to the resolution

$$\frac{1}{2}\Delta_\tau^{Si} \quad \text{(kev)} \tag{8}$$

From expressions (7) and (8) it follows that in order to decrease the contribution of the thermal noise to the channel resolution it is necessary to have a resistance R as large as possible.

For working with silicon detectors, an amplification channel was used, the circuit diagram of which is presented in Figure 2. A stage (ПП1, ПП2) constructed by the stage scheme for inclusion of the transistors is used as the preamplifier. This stage does not change the phase of the input voltage which is convenient for introducing feedback $C_{feedback}$. The magnitude of the capacitance $C_{feedback}$ is chosen equal to 2 ± 0.4 pf. It does not seem possible to make it smaller since the effect of the spurious capacitances worsening the stability of the system increases.

In reference [1] the relation is presented for the maximum signal/noise ratio as a function of the input parameters of the preamplifier from which it follows that in order to decrease the characteristic noise of the preamplifier it is necessary to decrease the emitter current of the first transistor of the stage. However, this is valid until the base current exceeds the detector current and the return current I_{return}. The further reduction in I_e decreases the amplification, but the noise in this case does not change and the signal/noise ratio decreases.

In the region of large values of I_e the resolution becomes worse. This is explained by the increase in the diffusion capacity of the transistor which is proportional to I_e, that is, the inertia of the transistor.

In Figure 3 we have the experimental noise characteristics of the stage preamplifier for various values of β and I_{return} of the transistors. The presented curves show that in order to decrease the contribution of the characteristic noise of the transistors to the channel resolution, it is necessary to select high-frequency transistors with maximum β for small I_e and with minimum I_{ret} for the preamplifier.

For the stage preamplifier (Figure 2), transistors of the 2T306G type were selected with $90 < \beta < 200$ for I_e = 150 milliamps, U_c = 3 volts and $I_{ret} \leq 0.1$ microamps.

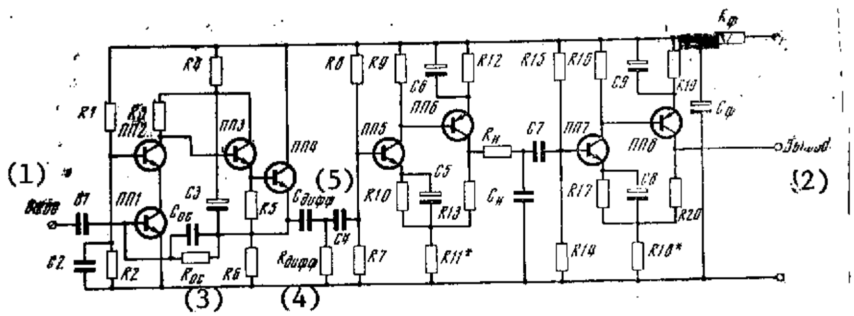

Figure 2. Circuit diagram of the amplifier.

Key: 1. input
2. output
3. $R_{feedback}$
4. diff
5. C_{diff}

The amplification coefficient of the preamplifier with respect to a voltage at a frequency of 10 kilohertz is 500 (the duration of the input signal τ_{inp} = 3 microseconds). The dynamic error $C_{dyn} \geq$ 1,000 picofarads. The intake current was less than 2 milliamps.

In order to decrease the effect of spurious parameters of the preamplifier on the differentiating circuit (R_{diff} C_{diff}) it is connected after the emitter

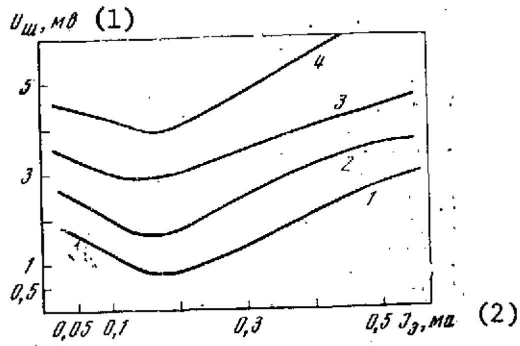

Figure 3. Noise characteristics of the stage preamplifier for various values of β and I_{ret} of the transistors. 1 -- 2T306G transistors; $\beta_1 = \beta_2 = 120$, $I_{ret} \leq 0.05$ microamps; 2 -- 2T306V transistors: $\beta_1 = \beta_2 = 90$, $I_{ret} = 0.1$ microamps; 3 -- transistors 2T301Ye; $\beta_1 > \beta_2$, $I_{ret} \leq 0.5$ microamps; 4 -- 2T301D transistors: $\beta_1 < \beta_2$, $I_{ret} \leq 0.5$ microamps.

Key: 1. U_{noise}, millivolts 2. I_e, milliamps

repeater (the transistors ПП3, ПП4). In order to transmit the leading edge of the detector pulse, the duration of which is equal to 0.1 microseconds, the time constant of the differentiating circuit is selected equal to $\tau_{diff} = 0.24$ microseconds.

Inasmuch as in the preamplifier the charge sensitivity does not depend on C_{inp} (it is defined only for $C_{feedback}$), the ouput voltage of the noise is proportional to the total noise fed to the input, that is,

$$\bar{U}^2_{ш} = \bar{U}^2_{т} + \bar{U}^2_{к},$$
(1)

Key: 1. $\bar{U}^2_{noise}$

where $\bar{U}^2_T$ is the thermal noise of the resistances at the input of the preamplifier; U^2_K is the natural noise of the stage preamplifier.

The mean square voltage of the natural noise of the staged preamplifier is determined by the equivalent noise resistance I_e at its input:

$$\bar{U}^2_{к} = KTR_0\Delta f,$$

which makes a contribution to the resolution

$$\frac{1}{2}\Delta_{\kappa}^{Si}(\text{kev}) \approx 1{,}4\sqrt{R_{э}}. \quad (9)$$

The total noise contribution to the channel resolution will be

$$\frac{1}{2}\Delta^{Si}(\text{kev}) \approx 6{,}4\cdot 10^{6}\sqrt{\tau/R} + 1{,}4\sqrt{R_{э}}. \quad (10)$$

The integrating circuit (R_iC_i) is included between two sections of the basic amplifier. Each section of the basic amplifier is encompassed by negative feedback (R_{11} and R_{13}). The feedback coefficient of the first section of the amplifier is: $\beta_1 \approx R_{11}/(R_{11} + R_{13}) = 0.01\text{-}0.023$. The amplification coefficient of the section $K_1 \approx 1 + R_{13}/R_{11} \approx 35\text{-}40$ respectively.

Thanks to the strong negative feedback the amplifier section has high input impedance. The intake current of the entire amplifying channel does not exceed 3.5 milliamps.

BIBLIOGRAPHY

1. Akimov, Yu. K., et al., POLUPROVODNIKOVYYE DETEKTORY YADERNYKH CHASTITS I IKH PRIMENENIYE (Semiconducting Detectors of Nuclear Particles and Their Application), Moscow, Atomizdat, 1967.

2. Reynfel'der, V. A., RAZRABOTKA MALOSHUMYASHCHIKH VKHODNYKH TSEPEY NA TRANZISTORAKH (Development of the Low-Noise Input Circuits Based on Transistors), Moscow, Sovetskoy radio, 1967.

3. Tsimovich, A. P., YADERNAYA RADIOELEKTRONIKA (Nuclear Radio Electronics), Moscow, Nauka, 1967.

4. Gonorovskiy, I. S., RADIOTEKHNICHESKIYE TSEPI I SIGNALY (Radio Engineering Circuits and Signals), Part 1, Moscow, Sovetskoye radio, 1966.

5. Lozhnikov, A. P., Sonin, Ye, K., KASKADNYYE SKHEMY NA TRANZISTORAKH (Staged Transistorized Circuits), Moscow, Energiya, 1969.

6. Dirnili, J., Northrop, D., POLUPROVODNIKOVYYE SCHETCHIKI YADERNYKH IZLUCHENIY (Semiconductor Nuclear Radiation Counters), Translated from the English, Moscow, Mir, 1966.

N74-33984

UDC 629.7.086

SERVOSYSTEM WITH AN UNDULATORY REDUCING GEAR

[by A. I. Romashchenko, V. A. Samoylenko, I. A. Grishin, Yu. S. Tatarchuk]

[Text] A discussion follows of experience in developing a potentiometric servosystem with a dc microservomotor, which is the builtin drive of an undulatory reducing gear. The operation of the system and the structural design of the undulatory reducing gear are described. The results are presented from analyzing some tests of various types of undulatory reducing gear generators. There are 8 illustrations and 9 references.

The proposed system is designed to control a dc micromotor by the armature circuit. During its development the following basic factors were considered:

a) The system must be optimal with respect to speed;

b) Autooscillations are not allowed;

c) The error with respect to angle must be no more than 10 angular minutes;

d) The number of power supplies is minimal;

e) The system must have high energy indexes.

Considering the above listed requirements, a relay control system was selected for the motor.

The block diagram is presented in Figure 1. The error signal from the comparison circuit goes to the input of the electronic amplifier and is demodulated by the demodulator.

Depending on the signal phase, the relay element RE1 or RE2 responds which controls the corresponding switch via the emitter repeaters EP1 or EP2. The switch commutes the base circuits of the power transistors of the reversing power amplifier, the collector circuit load of which is also the motor armature circuit.

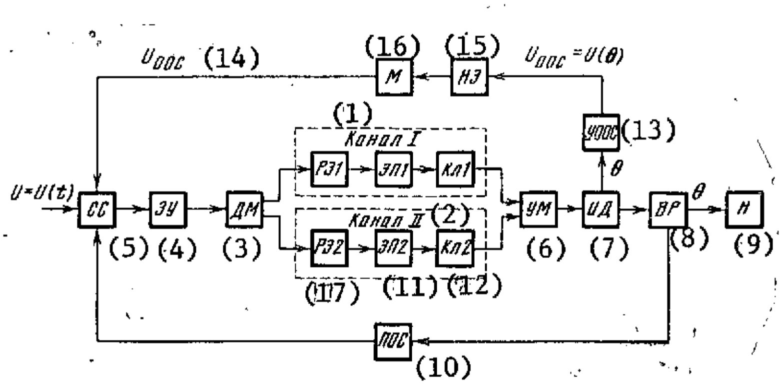

Figure 1. Block diagram of the control channel.

Key:
1. channel I
2. channel II
3. demodulator
4. electronic amplifier
5. comparison circuit
6. power amplifier
7. motor armature
8. undulatory reducing gear
9. load
10. line potentiometer
11. emitter repeater
12. switch
13. negative feedback circuit
14. $U_{\text{negative feedback}}$
15. nonlinear element
16. modulator
17. relay element

The useful load of the output shaft is connected with the shaft of the motor via an undulatory reducing gear. The line potentiometer is used as the feedback sensor with respect to the load shaft feedback angle. The shaft of this potentiometer is connected to the motor and the load via the undulatory reducing gear.

The system is stabilized by introducing negative feedback with respect to the speed of the motor encompassing all of the stages. The feedback voltage is selected by the negative feedback circuit. The feedback is essentially nonlinear as a result of the presence in its circuit of a nonlinear element. Then the feedback voltage is converted by the modulator and fed to the comparison circuit.

The variation law of the output shaft angle with time considering the reversing programmed circuit executed from magnetically controlled contacts (K1-K10) (Figure 2) which change the voltage amplitude on alternate closure. The difference between this voltage and the voltage on the angle feedback potentiometer is summed algebraically with the velocity negative feedback signal and is fed to the amplifier input. The period of the closure of the contacts is 2 seconds; the time for working out one step corresponding to an angle of 12 degrees will be about 1 second. Thus, the position of the output shaft is uniquely determined by the number of the selected contact, that is, the given operating program of the system.

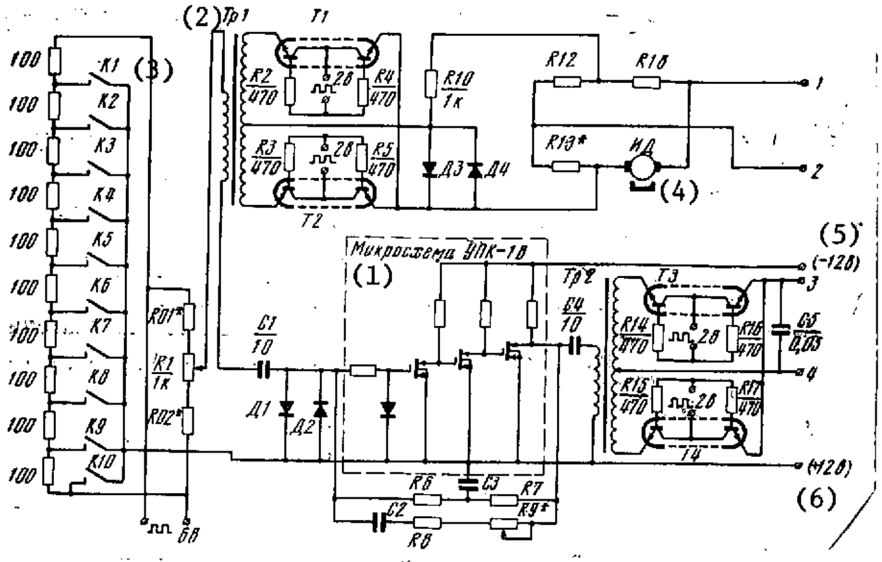

Figure 2. Signal shaping stages.

Key: 1. UPK-1V microcircuit
2. Tr1 transistor
3. K... = contacts
4. motor armature
5. -12 volts
6. +12 volts

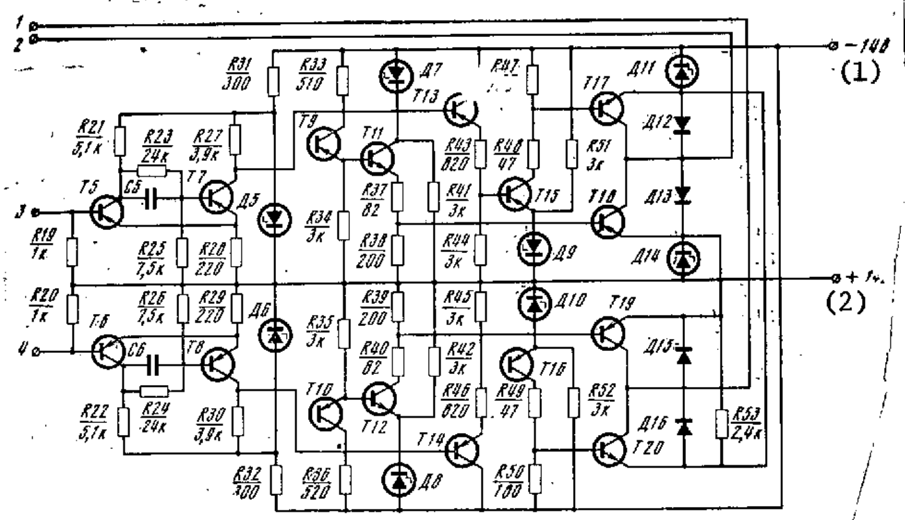

Figure 3. Relay amplifier.

Key: 1. -14 volts 2. +14 volts

The error signal made up of the algebraic sum of the mismatch signal of the comparison circuit and the speed negative feedback signal of the motor goes through the capacitance C1 to the input of the electronic amplifier.

The amplifier is a three-stage integrated UPK-1V microcircuit. The amplified signal from the output transformer Tr2 is rectified by the IP-1A integrated microcircuit demodulator. The negative velocity feedback signal modulator is also assembled on the basis of the IP-1A.

The application of microcircuits has provided significant gains with respect to size and weight and also intake power. For comparison it is necessary to note that the amplifier with the same amplification coefficient based on bipolar transistors was assembled from four transistors, 11 resistors and four capacitors.

Depending on the mismatch signal phase at the demodulator output, a constant voltage of one polarity or another appears. On reaching the response threshold the signal forces the electronic relay of one of the two identical channels to respond. If the signal polarity is such that the sign is negative at socket 3 and the sign is positive at socket 4, then the ER1 relay responds which is assembled from the T5 and T7 transistors (Figure 3).

In the initial state the transistor T7 is saturated by a base current with respect to the divider R21, R23, R25. Its collector current flowing through the common emitter to the resistance R28 blocks the transistor T5.

The signal from the demodulator output is applied negative to the base of the transistor T5 and blocks it. The voltage on the collector of the transistor T5 drops, and the avalanche process of blocking the transistor T7 and unblocking the transistor T5 begins.

The collector circuit of the transistor T7 is loaded at the inputs of the emitter repeaters T9 and T13 which control the base circuits of the switches T11 and T15. When trying to control the switches directly from the outputs T7, T8, a significant effect on the operation of the relay from the variable input currents of the switches was discovered.

In the initial state the switch T11 is open and the switch T15 is closed. The potentials of the switch emitters are rigidly recorded by the stabilitrons D7 and D9 the initial current of which is given by the resistors R41 and R51.

The response of the relay leads to unblocking of the transistor T15 and blocking of the transistor T11. The switch T11 breaks the current circuit of the base of the T18 power transistor, and the latter is blocked; the switch T15 saturates the base of the transistor T17. Thus, when the signal arrives at the relay input equal to the response threshold or exceeding it, the power transistors "change places" with respect to conductivity. As a result, the following feed circuit of the motor armature ID is formed (here the outputs 1 and 2 shown in Figures 2 and 3 are connected to each other correspondingly): the negative of the power supply (-14 volts) -- the D11 diode -- transistor T17 -- resistance R13 -- motor armature winding -- transistor T19 -- diode D14 -- the positive of the power supply (+14 volts). The motor turns the sliding contact of the feedback potentiometer R1, thereby decreasing the mismatch signal. With a decrease in the signal to the release threshold, the relay is switched to the initial state; the switches T11 and T15 return the power transistors T17 and T18 to the initial state: T17 is blocked, T18 is unblocked, creating a dynamic braking circuit for the motor; the winding of the armature is short-circuited through the R13 (see Figure 2) -- open transistor T18 -- diode D15.

On variation of the signal phase the relay of the second channel made up of the transistors T6 and T8 responds. The switch T12 blocks the power transistor T19, the switch T16 unblocks the power transistor T20. The voltage on the armature winding is now applied in the opposite polarity, that is, by changing the signal phase the motor is reversed.

The negative feedback with respect to the speed of the motor is used to stabilize the system and it is taken from the tachometric bridge, the arms of which are formed by the armature winding of the ID and the three resistors R12, R13, R18 (see Figure 2). The feedback voltage is fed from the bridge diagonal to the divider from the linear and nonlinear resistances. Two diodes D3 and D4 are used as the nonlinear element. Then the feedback voltage is modulated by the converter executed from the microcircuits T1 and T2 of the IP-1A type and the transformer Tr1 (see Figure 2). From the secondary winding of the transformer Tr1, the feedback voltage in opposite phase is fed to the amplifier input by the mismatch signal.

For an amplification coefficient on the order of 400 and a response threshold of the relay of 0.5 volts the magnitude of the calculated error reduced to the output shaft and determined by the sensitivity threshold of the circuit was 5 angular minutes. Here, the steepness of the characteristic of the potentiometer -- the feedback sensor -- was 0.8 mv/deg. Further improvement of the static accuracy of the system as a result of an increase in the amplification coefficient can lead to the occurrence of autooscillations. Autooscillations can be eliminated by selecting the depth of negative feedback with respect to speed.

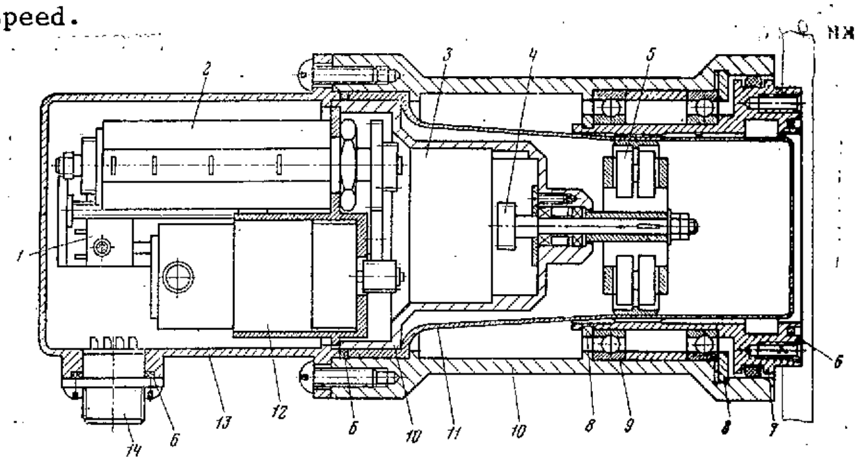

Figure 4. General view of the electromechanical module. 1 -- blocking mechanism; 2 -- potentiometer; 3 -- intermediate reducing gears; 4 -- pinion shaft; 5 -- generator; 6 -- packing; 7 -- rigid gear; 8 -- stop ring; 9 -- ball-bearing; 10 -- housing; 11 -- flexible shell; 12 -- microelectric motor; 13 -- cover; 14 -- parting seal.

The system was tested for operation in the temperature range from -10 to +50°C.

The power supply for the divider of the programming device, the feedback potentiometer, the base circuits of the modulator and the demodulator came from the windings of the converter transformer putting out a square voltage at 2,000 hertz.

The servomechanism of the servosystem is an electromechanical module in the form of an undulatory reducing gear with builtin servomotor, an intermediate cylindrical reducing gear, a feedback potentiometer and other elements of the electric control circuit (Figure 4). All the elements are located in the sealed cavity of the module formed by the stationary flexible shell 11 of the undulatory reducing gear and the cover 13.

The parameters and the calculations were chosen by the procedure discussed in reference [6].

The dc micromotor 12 turns the pinion shaft 4 of the generator 5 via the intermediate cylindrical reducing gear 3. The generator deforms the stationary flexible shell 11 so that two zones of coupling of the teeth of the shell with a rigid gear 7 occur. The rigid gear 7 serves as the output shaft of the module. Its supports are the ball bearing 9 with the idlers 8. The cylindrical reducing gear has an intermediate output connected to the feedback potentiometer shaft 2 and the blocking mechanism 1.

For practical execution of the design a number of problems of a technological nature were solved successfully. Thus, the process was developed and introduced for manufacturing the shell -- a thin walled steel heat treated case of complex shape with small-modular toothed rim for outer coupling; a process was developed and tested for manufacturing the rigid gear with inside coupling. This permitted the manufacture of models of the undulatory transmissions and the performance of some tests. During the testing, a very important role of the generator in insuring the normal operation of the transmission was discovered. The following types of generators were tested.

1. Generator of Forced Deformation of Sliding Friction

This generator was used in the initial step for control assemblies, adjustment and checkout of the operation. In the structural design, this type of generator is not considered in view of the great losses to friction.

2. Generator of Forced Deformation of Rolling, Regulatable, Ball Friction without an Outer Ring (Figure 5)

In this experiment the generator quickly becomes unadjustable as a result of rolling of the track under the balls in the flexible gear which leads to the appearance of a gap in the toothed coupling and an increase in noise as a result of the gaps between the balls.

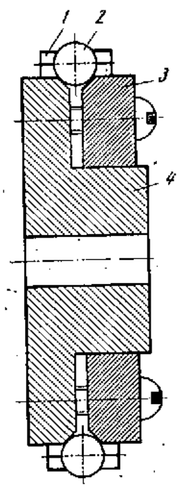

Figure 5. Ball forced deformation generator. 1 -- separator; 2 -- ball; 3 -- jaw; 4 -- boss.

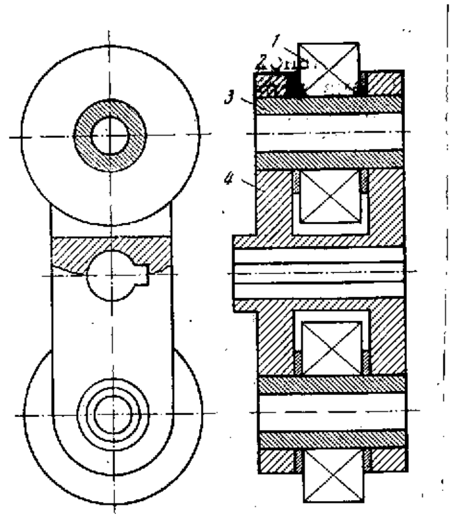

Figure 6. Two-roll generator of free deformation. 1 -- roll (ball bearing); 2 -- ring; 3 -- finger; 4 -- pole.

3. Generator of Forced Deformation of Rolling Friction, Multi-roll

This generator is kinematically similar to the preceding generator, but instead of balls it has cylindrical needle-like rolls. It has a very high load capacity, but it has increased resistance to rotation which limits its application in high-speed units.

4. Generator of Free Deformation, Two-Roll, Unregulatable (Figure 6).

This type is the simplest rolling friction generator. It has low moment of resistance to rotation, but it does not insure gapless coupling in the assembly. During operation the track in the flexible gear is quickly rolled out.

5. Free Deformation Generator, Two-Roll, Regulatable

The regulation is realized by using eccentric fingers for the rolls. The generator permits gapless coupling at the initial time after assembly; then as breakin takes place it becomes similar to the described nonregulatable generator.

6. Free Deformation Generator, Two-Roll, with Increased Pliability (Elasticity) of the Pole and Packing Ring.

The presence of elastic elements noticeably improves the operation of the transmission both with respect to accuracy (gapless) and with respect to reserves.

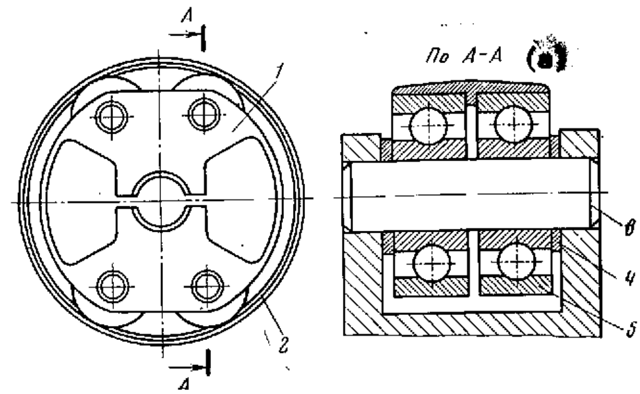

Figure 7. Four-roll free deformation generator.
1 -- pole; 2 -- packing ring; 3 -- finger; 4 --
ring; 5 -- roll (ball bearing).

Key: a. section through A-A

7. Free Deformation Generator, Four-Roll, Regulatable with Packing Ring (Figure 7)

The shell itself, the form of deformation of which depends on the angle between the axes of the rolls is used here as the pliable (elastic) element. The transmission with the given generator turned out to be highly unworkable in view of the fast failure of the shell as a result of cracks along the tooth depressions.

During the tests the measurements were taken of the shape of the deformation of the toothed rim for various types of generators with a circuit for comparison of it with the theoretical deformation curve. The shells of the generators types 3, 4 and 7 were measured. The results of the measurements are presented in the graph (Figure 8). The shape of the shell deformation of a generator type 3 coincided in practice with the theoretical curve presented in the figure. The shape of the curve for the free deformation generators differs very little from theoretical; for the type 7 generator this is especially noticeable in view of the presence of the "troughs" in the interval between the roles which were close together. This doubles the number of inflection points of the shell. An analysis of the curves obtained permits the conclusion that near the contact point of the shell with the roll there are sections with a small radius of curvature which increases the bending tension. All of this taken together can essentially reduce the transmission reserves.

The described servosystem was tested on a model for rotation of the analyzer-sensor with respect to a given program. Its application for the control of motors having starting currents to 4 amps is possible.

Conclusions

1. In the proposed system the possibility of joint operation of the integral amplifier built of MOS-transistors with standard elements of the servosystems

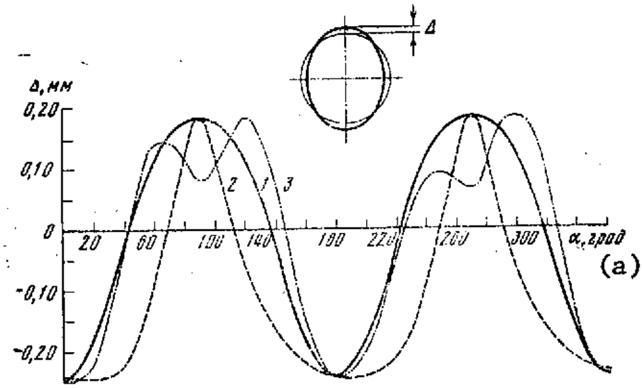

Figure 8. Deformation of the flexible gear of the undulatory reducing gear. 1 -- theoretical curve; 2 -- two-roll free deformation generator; 3 -- four-roll free deformation generator.

Key: a. degrees

was checked out in practice. The application of the IP-1A integral breakers permitted the creation of highly stable signal converters and reduction of the conversion errors to a minimum. A further increase in the specific content of the microcircuits in the servosystems is opening up the prospects for increasing the reliability, significantly reducing the size, weight and intake power.

2. In kinematically precise (slow) transmissions it is preferable to use the generators of forced deformation of rolling friction by comparison with the free deformation generators.

3. In instrument (low power) high speed transmissions it can be efficient to use free deformation generators.

4. In small-modular instrument undulatory transmissions, along with applying the elements which are regulatable on assembly, it is preferable to introduce pliable (elastic) elements which can frequently be adjusted during operation.

5. The packing ring in the free deformation generators improves the fitness of the undulatory transmission since it can be executed from harder steel than the shell, the hardness of which is limited by the tooth cutting conditions.

BIBLIOGRAPHY

1. Pavlov, A. A., SINTEZ RELEYNYKH SISTEM, OPTIMAL'NYKH PO BYSTRODEYSTVIYU (Synthesis of Relay Systems which are Optimal with Respect to Speed), Moscow, Nauka, 1966.

2. Pankram'yev, L. D., et al., IMPUL'SNYYE I RELEYNYYE SLEDYASHCHIYE PRIVODY POSTOYANNOGO TOKA S POLUPROVODNIKOVYMI USILITELYAMI (Pulse and Relay dc Servo Drives with Semiconductor Amplifiers), Moscow, Energiya, 1968.

3. Konev, Yu. I., TRANZISTORNYYE IMPUL'SNYYE USTROYSTVA UPRAVLENIYA ELEKTRO-DVIGATELYAMI I ELEKTROMAGNITIYMI MEKHANIZMAMI (Transistorized Pulsed Devices for Controlling Electric Motors and Electromagnetic Mechanisms), Moscow, Energiya, 1964.

4. Kossov, O. A., USILITELI MOSHCHNOSTI NA TRANZISTORAKH V REZHIME PEREKLYU-CHENIY (Switching-Mode Transistorized Power Amplifiers), Moscow, Energiya, 1964.

5. Lipman, R. A., POLUPROVODNIKOVYYE RELE (Semiconductor Relays), Moscow, Gosenergoizdat, 1963.

6. Shuvalov, S. A., Ivanov, M. N., Popov, P, K., Finogenov, V. A., Amosova, E. P., "Procedure for Calculating the Coupling Configuration of Undulatory Gears," IZV. VUZOV. MASHINOSTROYENIYE (News of the Institutions of Higher Learning. Machine Building), No 9, 1969.

7. Shuvalov, S. A., Ivanov, M. N., Popov, P. K., Finogenov, V. A., Amosova, E. P., Sheyko, V. V., "Structural Design and Calculation of the Basic Elements of Undulatory Transmissions," IZV. VUZOV. MASHINOSTROYENIYE, No 10, 1969.

8. Chernova, L. S., "Some Problems of the Configuration and Kinematic Accuracy of Single-Stage Undulatory Gears for Instrument Purposes," Author's Review of Dissertation for the Scientific Degree of Candidate of Technical Sciences, Leningrad, Northwestern Correspondence Polytechnical Institute, 1970.

9. Ginzburg, Ye. G., VOLNOVYYE PEREDACHI (Undulatory Transmissions), Leningrad, Mashinostroyeniye, 1969.

N74-33985

UDC 621.314.1

STATIC DC VOLTAGE STABILIZER-CONVERTER

[by V. I. Osadchiy]

[Text] A description follows of advantages of a static dc voltage converter combining the functions of the feed voltage stabilizer simultaneously. A comparison is made between the circuits for the known static stabilizer-converter and that developed by the author. A characteristic feature of the improved system is the increased stabilization coefficient, low output impedance and the possibility of smooth regulation of the output voltage. A practical diagram is presented for the improved high voltage stabilizer-converter and its parameters. There are 2 tables, 2 illustrations and 6 references.

Transistorized voltage converters which convert low dc voltage of one magnitude to various ac or dc voltages of other magnitudes [1-3] are widely used for feeding radio electronic instruments. One of the requirements imposed on the converters is stability of the ouput voltage on variation of the feed voltage. Frequently the voltage feeding the converter is stabilized for this purpose.

The most widespread types of stabilizers are continuous-action compensation voltage stabilizers. It is possible to find a description of the operation of these stabilizers in the corresponding literature [4]. A deficiency of the feed module comprising the feed voltage stabilizer and the voltage converter is the complexity of the device made up of two units. It is desirable to have a voltage stabilizer-converter in which the switching transistors simultaneously execute the functions of regulating transistors.

For the development of the stabilizer-converter described in this article, the method of stabilizing the output voltage of the converter as a result of automatic regulation of the base currents of the switching transistors was used. Here, the excess voltage of the power supply falls alternately on the converter transistors, keeping the variable voltage on the primary winding of the transform stable.

In contrast to the widespread operating mode of the two-cycle voltage converter with saturation of the transformer core, in the stabilizer-converter the transistor switching takes place when the collector current reaches a value of $I_k = B_{st} I_b$, that is, before saturation of the core takes place (I_b, I_k are the base and collector currents respectively in the saturation mode; B_{st} is the amplification factor in the saturation mode).

Usually the operating mode of the two-cycle converter without the transformer core's going into the saturation mode is rarely used since the losses on the transistors increase significantly as a result of the absence of excess base currents characterized by the saturation coefficient. In the case where instead of the feed module made up of the feed voltage stabilizer and the converter, the stabilizer-converter is used in which the transistors simultaneously perform the functions of regulating transistors, the operation of the stabilizer-converter without transformer core saturation permits an increase in the efficiency. This is explained by the fact that in the power supply module with an input stabilizer, the two transistors are included in series with the load: the regulating transistor of the stabilizer and the converter transistor. In the stabilizer-converter there is only one converter transistor included.

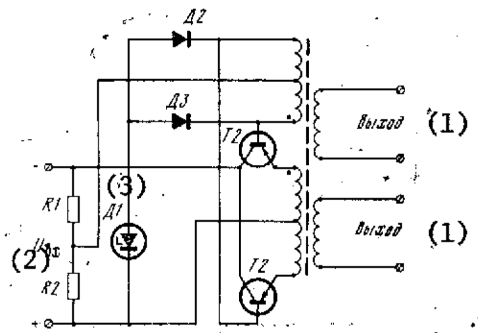

Figure 1. Schematic of the stabilizer-converter with common collector.

Key: 1. output 2. U_{inp} 3. D1

The operation of the converter without going into the saturation mode of the transformer core also permits a decrease in the losses in the core and exclusion of the distortion of the pulse shape as a result of the effect of scattering inductance. In addition, the number of circuit elements is reduced as a result of excluding the regulating transistor of the stabilizer and other auxiliary elements. The thermal regime of the regulating element is also facilitated since in the stabilizer-converter the scattering power on the regulating element is distributed equally between the two transistors.

In the literature [5] there is a description of the transistorized stabilizer-converter included with a common collector where on variation of the feed voltage the stabilization of the output voltages is realized as a result of establishing the voltage in the base circuits of the transistors of the converter using the stabilitron. The schematic of this stabilizer-converter is presented in Figure 1. For the steady-state mode of operation the stabilitron D1 alternately is connected to the bases of the open transistors by means of the diodes D2 and D3 which are alternately unblocked by the feedback winding emf.

The deficiencies of this type of stabilizer-converter are the following:

The low stabilization coefficient and large output impedance since for voltage stabilization in the circuit without transistors a parametric stabilizer is used which does not have a feedback circuit connected to the converter output;

The difficulty of setting the required voltage on the primary winding of the transformer as a result of the necessity for choosing stabilitrons with the required stabilization voltage and absence of the possibility of continuous regulation of the output voltage respectively.

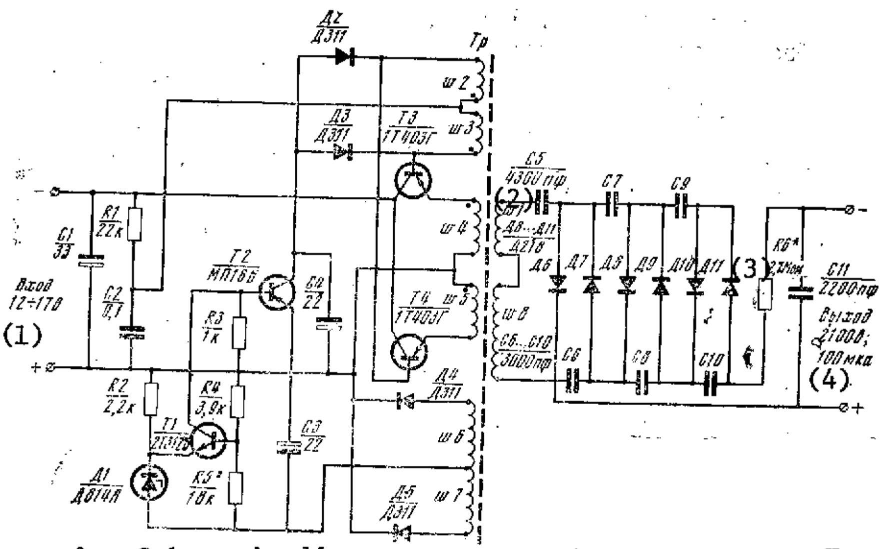

Figure 2. Schematic diagram of the improved stabilizer-converter with a common collector.

Key: 1. input 12-17 volts
2. 4,300 picofarads
3. 2.7 megohms
4. output 2,100 volts; 100 microamps

The purpose of developing the stabilizer-converter was also elimination of the indicated deficiencies. The electrical circuit diagram of the improved stabilizer-converter is presented in Figure 2 [6].

Instead of the stabilitron in the base circuit of the transistors a parallel emitter repeater based on the T2 transistor is installed, the base of which is connected to the collector of the feedback amplifier based on the transistor T1. The measuring element of the feedback amplifier is executed in the form of a nonlinear bridge made up of a parametric stabilizer using the diode D1 and the divider based on the resistors R4, R5 connected to the rectifier based on the diodes D4, D5 of the secondary winding of the transformer. The introduction of the T1 transistorized feedback amplifier into the circuit, the measuring element of which was connected to the converter output permitted a sharp increase in the stabilization coefficient, a decrease in the output impedance and by selecting the divider R4, R5 establishment of the required voltage on the primary winding of the transformer.

The improved stabilizer-converter operates in the following way. On connection of it to the power supply, a negative voltage is fed to the bases of the transistors T3 and T4 through the resistor R1 and the feedback winding. This voltage unblocks one of the transistors. The autooscillation process is set up. The transistors T3 and T4 and the diodes D2 and D3 connected to their bases are unblocked alternately under the effect of negative pulses reaching the circuits of their bases from the feedback windings. Here, the collector of the transistor T2 is periodically connected through the diodes D2 and D3 to the base of the transistor T3 or T4 which is open at the given point in time, fixing the voltage in their base circuits and stabilizing the voltage on the primary windings in the emitter circuits of these transistors. On variation of the feed voltage or the load current the output voltage of the secondary windings become greater than or less than the given level. On the diagonal of the nonlinear bridge of the measuring element an error signal appears which is amplified then by the transistor T1. The amplified control signal which is the base current of the parallel emitter repeater based on the transistor T2 operating in the corresponding phase changes the voltage on this transistor. The base current of the transistors of the converter and the voltage drop on them vary correspondingly, maintaining the voltage on the primary winding in the emitter circuits at the given level.

Table 1

Power supply unit	U_{inp}, volts	U_{out}, volts	I_{load}, milliamps	K	efficiency for U_{inp}=17v	f_{switch}, kilohertz
Stabilizer-converter	12-17	1800 (2100)	0.1	100	0.5	10
Feed voltage stabilizer and converter	12-17	1800 (2100)	0.1	50	0.2	5

Thus, the stabilizer-converter with common collector operates without the core of the transformer in the saturation mode which permits use of the advantages of operating in this mode: decreasing the losses in the core and excluding the effect of the scattering inductance on the shape of the square pulses. This is especially important when developing high-voltage voltage converters which have large scattering inductance as a result of a large number of turns of the secondary winding of the transformer. When developing the circuit the application of the converter with a common collector permitted electrical connection of the collectors (the cases) of the converter transistors and installation of them in the same radiator heat exchanger without insulating spacers which is especially important when the transistors execute the functions of regulating transistors.

Table 2

Windings	No of turns	Type of conductor	Conductor diameter, mm	Type of core
$w1$	1500	PEV-1	0,1	Sh7 × 7 M2000NM
$w2$-$w3$	105	"	0,1	
$w4$-$w5$	80	"	0,1	
$w6$-$w7$	80	"	0,1	
$w8$	1450	"	0,1	

The results of the experimental testing of the high voltage stabilizer-converter by the scheme depicted in Figure 2 are presented in Table 1. For comparison, in this table the parameters of the power supply and the high voltage converter are presented.

The error in the ouput voltage of the stabilizer-converter on variation of the ambient temperature from -20 to +50° C is no more than ±0.5 percent.

The type of semiconducting devices used and the magnitudes of the resistors and the capacitors are presented in the circuit. The transformer data are given in Table 2.

The following requirements are imposed on the transformer winding: the winding is made in the order of numbering of the windings, winding w2, w3 and w4 and w5 are wound in two conductors simultaneously.

BIBLIOGRAPHY

1. ISTOCHNIKI ELEKTROPITANIYA NA POLUPROVODNIKOVYKH PRIBORAKH. PROYEKTIROVANIYE I RASCHET (Electric Power Supplies Using Semiconductor Devices. Planning, Design and Calculation), Edited by S. D. Dodik and Ye. I. Gal'perin, Moscow, Sovetskoye radio, 1969.

2. Zhuravlev, A. A., Mazel', K. B., PREOBRAZOVATELI POSTOYANNOGO NAPRYAZHENIYA NA TRANZISTORAKH (Transistorized dc Converters), Moscow, Energiya, 1964.

3. Shvarts, S., POLUPROVODNIKOVYYE SKHEMY (Semiconductor Circuits), Translated from the German, Moscow, IL, 1962.

4. Karpov, V. I., POLUPROVODNIKOVYYE KOMPENSATSIONNYYE STABILIZATORY NAPRYAZHENIYA I TOKA (Semiconductor Compensation Voltage and Current Stabilizers), Moscow, energiya, 1967.

5. Zdorichenko, V. M., "Stabilizer-Converter. USSR Author's Certificate No 180642," BYULLETEN' IZOBRETENIY (Invention Bulletin), No 8, 1966.

6. Osadchiy, V. I., "Stabilizer-Converter. USSR Author's Certificate No 286051," BYULLETEN' IZOBRETENIY, No 34, 1970.

N74-33986

UDC 621.376.3:621.398

SHORTWAVE TELEMETRIC SYSTEM

[by K.K. Valenchuk, V. V. Shcherbakov, V. A. Yefremkin]

[Text] We have studied aspects of the application of frequency modulation when constructing a telemetric system in the shortwave band. The operating principles, the construction of the system and the decision-making device are described. The experimental data are presented. The equipment can be used on sounding balloons. There are 5 illustrations, 1 table and 4 references.

In transmitting telemetric information in the shortwave band it is of interest to use frequency modulation with a relatively low modulation index. Let us consider two aspects of the problem.

When receiving signals in the suprathreshold range FM gives a gain in the P_s/P_n ratio at the detector output by $\sqrt{3}$ D times (D is the modulation index) by comparison with using amplitude modulation [1, 2]. The fact is extremely important and characteristic for systems with frequency modulation that their efficiency rises for small values of the signal/noise ratio, that is, in the vicinity of the threshold [2]. On the other hand it can turn out that from the point of view of informativeness the pass band of the receiver on FM is better used than on AM although "...the exchange ratio between the communications channel band and the signal/noise ratio at the output with FM is not advantageous. The exchange ratio between the communications channel band the signal/noise ratio at the output, analogous to the ratio in the ideal system, is insured only in systems with PCM (pulse-code modulation)" [1].

Let us consider the problem of more efficient use of the pass band in more detail. For low information transmission rates (about 50 bits/sec) the frequency band on the air waves when using AM is small: 50-100 hertz. If we use simply AM, then in order to decrease the noise level at the receiver output it is necessary to have a receiver pass band also on the order of 100 hertz. However, in this case it is difficult to insure stability of the radio line frequency with respect to the receiver tuning frequency. In the shortwave band the relative instability of the carrier frequency by comparison with the tuning frequency of the receiver is difficult to insure even on the order of 100 hertz. It is comparatively easy to obtain a relative instability on the order of 10^3 hertz. Consequently, if nontunable communications are required, then in this case for information reception a total of 10 percent of the radio channel pass band is used. If we use FM, then with a signal band of 8-10 kilohertz for information reception at least 80-90 percent of the pass band of the channel is used, and only 10-20 percent to insure nontunable communications.

There is a third peculiarity of FM which permits simplification of the receiver -- this is constancy of the amplitude of the output signal at the output of the frequency detector with constant frequency deviation independently of the input signal level at the receiving channel. This permits construction of a system for separation and recording of information without using the circuits for instantaneous stabilization of the amplification coefficient of the low frequency channel.

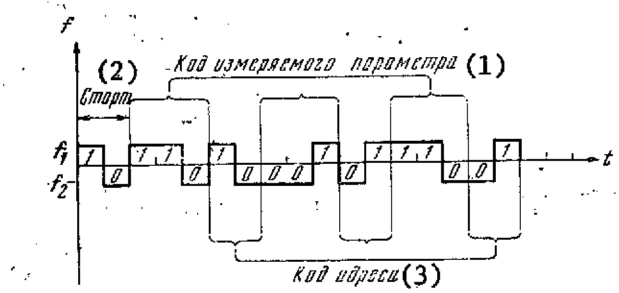

Figure 1. Time diagram of the code combination of one message -- word.

Key: 1. code of the measured parameter
2. start
3. address code

The description of the telemetric system and some experimental data are presented below.

The developed system is designed for transmitting analog telemetric data in the shortwave band with subsequent recording of it on punch tape of the receiving complex generator to process it further on a digital computer. The system is designed for transmitting 30 messages in 17 bit code with a transmission cycle equal to about 90 seconds. In Figure 1 we have the time diagram of the code combination of one message -- word. Each word begins with the start message comprising two elements, a 0 and a 1 arriving in series in two cycles. After this message comes the code for the measured parameter separated by the address code elements. The duration of the transmission of one message is 340 milliseconds.

In Figure 2 we have the block diagram of the system.

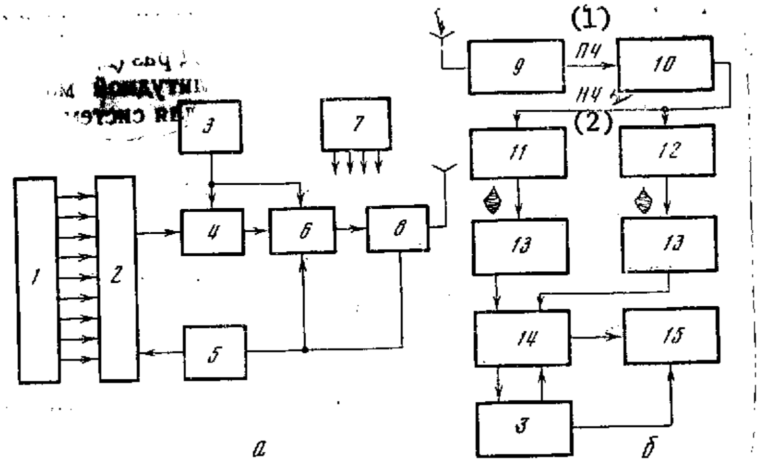

Figure 2. Block diagram of the system. a -- measuring complex; b -- receiving complex; 1 -- sensors; 2 -- commutator; 3 -- cycle pulse generator; 4 -- analog-digital converter; 5 -- time-program device; 6 -- modulator; 7 -- feed module; 8 -- transmitter; 9 -- shortwave receiver; 10 -- limiter-amplifier (frequency detector); 11 -- filter F1; 12 -- filter F2; 13 -- decision making circuit; 14 -- code shaper; 15 -- recorder.

Key: 1. intermediate frequency 2. low frequency

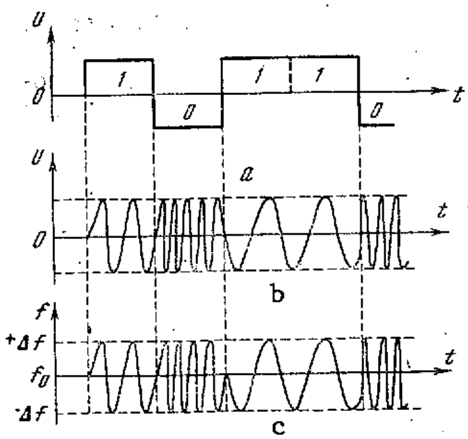

Figure 3. Output signal shaping diagram. a -- transmitted message; b -- signal from the modulator output; c -- signal from the shortwave transmitter output.

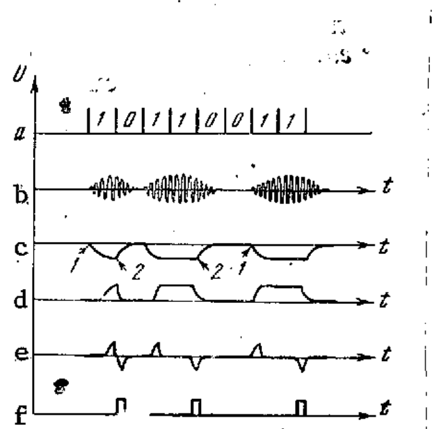

Figure 4. Voltage diagrams of the decision making device. a -- transmitted message; b -- filter output; c -- detector output; d -- selector output; e -- differentiating circuit output; f -- output of the unit.

Measuring Complex

The operating time diagram of the entire onboard complex is given using the time-program device. The synchronization of the operation of the analog-to-digital converter and modulator is realized by means of the cycle pulse generator. The system carried out triple transmission of each measurement which permits an increase in the reliability of the received messages by processing them on a digital computer.

The radio signal is shaped in the following way. Under the effect of the code in the modulator from the analog-to-digital converter commutation of the subcarrier frequencies f_1 and f_2 is realized. The signal obtained in this way (in which the element 1 corresponds to a frequency of f_1 and the element 0 to a frequency of f_2) goes to the transmitter input and realizes frequency modulation of the carrier (Figure 3).

Receiving Complex

The intermediate frequency signal from the receiver output is detected by the frequency detector and goes to the filter input. The filters realize selection of the signals of the subcarriers f_1 and f_2. The decision-making devices which define the time of completion of the arrival of the signals with a frequency of f_1 and f_2 are connected to the filter outputs.

The signals from the decision making devices go to the code shaper which reproduces the transmitting code. The received code is recorded in the register. By using the cycle pulse generator the operation of the onboard and ground complexes is realized, and the boundaries of the elements are defined in the received message.

The start-stop method of synchronization is used in the system. The information "word" reception begins with the time of arrival of the start message after the pause comprising two elements, 0, 1 arriving in series one after the other in two cycles. The phase correction of the cycle pulse generator takes place at the time of replacement of the 0 element by the 1 element during reception of the entire information word. This offers the possibility of quickly synchronizing and not imposing increased requirements on the stability of the cycle pulse generator frequency, but increased requirements are imposed on determining the element exchange boundary. The problem is solved in the decision-making device the operation of which is described below.

Decision-making Device

On receiving the pulses (radio pulses) the signals are sharply distorted by noise which leads to the occurrence of double-type errors [3]: the error as a result of displacement of the front and truncation of the pulse and anomalous errors which appear on suppression of the signal by noise and in the case of a pulse response when the noise surges are received as the signal.

The probability of the occurrence of the listed errors depends on the signal processing scheme. The noiseproofness of the receiver is essentially determined by the decision-making device used. It must provide reliable and precise recording of the time position of the received information-pulse (radio pulse) element.

In the general case the device comprises an assembly for the detection and recognition of the signal in the noise and a circuit for measuring (recording) the time position of the pulse received. Most frequently, a combination device is used for detection and measurement of the time position of the pulse by means of a threshold device. With this method, the time of exceeding some threshold (a given level) is taken as the time position of the signal. This method of reckoning gives the lowest accuracy and the highest probability of the appearance of an anomalous error [4]. With equiprobability of the appearance of a 0 and a 1, the threshold is selected corresponding to 0.5 U_{max} of the signal. In this case the error in determining the time of appearance of the pulse can reach (0.2-0.4)T where T is the symbol duration.

The most optimal method is recording the pulse by the position of the maximum of the suprathreshold surges. The position of the maximum value of the surge is determined by the position of the zero of its derivative. The surge is fed to the differentiating circuit, then to the amplifier, the limiter and the shaping circuit which is triggered by a negative voltage flash. In this case we obtain an output pulse, the leading edge of which coincides with the point of the maximum selected pulse.

In the described system the differentiation method is used, but in order to record the pulse with a flat peak, without the application of a delay line.

For reception of a radio pulse at the output of the band filter we obtain a radio pulse with a flat peak and exponential front since usually the following relation is satisfied [4]: $\Delta F = n/T$ ($n \geq 0.5$) where ΔF is the filter band; T is the radio pulse duration. On reception of a packet of pulses with the same name, we have a pulse with a flat peak (Figure 4,c).

The decision making device determines the time of the end of the pulse or the packet of pulses with the same name, that is, the position of point 2 (see Figure 4,c).

Point 1 (see Figure 4,c) which has the same steepness of the front as point 2 is not used since it lies in the region of effect of the noise in the absence of a signal. Point 2 is isolated after passage of the signal through the threshold device.

Let us consider the operation of the decision making circuit (Figure 5).

The signal from the filter goes to a paraphase amplifier executed from the PP1 transistor. Then amplitude detection of the signal takes place (see Figure 4,c). The voltage reproducing the envelope of the input signal from the filter goes from the output of the AM detector to the maximum amplitude selector executed from the PP2 transistor. The required threshold is established by the resistor

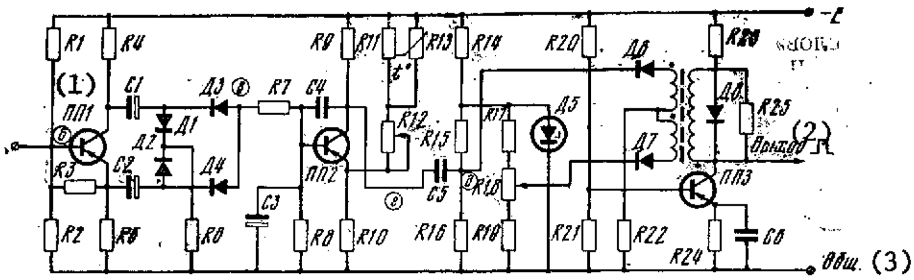

Figure 5.

Key: 1. PP1 2. output 3. common

R12. The signal from the output of the threshold device (see Figure 4,d) goes to the C5R15R16 differentiating circuit, the time constant of which is selected so that differentiation of the signal will be insured with its rated level without the effect of noise.

The negative differentiated signal drop starts the diode-regenerative comparator which emits the pulse, the leading edge of which corresponds to the time of completion of the input radio pulse (diagram e, Figure 4). The level of starting the comparators is established by the resistor R18 somewhat below the zero line (about 0.1-0.15 volts with a magnitude of the negative pulse with the differentiating circuit of 1.5 volts). For the given schematic the noise surge exceeding the level does not trigger the comparator since it is not differentiated in view of the short duration.

The experiment demonstrated that on variation of the P_{signal}/P_{noise} ratio from 10 to 1.4, the variation of the position of the output pulse is about 0.05 T_{pulse}.

Experimental Results

The above described system was checked for noiseproofness under laboratory conditions. At the receiver output the band of which was set equal to 10 kilohertz a signal was supplied from the simulator. The noise in the 6 megahertz band from the G2-1 noise generator was input to the intermediate frequency amplifier at the output of which, that is, at the input of the frequency detector, the voltmeter VZ-5 measured the signal level without noise U_{sig}; then it measured the noise level without the signal U_{noise}. The measurement was made with the automatic gain control shut off. Then the U_s/U_n ratio was found. Then with the signal included with the noise, the information was recorded and the probability of correct recording of the information words was calculated.

The experimental data are presented below:

U_s/U_n ratio	1,58	1,36	1,30	1,22	1,11
Probability of correct recording of the pulse packets	0.994	0.99	0.97	0.603	0.13

The noiseproofness of the system was also checked under the effect of pulse noise at the receiver input from the G5-6A generator. The signal/noise ratio was measured by the above-described procedure.

With a pulse noise repetition frequency of 3 kilohertz and duration of 1.5 microseconds (I), 1.5 kilohertz and 375 microseconds (II) and 1.0 kilohertz and 500 microseconds (III), the U_s/U_n ratios and the probabilities of correct recording were the following:

	I			II			III		
U_s/U_n	1,44	1,36	1,29	1,4	1,3	1,29	1,4	1,37	1,32
Probability of correct recording	1	0,995	0,9	0,984	0,96	0,8	0,96	0,95	0,92

BIBLIOGRAPHY

1. Teplyakov, I. M., RADIOTELEMETRIYA (Radiotelemtry), Moscow, Sovetskoye radio, 1966.

2. Kantor, L. Ya., METODY POVYSHENIYA POMEKHOZASHCHISHCHENNOSTI PRIYEMA CHM SIGNALOV (Methods of Increasing the Noiseproofness of the Reception of FM Signals), Moscow, Svyaz', 1967.

3. Karamov, Z. S., Fomin, A. F., ELEMENTY I UZLY ANALOGOVYKH RADIOTELEMETRICHESKIKH SISTEM (Elements and Assemblies for Analog Radiotelemetric Systems), Moscow-Leningrad, Energiya, 1968.

4. Nemirovskiy, M. S., POMEKHOUSTOYCHIVOST' RADIOSVYAZI (Noiseproofness of Radio Communications), Moscow-Leningrad, Energiya, 1966.

N74-33597

UDC 621.373.5

TRANSISTORIZED BLOCKING GENERATOR

[by A. V. Popkov]

[Text] Test results are given for a high speed transistorized blocking generator. There are 4 illustrations and 1 reference.

For the shaping of nanosecond pulses it is possible to use a driven blocking generator circuit with one power storage element -- a pulse transformer. Such circuits have a small number of elements, and the output parameters depend weakly on the uncontrolled current $I_{k.0}$. In addition, in the driven state they do not consume power from the power supply.

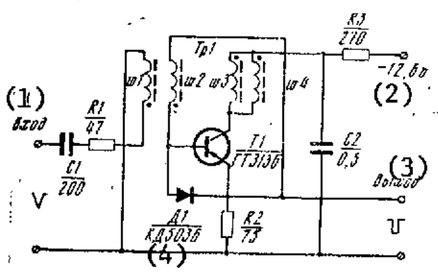

Figure 1. Schematic diagram of a driven blocking generator.

Key: 1. input
2. -12.6 volts
3. output
4. D1/KD5036

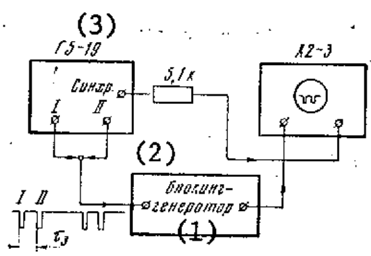

Figure 2. Block diagram of measuring the dead time of the blocking generator.

Key: 1. synchronization
2. blocking generator
3. G5-19

A study was made of a driven blocking generator assembled according to the diagram (Figure 1) analogous to that proposed in reference [1]. As the energy storage element a transformer based on a toroidal ferrite core was used. The base winding w2 connects the base of the transistor to the emitter which insures high current flowing through the base-emitter junction. This made it possible to obtain a good ouput pulse buildup front (τ_{front} = 10 nanoseconds).

One of the collector windings of the transformer w4 is wound together with the base winding w2 to increase the positive feedback for response of the circuit. The ferrite core of the pulse transformer Tr1 had an initial magnetic permeability of 600 and dimensions of K4 × 2.5 × 2 mm. The windings were made of PELShO-0.09 conductor with the following number of turns: w1 = 8, w2 = w4 = = 2, w3 = 10. In the given case the diode D1 protects the base-emitter junction from breakdown during the generation of the pulses.

In the circuit the GT313B high frequency transistor was used (β = 65). The transistors of this type have β = 4.5-10 on a frequency of 100 megahertz and a feedback circuit time constant of 40 nanoseconds.

The duration of the output pulse of a blocking generator can be regulated by changing the number of turns of the w3 collector winding. Here, with an increase in the number of turns, the pulse duration decreases. This is obvious from the results of the measurements presented below and obtained for the following parameters of the start pulses: the amplitude U_{inp} = 3 volts, the duration τ_{inp} = 40 nanoseconds, the recurrence frequency F = 5 megahertz:

No of turns of w3	0	6	8	9	10
Pulse duration τ_{out}, nanoseconds	50	48	37	30	26

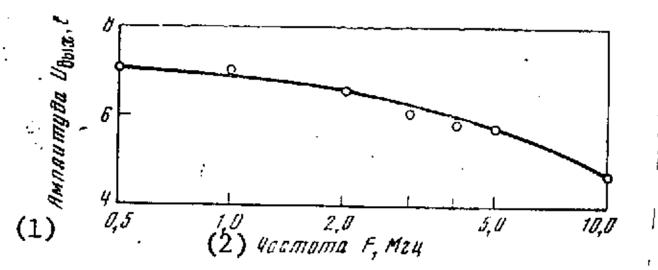

Figure 3. Amplitude of the output pulse of the blocking generator as a function of the start pulse frequency.

Key: 1. amplitude U_{out}, volts 2. frequency F, megahertz

In order to estimate the speed of the blocking generator, the dead time was measured. In Figure 2 we have a block diagram for the measurement. The triggering was done from the G5-19 pulse generator; here, the pulses were fed to the input of the circuit via a triplet from the two outputs of the generator. The output signals of the investigated circuit were observed on the screen for measuring the transient characteristics Kh2-3. The recurrence rate of the pulses was set to the maximum for the given type of generator equal to 5 megahertz. With a II pulse delay (see Figure 2) of 100 nanoseconds with respect to pulse I at the input of the blocking generator, a periodic pulse train was obtained with a recurrence rate of 10 megahertz. The circuit operated stably on this frequency; here the input and output pulses had the following parameters: U_{inp} = 2 volts, τ_{inp} = 10-40 nanoseconds, U_{out} = 4.5 volts, τ_{out} = 26 nanoseconds.

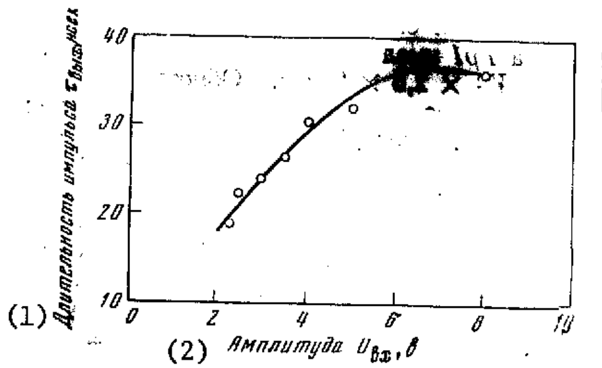

Figure 4. Duration of output pulse as a function of start pulse amplitude.

Key: 1. pulse duration τ_{out}, nanoseconds
2. amplitude U_{inp}, volts

In order to determine the dead time of the blocking generator, the delay time τ_{del} of pulse II was decreased until the second pulse dropped in the pair of pulses observed on the oscillograph screen. The minimum delay time is equal to the dead time of the circuit, and in our case it was 40 nanoseconds. Thus, there is a possibility of starting the given blocking generator with a maximum frequency to 25 megahertz.

Some characteristics of the investigated blocking generator were determined. Thus, in Figure 3 the amplitude of the output pulse is shown as a function of the trigger frequency.

The duration of the output pulses depends on the amplitude of the trigger pulses. This relation is presented in Figure 4. The data were obtained for $\tau_{inp} = 40$ nanoseconds and F = 5 megahertz. The dependence of the duration of the output pulses on the amplitude of the trigger pulses complicates the use of the given blocking generator as the input shaper in the amplitude analyzers. However, it is possible to recommend it as the nanosecond pulse shaper in cases where operation on a low-resistance load is required (75 ohms), and the start pulses have constant parameters.

BIBLIOGRAPHY

1. Mineyev, Yu. V., "Shaping Nanosecond Pulses by a Transistorized Blocking Generator," PRIBORY I TEKHNIKA EKSPERIMENTA (Experimental Instruments and Techniques), No 5, 1966.

N74-33988

UDC 629.785.002.2

PRODUCTION TECHNOLOGY

PROSPECTIVE AREAS IN THE PRODUCTION TECHNOLOGY OF SCIENTIFIC EQUIPMENT FOR SPACE RESEARCH

[by A. V. Breslavets]

[Text] The average labor of individual types of operations in the percentage ratio of the total labor consumption of manufacturing scientific instruments and apparatus for space research is presented. The prospective areas in the production technology of billet, machining, mechanical assembly, installation and assembly, adjustment and regulation and testing and control operations are noted. Basic recommendations are made with respect to further reduction of labor consumption and an increase in the productivity of labor when manufacturing scientific equipment for space research. There are 4 references.

The successful performance of basic research requires continuous increase in the nomenclature and the number of scientific instruments and equipment developed and manufactured in experimental production.

Here, both the development and the manufacture of the instruments and equipment must be carried out in extremely compressed times with simultaneous insurance of the required high-quality, reliability and constant reduction in cost.

The presented analysis of the manufacturing cost of the scientific equipment and instruments demonstrated that it is determined above all by the tediousness of their manufacture and experimental production. Therefore, it is necessary sharply to increase the growth rates of the productivity of labor of all types of operations performed by experimental production when manufacturing equipment and instruments. The increase in productivity of labor and the experimental production, considering its unique (small series) nature, can be insured above all by using new progressive materials, introducing all-purpose high-production equipment and instruments, mastering the latest technological processes, the performance of operations with respect to broad standardization and normalization of the technological equipment and tools and also by improving the forms of cooperation and specialization used.

These measures have special significance for the production of the scientific instruments inasmuch as the distinguishing feature of the given production is the large nomenclature of the instruments, their structural-technological complexity requiring multiple forms of separation of production, the constant mastery of new, theoretically distinguished technological processes, in a number of cases changing the nature of manufacture of the instruments basically. Under these conditions an important source of increasing the productivity of labor will be an increase in the level of technological processing of the structural elements of the new instruments in the direction of standardization of the parts and unitization of the technological processes, the application of group processing techniques, broad use of all-purpose assembly attachments and equipment.

The application of the means of computer engineering when selecting the optimal version of the technological preparation of production and dispatching of the production process, the introduction of the means of low mechanization of technological processes and the scientific organization of labor in all parts of the production process have a significant effect on increasing the productivity of labor and reducing the instrument cost. Accordingly, it is of interest to investigate the most important prospective areas in production technology for scientific space equipment by individual forms of operations.

The average proportion of the labor consumption of individual forms of operations developing in practice in percentages of the total labor consumption of the manufacture of scientific instruments and equipment is presented below:

Billeting operations	7
Framing and fitting operations	8
Machining	20
Mechanical assembly operations (assembly of precision mechanics units)	12
Installation and assembly operations	22
Adjustment and regulation operations	19
Testing and control operations	12

Billeting

Improving the technical level of the billeting is connected above all with the introduction of progressive methods of the formation of billets having minimum tolerances for machining and improved finishing of the surface, the introduction of machines for processing the pressure parts with simultaneous decrease in the equipment fleet for machining with the removal of shavings. The application of billets obtained by the method of pressure die casting permits the use factor of the metal to be brought to 0.9-0.95 percent and a sharp reduction in the labor consumption of subsequent machining. When using billets made by chill casting and the lost-wax method, a significant increase in accuracy and surface finish to fourth and fifth class are insured which in a number of cases completely excludes the necessity for subsequent machining. The application of special profiles of the rolled products for the production of framing elements, bays, modules, chassis and other parts instead of casting, welding and machining permits a reduction in the labor consumption of this type of operation by 2-3 times and a reduction in the metal consumption by 40-60 percent. The introduction of new polymer materials and, in particular, new thermoplastic masses permitting an increase in quality of the external finish, improvement of technical characteristics of the parts, an increase in the productivity of labor as a result of exclusion of subsequent machines deserves attention in the billeting production. The application of polymer materials permits the solution of complex technical-economic problems: in some cases these materials correspond better than metals to the requirements of the structural design, and in other cases they are used as substitutes for expensive metal.

The transition of the billeting production from machining to obtaining parts by the method of stamping and pressure working permits achievement of a growth in the productivity of labor by 2-3 times with simultaneous significant increase in the use coefficient of the material. On this level the introduction of the method of inverse extrusion, rolling processes, electrohydraulic and magnetopulse stamping, explosive forming and also the introduction of the technological processes of manufacturing parts by the methods of liquid and hot stamping offer a highly productive effect.

In connection with the small series and single nature of the production of scientific instruments it is especially effective to introduce the method of element by element stamping for which it is not necessary to manufacture special dies and it is possible to obtain parts of relatively complex shape with insignificant labor consumption in their manufacture. Obtaining billets of the type of cores, bushings, flanges, housing, bearings and other parts by the method of powder metallurgy also permits significant reduction in labor expenditures as a result of a decrease in tolerances for subsequent machining or complete exclusion of subsequent machining.

Fitting and Framing Operations

The labor consumption of the fitting and framing operations under the conditions of individual production of instruments is highly significant and is almost 8 percent of the total labor consumption. As the prospective areas in improving the technical level of fitting and framing operations it is necessary to consider further introduction of the means of mechanization, production equipment and other fittings, which, above all, include the following:

Pneumatic and mechanical devices for cutting the sheet material, cutting angles in the parts, cutting out the outlines of parts of the chassis type, cutting out square holes, grooves, various flexible sections and gluing the parts of the frames;

The jig turret process, prices of the "multiple mold" type, flexible disc and other quickly adjustable and all-purpose machine tools;

All-purpose assembly stocks for welding, gluing and riveting the frame elements permitting argon-shielded and carbon dioxide-shielded welding, and also gas welding and electric arc welding;

The sheet breakthrough and cutting punches for manufacturing small-series parts;

The all-purpose assembly attachments for drilling, milling, planing and other assembly and finishing operations;

Low mechanization media -- the fitting and assembly operations -- mechanized clamps, clips, screw drivers, wrenches and other tools.

The operations with respect to the application of galvanized, chemical and paint and varnish coatings (also belonging to the fitting and framing operations) are not characterized by great labor consumption, but they have important significance in insuring the quality, reliability, service life and improvement of the external type of instrument and equipment. In this field the prospective area in the technological process is the introduction of new types of coatings such as cyanide, chemical nickel plating, painting in an electrostatic field, painting by the pouring method, and others.

Machining

In scientific instrument-making machining basically includes the machining of complex housing parts, the parts and assemblies for precision machinery, the parts of various types of kinematic transmissions, and so on; here the labor consumption of machining reached on the average 20 percent of the total labor consumption of manufacturing the instrument. It is necessary to note that with an increase in the technical level of the billeting production, with the introduction of progressive processes of embossing the billets in the mechanical sections, the volume of rough grinding operations is reduced sharply and the proportion of the finish operations increases correspondingly.

All of this stimulates broader use of the most economical and high-precision machine tools. In addition, the specific requirements arising from the complexity of the parts and assemblies manufactured in the mechanical sections for the instruments and their high precision also stimulate significant reduction in the number of lathes, milling machines, low-precision planes and a further increase in the fleet of precision, grinding, electroerosion and other machine tools for electrophysical and electrochemical methods of machining.

A reduction in the labor consumption of machining in scientific instrument making for outer space is continuously connected with further introduction of progressive forms of organization of labor and improvement of the machining techniques. The most prospective areas in improving the technical level in machining production must, above all, take into account the following:

Modification of the metal-working equipment for improving its speed and accuracy characteristics;

Broader application of hard-alloy and diamond cutting tools permitting machining at high speeds and insuring high quality of the machined surfaces;

The introduction of group machining of the parts, the creation of specialized work areas and variable flow lines;

The expansion of the area of application of electrophysical and electrochemical methods of machining with the removal of shavings;

The conversion to diamond machining of precision parts made of metal and parts made of germanium, silicon, ferrite, pyroceramic, quartz, glass and other hard materials and alloys.

The introduction of machine tools with programmed control and unitized machine tools made of standard assemblies and parts is an enormous reserve for the growth of productivity of labor in machining.

Mechanical Assembly Operations

With respect to labor consumption these operations constitute about 12 percent of the total labor involved in manufacturing an instrument or apparatus; here, the primary proportion goes to manual operations with respect to assembly and regulation of the precision mechanisms and elements among which the most frequently encountered are periscope units, programmed and staged current distributors, electrical commutators, step-by-step motors, and various types of reducing gears, including undulating transmissions and other elements of instruments characterized by precision and exceptionally high requirements on the assembly and adjustment culture. In connection with the individual nature of the production of scientific instruments and the theoretical structural-technological difference of the manufactured assemblies in precision mechanics at the present time it does not seem possible significantly to increase the level of mechanization of manual operations of this type, and therefore it is necessary to some degree to consider it justifiable to use the selective method of assembly. However, increasing the manufacturing accuracy of the parts when machining them significantly reduces the labor consumption of the assembly and adjustment operations. Among the most prospective areas in the improvement of the productivity of labor during assembly and regulation of the precision mechanics assemblies it is necessary to consider the following:

Improving the accuracy of machining the parts to complete exclusion of finish operations during assembly;

Expansion of the nomenclature of the all-purpose assembly tools and equipment used (the calibrated attachments for pressing and removing bearings, calibrated wrenches, screw drivers, and so on);

Introduction of automated precision finishing machine tools and automated breakin units;

Introduction of mechanized and automated methods and equipment for monitoring the regulatory operations and performing tests;

Improving the overall production culture.

Installation and Assembly Operations

The most characteristic feature of the production of scientific equipment is the significant proportion of the installation and assembly operations making up more than 20 percent of the total labor consumption. As a rule, these operations are poorly subjected to mechanization, and under the conditions of individual production they are in the majority of cases manual. In order to decrease the labor consumption of this type of operation, the efforts of the equipment developers and designers must be directed primarily at broader introduction of the functional-assembly method of planning and design, the application of methods of constructing equipment in various modular and micro-modular designs, the creation of equipment where this is technically and economically expedient with the use of microminiature integrated and hybrid microcircuits.

The application in the new developments of standardized assemblies and modules and also structural designs borrowed from the preceding developments and previously mastered in experimental production essentially reduces the labor consumption and costs of the installation and assembly operations.

The individual nature of the production of scientific equipment and instruments with great variety and multinomenclature of the parts does not permit the introduction of the complex-mechanized flow and conveyor lines widely used under the conditions of series and mass production of the installation and assembly operations. However, the performance of the set of operations with respect to classification, standardization, normalization and unitization permits under the conditions of individual production the organization of specialized work areas and sections in which it appears possible to use the methods and apply the means of mechanization characteristic of series and large series production. The specialization of the work areas with respect to types of operations permits equipment of the work areas with the most advanced specialized assembly and installation tools and equipment, a reduction in the operation category, a significant reduction in the labor consumption of the individual assembly and installation operations and significant improvement of the labor conditions on performance of these operations.

One of the most prospective areas in the organization of specialized work areas and sections is the creation of specialized sections with respect to performance of the prefabrication operations of the installation and assembly work. In spite of the great variety of schematic elements and parts installed on the mounting plate, whether using three-dimensional or printed installation, they can be combined into defined groups and classes. The technological processes performed in the specialized prefabrication section for each group and class of elements are characterized by identicalness of the procedures and operations which permits the assignment of defined transitions and operations to defined equipment or work areas. Here, the work areas and the equipment are available for execution of the transitions of the billeting operations and they are specialized with respect to forms of operations performed. The work area specialized in this way can be equipped with highly efficient all-purpose equipment and tools:

The machine tools and tha automata for dimensional cutting of wiring and jumpers with simultaneous removal of the insulation and twisting of the strands;

Machine tools and devices for pinning the plates and fitting the hollow rivets from tape;

Automated units for marking and dimensional cutting of the vinyl chloride insulation tubes;

All-purpose pneumatic devices for molding the radio elements with the basic leads with simultaneous cutting of them to the given length;

Specialized devices for tinning the jumpers and leads of the radio elements.

The execution of prefabrication installation and assembly operations in the specialized prefabrication sections permits a reduction in their labor consumption by 50-60 percent. Analogous specialized sections can easily be built for execution of open and torroidal windings, the manufacture of single layered and multilayered printed mounting plates and other operations of installation and assembly production remaining labor-consuming manual operations and forming a huge reserve for the improvement of the productivity of labor.

Adjustment-Regulation and Monitoring and Testing Operations

The adjustment-regulation and monitoring and testing operations are an inseparable part of the technological process of manufacturing scientific equipment, and they constitute more than 30 percent of the total labor consumption. Here, under unit production conditions the adjustment and regulation operations are performed by the most qualified adjustment and regulation personnel. In order to decrease the labor consumption of these operations and for the possibility of using manpower with lower qualifications, the most prospective area, just as for the installation and assembly operations is broader application of the functional-assembly method of planning and design using ready-made modular, micromodular and microminiature circuits and structural elements not requiring additional adjustment and regulation operations. The labor consumption of adjusting the equipment using micromodules and integrated hybrid microcircuits is two to three times less than the labor consumption of the adjustment and regulation of analogous equipment made from ordinary discrete elements.

Another prospective area in the reduction of the labor consumption of the adjustment and regulation operations is broader equipment of the adjustment sections with all-purpose mechanized devices, test units and checking and monitoring panels assembled from standardized assemblies and modules of control radio measuring equipment. The all-purpose mechanized devices and test units permit easy mechanization in spite of the variety of schematic solutions to the equipment, such operations as signal testing of closed and open circuits, checking the insulation resistance, checking insulation strength, and so on. Here no finish work or adjustment of the devices and the test units themselves are required since the required checkout program is given by moving the switches located on the control panel of the test unit or the monitoring and checking device to the corresponding position.

The monitoring and testing panels assembled from standardized assemblies and modules of radio measuring equipment permit under the condition of unit production easy recomposition of them providing special measurements necessary only for the given specific circuit. Thus, there is no necessity for large capital expenditures on the manufacture of specialized panels, and the adjustment labor is sharply reduced.

In order to reduce the labor of the adjustment and regulation operations, further improvement of the technological processes of the adjustment and regulation has great significance as a result of the proper grouping of the operations and efficient organization of labor, the introduction of low-mechanization means, the specialization of adjustment and regulation work areas and sections, the creation of new methods of adjustment and regulation corresponding to the requirements of automating the adjustment and regulation processes.

A further reduction in labor consumption and improvement of the productivity of labor of the adjustment-regulation and monitoring and testing operations is the all-around problem encompassing the problems of structural design of the scientific equipment, the organization of production, the development, manufacture and introduction of automated and mechanized equipment.

The adjustment, regulation, monitoring and testing are the most responsible, very specific steps in the production of scientific equipment and instruments for space research. Obtaining stable parameters of the scientific equipment and, consequently, the progress in the space experiment as a whole depend to a large degree, if not completely, on the quality of execution of the adjustment, regulation and test operations.

BIBLIOGRAPHY

1. Kalita, Ye. D., "Basic Paths of Technological Reequipment of Enterprises and Raising the Level of Mechanization and Automation of Production Processes," OBMEN OPYTOM V RADIOPROMYSHLENNOSTI (Exchange of Experience in the Radio Industry), NIIEIR, No 3, 1968.

2. Pyatlin, O. A., "Basic Areas in the Improvement of the Technology of Assembly-Installation and Regulation Operations," OBMEN OPYTOM V RADIOPROMYSHLENNOSTI, NIIEIR, No 3, 1968.

3. Bronnikov, M. B., Perminov, B. P., "Mechanization and Automation of Technological Processes for the Assembly and Installation of Radio Equipment," OBMEN OPYTOM V RADIOPROMYSHLENNOSTI, NIIEIR, No 7, 1967.

4. Mal'kevich, V. L., Rudnev, N. I., "Some Paths of Mechanization of Billeting Operations during Assembly and Installing of Radio Equipment," OBMEN OPYTOM V RADIOPROMYSHLENNOSTI, NIIEIR, No 5, 1970.

N74-33989

UDC 629.785

PROCESS OF MANUFACTURING SMALL-MODULE GEARS WITH INTERNAL COUPLING

[by V. P. Romanenko, A. P. Steblov, G. V. Delektorskiy]

[Text] A study of small-module geared coupling of an undulatory transmission, the versions of the manufacture of gears with internal coupling and the instruments and equipment used is made. There are 3 illustrations.

The undulatory transmission is a new type of transmission. The name "undulatory" is connected with the fact that the conversion of motion in the mechanism of this transmission is realized by the displacements of the deformation wave of one of the elements which is made flexible and the corresponding synchronous displacement of the coupling zone or the friction contact of the rigid elements. The displacement of the deformation wave of the flexible element is caused by the moving element of the mechanism or a nonmechanical device called the wave generator.

The possibility of obtaining large transmission numbers from a small size, the high kinematic accuracy of the transmission, the smoothness and the noiseless nature of their operation, the possibility of obtaining gapless reversible drives, the stability of the kinematic characteristics during prolonged operation under load, the quite high transmission efficiency, insignificant wear and satisfactory life of the basic parts, the multicouple contact of the teeth, the balance of the loads, the low sliding rates in the coupling and a number of other properties of undulatory transmissions have brought the attention of a large number of engineers and scientists to them. At the present time, the undulatory transmissions have become quite widespread in the form of special or general purpose reducing gears.

In the structural designs of undulatory transmissions there are parts which are highly complex from the technological point of view. Above all, this pertains to the flexible elements in which the requirements of high fatigue strength and accuracy are combined with low rigidity and extraordinary shape and also rigid elements with a small-module inside tooth.

In order to manufacture the undulatory reducing gears with a module of 0.2 mm, the following two methods were used: 1) the method of broaching with a small-module broach; 2) the method of burning through on an electroerosion tool.

In order to manufacture gears with an inside tooth by the broaching method, a small-module broach was made from the Kh12F1 and KhVG type tool alloy steel.

In order to insure a coupling without clearance between the gear and the inside tooth (Figure 1) the geometric parameters of the broach were selected, the diameter of the calibrating part of the broach and the height of the teeth. The broach and the tooth profile are illustrated in Figure 2. The teeth were broached on the screw-cutting lathe using the tailstock with small longitudinal feed of the tool. As a result, a gear was obtained with unsatisfactory finish machining of the tooth surface and the tooth profile corresponding to the profile of the broach depressions.

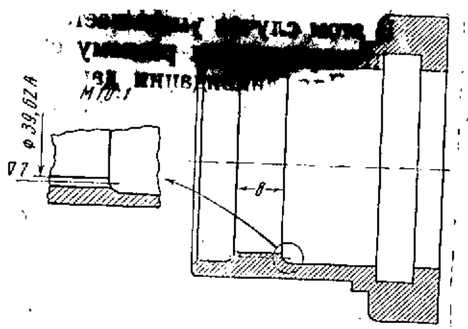

Figure 1. Gear with inside tooth.

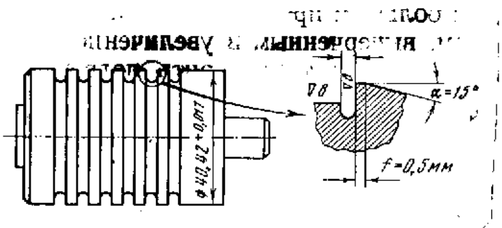

Figure 2. Broach and tooth profile

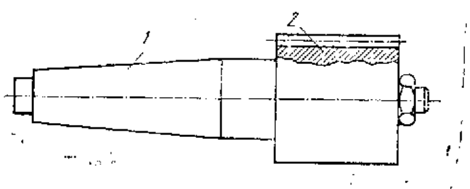

Figure 3. Electrode tool for manufacturing a gear with an inside tooth.

The deficiencies of the given method include the following:

1) When milling teeth the error in manufacturing the cutter is copied on the broach which leads to an increase in the circular pitch error on the tool, the tooth profile, and so on;

2) Inadequate finish of the side surfaces of the teeth of the broach correspondingly gives poor machining finish on the part;

3) During heat treatment the surface layer of the broach material is decarburized which leads to reduced strength of the broach;

4) After heat treatment the tool diameter varies within the limits of ± 0.03 mm.

In checking out the method of manufacturing the small-module gears with an inside tooth by a broach and seeing that it does not permit the required machining finish of the teeth, the decision was made to burn the inside teeth on an electroerosion tool. Initially the electrode tool was made of L62 brass, but an electrode made of this material has high relative wear and does not provide the required accuracy and finish. Therefore, type EEG graphite , which has a low relative wear, was taken as the material for the electrode tool.

The structural design of this tool appears in Figure 3. The electrode tooth is seated on the metal arbor 1. Teeth with a 0.2 mm module are threaded on the electrode. The electrode is sharpened to the required diameter and the teeth are cut in it jointly with the metal arbor.

During the process of burning out the teeth, the electrode suffers some wear which leads to an increase in area of the electrode contact with the product. In this case the current density per unit area decreases which leads to a sharp reduction in the productivity of the machining. In order to elminiate the given phenomenon it is necessary to shear the electrode, that is, cut its worn part off which leads to a decrease in the contact area of the electrode with the product, insures a stable machining process and cuts the labor of manufacturing the gear in half.

The advantage of the method of burning the gears on the electroerosion tool by comparison with the method of manufacturing the teeth by broaching consists in the fact that the accuracy of the gears and the tooth machining finish are improved. In addition, hardening of the tooth surface by about 10-15 percent takes place.

The ready-made small-module gears are monitored on a large projector by the method of comparing the tooth profile with the profile drawn on a magnified scale on paper. The given method permits checking the error of the circular pitch, the tooth profile, and so on.

N74-33990

UDC 629.785

PROCESS OF MANUFACTURING GRIDS FROM WIRE LESS THAN 0.025 MM IN DIAMETER BY THE GALVANIC GROWTH METHOD

[by V. A. Tsyshnatiy, N. F. Yedlichko, A. A. Yemel'yanov, L. M. Frolova]

[Text] The process of manufacturing grids, the peculiarities of the structural design, the fittings, the requirements on the tools and work area are discussed. There are 2 illustrations.

The grids are structurally executed in a circle with an L-type cross section. The diameter of the circle is 86 mm; the height is 2.5 mm; the width is 3 mm. Two layers of wire are wound at an angle of 90 degrees on the ring. The wire is tungsten-rhenium wire 15 microns in diameter with a winding pitch of 1 ± 0.1 mm. The monolithic nature of the grid is achieved by galvanic growth of nickel over the entire surface of the ring and the grid. In order to insure the necessary strength, the thickness of the coating must be no less than 0.5 diameters of the wire. The process of manufacturing the grid comprises the manufacture of the rings, the windings, the galvanic growth and checking the finished products.

The preparation of the rings reduces to their dressing and grinding under load until a smooth dull surface is obtained. The magnitude of the weight is selected experimentally. For the given rings the weight is 150-200 grams.

The ground rings are coated with nickel. The nickel coating process comprises degreasing, pickling, coating with nickel hydrocloride, copper and repeated coating with nickel sulfate.

The degreasing is done in an electrolytic degreasing bath for 15 minutes at an electrolyte temperature of 60-70° C and a current density of 5-10 amps/dm^2. Then the rings are washed in hot and cold water and pickled in a 10 percent solution of hydrochloric acid for 5-10 seconds.

After pickling the rings are washed in cold water. Then they are placed in a nickel hydrochloride bath. The charging is done without current with a delay of 45-60 seconds. Then a current with a density of 8-10 amps/dm^2 is included. The process lasts 10 minutes at a temperature of 18-23° C. On completion of

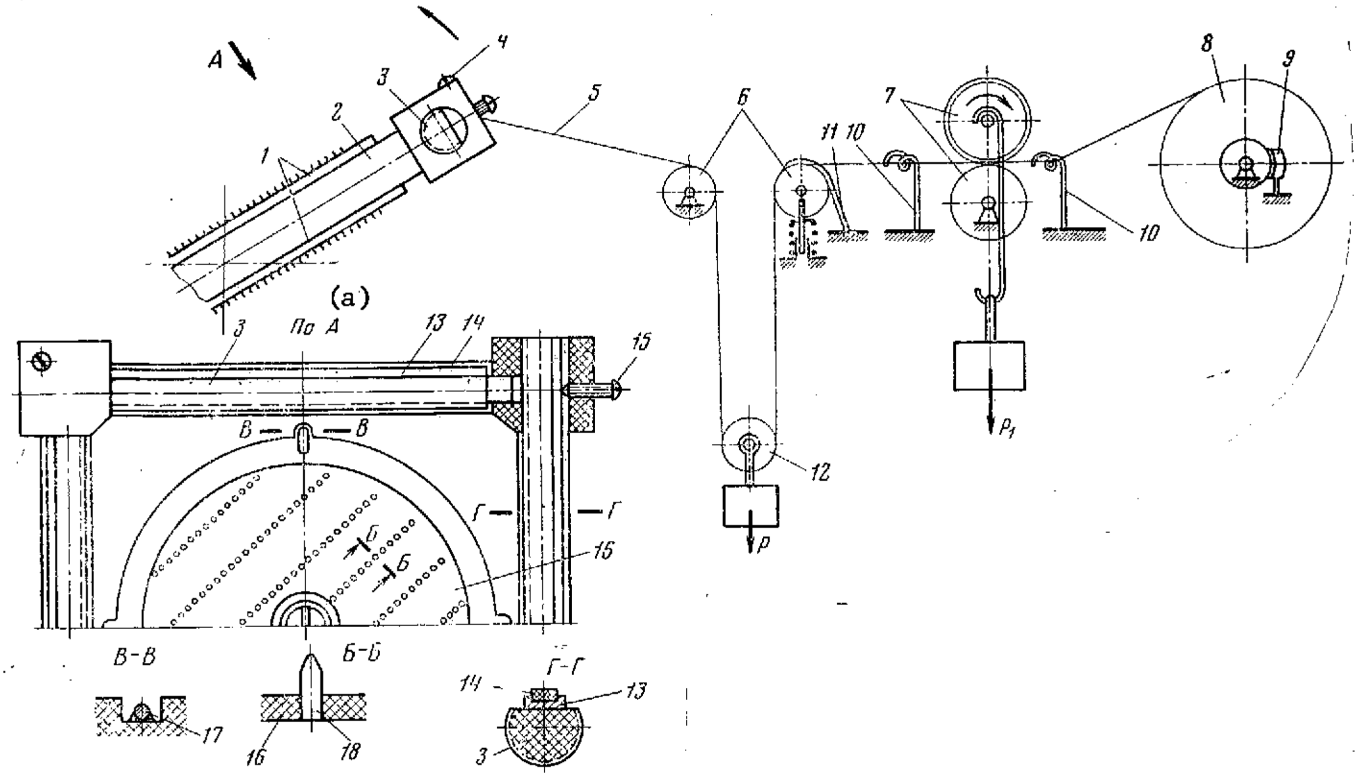

Figure 1. Attachment for winding a grid from wire less than 0.025 mm in diameter. 1 -- ring; 2 -- attachment; 3 -- screw for setting the winding pitch; 4 -- screw for attaching the wire; 5 -- wire; 6 -- guide rolls; 7 -- feed rolls; 8 -- coil with wire; 9 -- coil brake; 10 -- guides; 11 -- damper; 12 -- weighted roll; 13 -- tire; 14 -- packing;15 -- contact screw; 16 -- insert; 17 -- wire; 18 -- pins.

Key: a. section through A

the process the rings are quickly transferred to the bath with tap water and after washing they are placed in the nickel sulfate bath. The charging is done quickly under current. The current density in the bath is 0.3-0.5 amps/dm^2 at a temperature of 18-23° C with holding 1.5 hours.

Then the rings are again washed and loaded in the bath of copper sulfate for 40 minutes. The current density during copper plating is 1 amp/dm^2, and the temperature is 18-23° C. After copper plating, the nickel sulfate process is repeated along with washing in cold and hot water.

On completion of the coating, the quality control check is run on the coating. Before winding, the rings must again be rubbed with M20 powder to obtain a uniform dull surface. The removal of the coating to the copper is not permitted.

For the winding a lathe with center height 200-250 mm is used. Before winding the operating zone of the lathe (its levers, flywheels, boss, tool and attachment) are degreased by B-70 gasoline, and they are dried by a towel with alcohol. The tool is adjusted to the required pitch; the attachment is attached to the lathe centers, and a coil with wire and a special tension device are installed in the cutting tool holder (Figure 1). The tension is determined for each wire diameter and it is made equal to 0.45-0.7 Q_B where Q_B is the rupture strength. For wire less than 20 microns in diameter, the tensile strength is 0.6-0.7 Q_B. The weight for the tension on the wire must be selected with an accuracy to 20 percent.

In order to decrease parting during winding the wire must be force fed, and the coil with the wire must be braked. All of the fluctuations in the weight during winding are damped. For observation of the required pitch during winding on the attachment there must be provision for devices of the groove type in which the wires are laid. These devices prevent displacement of the wound wire in the galvanic baths The width of the groove or the radius of the cutting depression must be no more than 4-6 wire diameters. With long length of the wire span and small wire diameter (less than 20 microns) the attachment is executed with an insert 16 (see Figure 1). The wire is laid between the pins which hold it from displacement in the galvanic baths. This is especially important for low tension.

The device for holding the wire (the screws, inserts, and so on) must be movable in the direction of their axes: they are used to adjust the attachment for winding for laying the wire with respect to pitch.

When installing the attachment on the machine tool for doing the winding, the first row must be correctly oriented. It must be wound in the direction of the wire 17 (see Figure 1) as a result of which the ring acquires a bend (Figure 2). The bend in the ring is necessary to insure complete adjacency of the second series of wire to the first. The ends of the winding are attached into the screws 4 (see Figure 1) of the attachment, and they are further glued using polystrene glue.

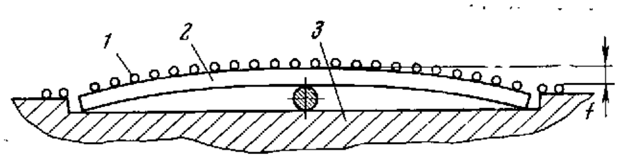

Figure 2. Schematic of the ring deformation under the effect of tension during winding of the wire. 1 -- wound wire; 2 -- ring; 3 -- attachment.

For winding the second row, the attachment is rotated in the plane of a frame by 90 degrees and again is placed in the lathe centers. The second row of the winding is made on top of the first. During winding maximum care must be exercised since in the case of a break the entire wound wire is lost. The presence of oil and grease on the surface of the rings and the grid is not permitted. The grid field must be clean, and no violation of the pitch is permitted. After winding the attachment is removed, the quality of the winding is checked visually, and the contact wire is connected. Then the wound attachments undergo electrochemical degreasing at a temperature of 60° C and with a current density of 5-10 amps/dm^2. After degreasing the attachment is cooled in water to a temperature of 30-40° C and it is washed in cold water. Then the attachment is placed for pickling in a bath with the following composition: chemically pure hydrochloric acid -- nine parts by weight; chemically pure nitric acid -- one part by weight.

The pickling proceeds for 30-60 seconds at a temperature of 18-23° C. On completion of pickling the attachment is washed in tap water and is placed without current in the nickel hydrochloride bath where it is held for 50 seconds, then the current with a density of 5-10 amps/dm^2 is included at room temperature. The coating must have an even light gray color. On completion of the coating in the nickel hydrochloride the attachment is quickly washed in cold tap water and it is loaded in the nickel sulfate bath. The duration of the growth process depends on the thickness of the coating and proceeds at a rate of about 5 microns/hour at a temperature of 18-25° C with a current density of 0.3-0.5 amps/dm^2. On completion of growth, the attachment is washed in cold and hot water and dried.

After cutting out the grid along the outer perimeter of the ring the grid is dehydrogenated at a temperature of 200-250° C for two hours. On completion of manufacture the coating quality and the size of the openings considering the coating are checked on the finished grid.

N74-33991

UDC 666.1.056:537.533.3

METHOD OF APPLYING A MIRROR REFLECTING LAYER TO INSTRUMENT PARTS

[by L. G. Alkhanov, I. A. Danilova, G. V. Delektorskiy]

[Text] A method follows for applying a mirror reflecting layer to the surfaces of parts, instruments, apparatus, and so on. A brief analysis is presented of the existing methods of obtaining the mirror surface. The advantages of the new method of obtaining the mirror surface and the range of its application are indicated. There is 1 illustration.

Many parts of modern machines, apparatus and instruments have complex shapes, high machining finish and an aesthetic appearance. The manufacture of such parts by machining on machine tools is in a number of cases either impossible or labor consuming and expensive. Especially great difficulties occur when manufacturing parts of spherical and parabolic shape and of the prism type with a mirror surface requiring grinding, finishing, polishing and the application of the mirror layer to the surface.

In such cases a polymer comes to our assistance. From the polymer, in the form of castings it is possible to obtain any type of billet and parts of complex configuration, but it is impossible to obtain a high quality mirror surface. The best known methods of applying the mirror layer to the surface include the surface machining to a finish of $\nabla 10$-$\nabla 14$ and then application of the mirror layer to it by deposition of aluminum, sulfur or other metals in a vacuum or by one of the chemical and galvanic methods with subsequent protection of the mirror surface.

The deficiencies of these procedures for the application of the mirror surface include the following:

a) Great labor consumption of machining under the mirror coating of complex outer and especially inner surfaces;

b) The necessity of machining to a high class of surface finish for each coated part;

c) The necessity for painting the surface of the deposited layer;

d) a high percentage of rejected parts made of brittle materials.

In order to eliminate the indicated deficiencies, a method has been developed for the application of the mirror layer not to the part, the surface of which is to be coated, but to an intermediate model which is a reverse copy of the coated part with the necessary linear and angular dimensions and considering the shrinkage factor of the polymer within the limits from 0.5 to 2 percent.

In order to apply the mirror layer, the surface of the model is machined with a finish of no less than ∇10. A mirror layer is applied to the surface of the model by chemical or other deposition of aluminum or silver. The model is made of organic glass.

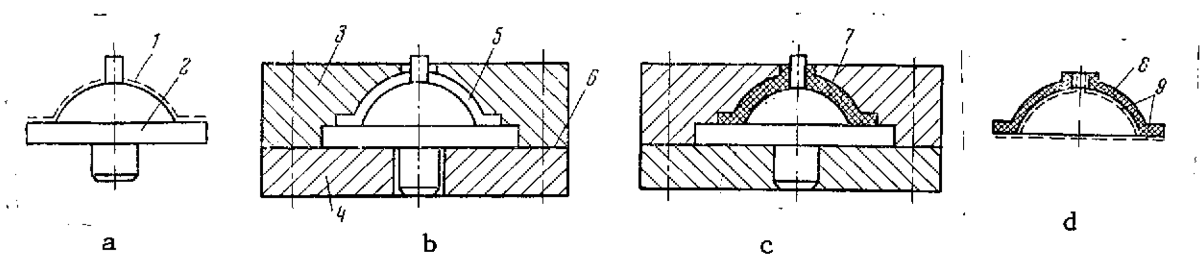

Schematic of the manufacture and the casting of parts in a metal die pressure cast mold. 1 -- deposited mirror layer; 2 -- standard model with push rod; 3 -- upper plate; 4 -- lower plate; 5 -- filled cavity; 6 -- parting plane of the mold; 7 -- mold with filled cavity; 8 -- part with transferred mirror surface; 9 -- mirror surface transferred to the part.

The model with the mirror layer is put in the metal die pressure cast mold and filled with epoxy. After pouring and polymerization of the compound, the part formed is extracted together with the model from the mold and as a result of the fact that the adhesion between the compound and the mirror layer is higher than the adhesion between the mirror layer and the model, the mirror layer remains on the part, and the model is removed. The model can be used more than once.

Advantages of New Procedure

1. The necessity drops out for processing each coated part to a high finish and accuracy class.

2. The labor consumption operation with respect to machining and finishing the complex outer and especially inner surfaces drops out.

3. There is no varnishing or painting.

4. The precision of the parts made of epoxy compound instead of glass and their vibration resistance are increased.

5. The weight of the parts and assemblies of the instruments and machines is reduced.

6. The coefficient of the technical level of the production technology is increased.

Pressure Die Cast Molds for Obtaining Parts with a Mirror Surface by the Transfer Method

Obtaining parts with exact dimensions and high surface finish by the pouring method depends above all on the quality of execution of the forming surfaces of the pressure die case mold.

The pressure die case mold used to manufacture parts applying the method of transferring the mirror surface must be manufactured very carefully. The dimensions of the working cavity of the mold are made considering the shrinkage of the poured material. The surface finish of the operating cavity of the mold must be quite high since it determines the finish of the surface of the manufactured part. The special design of the mold must be such that it can easily be assembled, dismantled and the model extracted from it. Here, the mold and the model dimensions must not be harmed.

The pressure die case molds can be manufactured not only from metal with subsequent chrome plating but also from other materials. The method of manufacturing the molds depends on the material from which it is made. For small series parts it is expedient to manufacture the pressure die cast molds from inexpensive material which is easily machined. In this case no great strength of the pressure die cast mold is required since it does not serve long. It is possible to manufacture such a pressure die cast mold from organic glass and polyvinyl fluoride (in individual cases manufacture from gypsum and plastiline is permitted). In order to manufacture such molds little time is required, and the pressure die cast mold is found to be cheap and available for manufacture in experimental production.

The standard model is made in accordance with the executed dimensions of the required part. In one way or another aluminum or silver (see figure, a) is applied to the surface. The model is installed on the lower plate 4; it is covered with the upper plate 3 (see figure, b) and the epoxy compound is poured into the cavity 5 (see the figure, c) after which it is held for no less than 12-16 hours for polymerization of the compounds. After removal from the mold the part with the transferred mirror surface is obtained (see the figure, d). The forming surfaces of the mold are covered with antiadhesive compound, for example, paraffin or a lubricant of the TsIATIM type for easier removal of the parts in the mold. In the molds made of polyvinyl fluoride or organic glass the forming surfaces are not covered since these materials do not adhere to epoxy resins.

In order to manufacture the cast parts, the epoxy resin or epoxy compound (types ED-5, ED-6, K-115, K-156, and so on) is selected depending on the structural design and the purpose of the parts.

Requirements Imposed on the Compounds and the Coated Surface

The technical requirements imposed on the compounds arise from their purpose.

The poured compounds must have the corresponding viscosity insuring good filling of the pressure die cast mold, mechanical strength in the polymerized state corresponding to the possible static and dynamic loads under operating conditions, low water absorption and waterproofness, high electric strength and specific volumetric resistance, stability of the electrical characteristics under operating conditions, thermal stability with cyclic variation of the temperatures and a low coefficient of linear expansion of the insulated material.

In order to lower the mechanical stress in the compound a filler is introduced. The fillers have a great effect on many of the physical-mechanical and electrical properties of the compounds and promote a reduction in their cost. By using a filler, depending on its type and amount, it is possible to increase the thermal conductivity of the epoxy compound, decrease the shrinkage and increase the mechanical strength. Among fillers it is possible to use powdered quartz sand, porcelain dust, aluminum oxide, fired talc, titanium dioxide, and Portland cement. In individual cases, depending on the purpose of the compound and the requirements imposed on it, powdered aluminum, bronze or brass powder, graphite and other materials are used as the filler. The introduction of the fillers unavoidably causes an increase in viscosity of the compound complicating its use. In order to reduce the viscosity and observe the technological process of the application, such compounds must be used in the heated state, especially in cases where the heating does not cause accelerated hardening. Pouring is the basic operation of realizing cast insulation from epoxy compound. The formation of a continuous insulating shell of the compound requires special equipment in the form of a split mold in which the part is attached and acquires its final shape and also the special technological process equipment.

In connection with the high adhesive properties characteristic of the epoxy compounds, the surface of the mold must be protected by the so-called separating or antiadhesion layer of material excluding adhesion to the epoxy compound. As the separating layer protecting the inside surface of the mold from adhesion to the compound, the TsIATIM type lubricants can be used. The applied lubricant stays on through five molding processes. In especially precision parts, it is necessary to check the lubricant after each removal.

The structural design of the mold has a great deal of effect on the quality of the product. When planning and designing the mold it is necessary to consider that it must be freely filled with compound, easily removed after hardening and provide for the possibility of removing the gas released from the compound without permitting it to accumulate under any of the parts of the mold in contact with the compound. The mold must permit free shrinkage of the compound during its congealing.

The surface of the part to which the mirror layer is to be applied is not subjected to special machining. The model with the applied layer is installed so that the mirror surface will be in the necessary position and the correct place. The process of the transfer of the mirror layer is technologically simple.

The deposited mirror layer does not exceed several angstroms, and it is not subject to control by an ordinary measuring instrument. The deposited layer is examined by transillumination visually. The presence of spots or holes seeming at first glance to be insignificant is clearly outlined on the transferred surface which is also a defect in the mirror surface. In order to avoid rejects it is necessary carefully to examine the deposited layer using a magnifying glass in doubtful cases.

Region of Application

The method of transferring the mirror surface can be applied in prisms with internal reflection in which the application of the mirror layer by the procedures known in practice is impossible, in marine lighting units, beacons, onboard devices, all types of lighting units and instruments for motor vehicle transportation and optical-mechanical devices. The products made from the epoxy compounds have increased shock and vibration resistance, and the application of a mirror layer to them by the transfer method simplifies the process of preparing the optical and reflecting surfaces of complex shape. The weight of the product is decreased significantly.

The deficiencies of the parts made of epoxy compounds must include comparatively low operating temperature range.

N74-33992

UDC 535.885.002

PROCESS FOR MANUFACTURING SLIT COLLIMATORS

[by V. P. Romanenko, A. A. Yemel'yanov, K. I. Churbakov]

[Text] Peculiarities are described of the manufacturing process and the control of elements of slit collimators, the structural design of the required equipment and the process or assembling the collimators. There are 3 illustrations.

The process of manufacturing the collimator includes the following operations:

1) The cutting of the billets out of steel t = 0.08 mm;

2) The bending or forming of the billets in a special die;

3) The assembly of the formed billets into packets and installing the packets in the collimator housing;

4) Checking the accuracy of formation of the shape of the honeycomb openings and the overall dimensions of the collimator;

5) Fixing the assembled and checked packets in the collimator housing using glue (compound);

6) Checking the fastening.

Part of these operations have some characteristic features. Thus, when cutting out the billets it is necessary to see that the direction of rolling of the material does not coincide with the direction of the longitudinal cut. When bending the plate must have two sides based against the base sides of the die (Figure 1); here the direction of rolling must be compared with the direction of bending the cells.

The packet is assembled from the molded plates by the method of laying one plate on another; here, the molded sides of the plates are arranged in mirror position relative to each other.

The collimator is assembled on frosted glass with illumination from below (Figure 2). When assembling the packet of plates it is necessary to see that

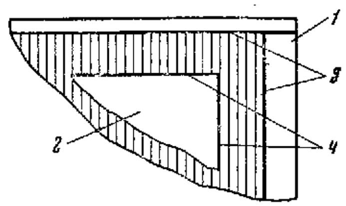

Figure 1. Basing of the billet. 1 -- die; 2 -- plate; 3 -- base sides of the die; 4 -- base sides of the plate.

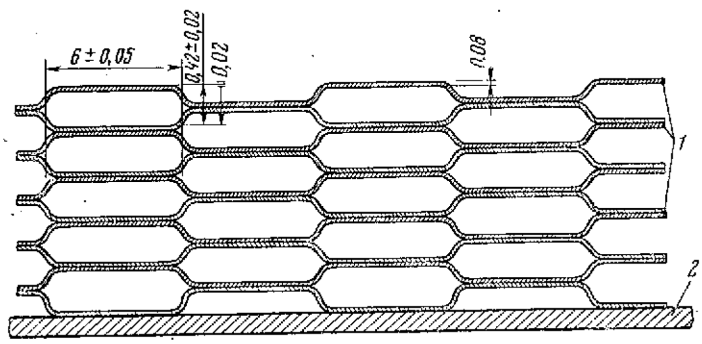

Figure 2. Assembly diagram of the collimator. 1 -- collimator plates; 2 -- wall.

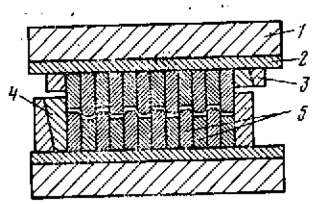

Figure 3. Transverse section of the flexible die. 1 -- plate; 2 -- insert; 3 -- clamp; 4 -- wedge; 5 -- plates.

displacements of the plates relative to each other do not take place, and the light cells are correctly formed. The coincidence of the plates can be controlled by means of a magnifying glass.

The assembled collimator packet is fixed (filled) from the ends by epoxy compound which prevents these plates from possible shift relative to each other. After fixing the plates the collimator is subject to drying in a thermal chamber.

The possibility of obtaining high-quality plates was solved after the application of the combination die which is shown in Figure 3.

The die plates are brought to the required size by individual fitting; then they are attached in a clamp by means of the wedge. The guides in the given die are the wedges and the strip of the lower plate.

When manufacturing the collimator plates from parts and billets, no traces of corrosion, scab, fracture, galling, the presence of nonmetallic inclusions, and so on are permitted.

The quality of the collimator is checked by means of the all-purpose UIM23 microscope.

N74-33993

UDC 621.3.001.4

CONTROL, QUALITY AND RELIABILITY

METHOD OF BOUNDARY TESTING OF THE ELECTRIC CIRCUITS AND ITS APPLICATION FOR CALCULATING ELECTRIC TOLERANCES

[by N. P. Red'kina]

[Text]A study of the method of boundary testing of electric circuits including the preliminary and the limiting test is made. Preliminary tests permit determination of the critical parameters causing the greatest deviation of the output parameter of the system. The boundary tests offer the possibility of determining the limits of the fitness of the system with simultaneous variation of its critical parameters. There are 3 illustrations.

The basic cause of the failure of the equipment is the irreversible changes taking place in the system elements as a result of which changes occur in the output parameters of the system, that is, they go beyond the limits of the technical specifications. The irreversible changes take place under the effect of the temperature, moisture, vacuum, radiation, aging and other factors.

In order to achieve the given reliability it is necessary when doing the design calculations to estimate the effect of one factor or another on the output parameters of the circuits. Beginning with the operating conditions, tolerances can be calculated for the output parameters of the systems with respect to all operating conditions (external environment, continuous operating time).

During the production process the possibilities for achieving the given reliability are expanded thanks to the experimental operations. The boundary tests on the mockups permit the calculated assumptions to be checked, and in the case of their lack of correspondence to the technical specifications, performance of the necessary finish operations on the circuits.

Laboratory tests on specific models do not offer the possibility of fully determining the quality of the equipment if they do not include the reliability tests. During the laboratory tests, it is not the aging of the elements or the effect of the variations of their parameters on the output parameters of the circuit that are considered. Neglecting these variations leads to the fact that the products can have low reliability.

Different steps in the development of the products correspond to defined methods of solving the reliability problems. In the early stages of development, the calculation of the electrical tolerances of the circuits and the boundary tests on the mockups are most effective.

In the given paper one of the methods of boundary testing is presented. Its purpose is to determine the limits of proper operation of the circuit for simultaneous variation of the parameters of the circuit elements. By using the boundary test method it is possible qualitatively to evaluate the limits of operation of the circuit with simultaneous variation of its element parameters.

The boundary values of the output parameters of the circuit must be less than the limiting values of the parameters determined by the calculated tolerances on these parameters, and the calculated tolerance, in turn, can be less than or equal to the tolerance assigned by the technical specifications:

$$\Delta N_{bound} < \Delta N_{calc} < \Delta N_{TS},$$

where ΔN_{bound} is the tolerance on the output parameter according to the boundary test data; ΔN_{calc} is the calculated tolerance; ΔN_{TS} is the tolerance with respect to technical specifications.

The boundary test method can be divided into two steps: 1) preliminary testing; 2) boundary testing.

Before proceeding to the tests, it is necessary for each circuit to establish the failure criterion which is determined by the output parameter of this circuit (there can be several output parameters). The most critical output parameters of the circuit are selected for the tests. The failure criterion is established beginning with the technical specifications for the product. After determining the failure criterion for the tests from all of the circuit elements, the most critical are selected, the variations of which have the greatest effect on the output parameter of the system.

After selecting the failure criterion and the critical parameters it is possible to proceed with preliminary testing. The purpose of these tests is to find the dependence of the output parameter of the circuit on each of the critical parameters:

$$y = f(x_i) \qquad (i = 1, 2, \ldots, n),$$

where y is the output parameter of the circuit; x_i is the critical parameter of the circuit.

In order to find $f(x_i)$, the critical elements of the circuit age artificially within the limits of the calculated tolerances which are defined in the following way:

$$\Delta x_i = \Delta x_{i_T} + \Delta x_{i_{cT}} + \Delta x_{i_B} + \dots,$$

where Δx_{i_T} is the tolerance on the temperature effect; $\Delta x_{i_{cT}}$ is the aging tolerance; Δ_{i_B} is the tolerance on the vacuum effect.

The taking of the functions $f(x_i)$ occurs for the rated values of all the remaining elements of the circuit.

The relations obtained are depicted on one graph which offers the possibility of quantitative evaluation of the degree of the effect of one element or another on the circuit and also determination of the unfavorable combinations of input parameters. It is especially important to establish the unfavorable combinations in cases where the direction of variation of the rated value of the element parameter under the effect of various disturbing factors is unknown.

Example

For an amplifier depicted in Figure 1, the amplification coefficient K was taken as the output parameter of the tests. The failure criterion $\Delta K_{bound} \leq$ $\leq \Delta K_{TS}$ where $\Delta K_{TS} = \pm 10$ percent is the tolerance given by the technical specifications.

The critical parameters in the given case are the resistances of the resistors R1, R2, R3, R4, R5, R6, R7.

The functions $f(R_i)$ are depicted in the graph (Figure 2). From the graph it follows that the elements R2, R3, R5 and R7 which are the most critical for this circuit have the greatest effect on the amplification coefficient.

The generalized graph (see Figure 2) was used to determine the unfavorable combinations of critical input parameters of the circuit. From this graph it is obvious that the unfavorable combinations are the following:

A simultaneous decrease in R5 and an increase in R7 from their rated values;

Simultaneous increase in R5 and decrease in R7 from the their rated values.

The boundary tests were made by the parameters which by the results of the preliminary tests turned out to be the most critical. Before proceeding to the tests, it is necessary to select the step size of the variation of Δx_i

C-2

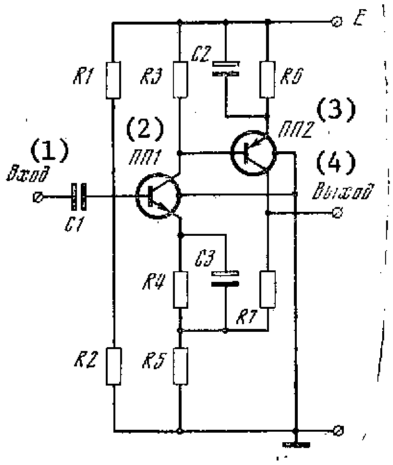

Figure 1. Amplifier circuit

Key: 1. input 3. PP2
2. PP1 4. output

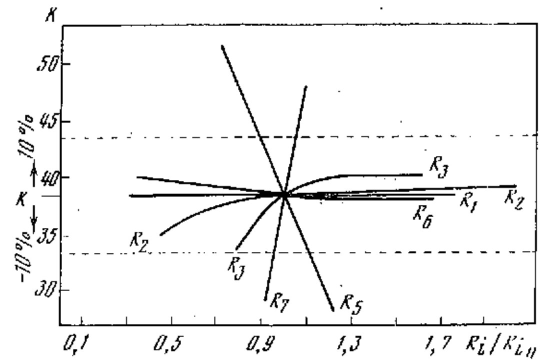

Figure 2. Generalized graph of the amplification coefficient as a function of the drift of the resistance of the resistors.

of the investigated parameters x_i. The relative rate of the physical-chemical processes in the elements which in the final analysis lead to variation of the magnitude of the parameter of this element must be identical for the elements of a defined type. Consequently, if in the circuit, for example, resistors of one type are used, then the test step size is taken equal to $\pm\Delta R_i/R_{i\ rated} = \text{const}$.

After selecting the test step size it is possible to proceed to the boundary tests. Simultaneously m critical parameters vary in the circuit with the selected step size $\Delta x_i/x_{i\ rated} = \text{const}$ for a defined type of element. The variation takes place from the rated values of the input parameters to those values for which failure of the circuit takes place in accordance with the failure criterion. The variation in values of the critical parameters takes place in the direction of unfavorable combinations. After each test step the output parameter is measured.

The results of the boundary tests are processed in the following way. The region of possible operation is constructed. The values of the output parameter of the circuit are plotted on the y-axis, and the relative variation of the input parameters of the circuit taken with respect to absolute magnitude (the test step size) is plotted on the x-axis.

Example

For the amplifier (see Figure 1) the test step size for the critical parameters R2, R3, R5 and R7 was selected equal to one percent. In Figure 3 we have the amplification coefficient as a function of the parameters R2, R3, R5 and R7 for their simultaneous variation with a step size of one percent in the direction of unfavorable combinations. Here N is the operating point, AB is the operating section of the circuit. If the point N is within the limits of the section AB, then the output parameter corresponds to the technical specifications. The emergence of the point N beyond the limits of the section AB corresponds to failure of the circuit. From the graph depicted in Figure 3 it is obvious that the maximum possible simultaneous drift of the resistances R2, R3, R5 and R7 must not exceed ± 5 percent.

The calculation of the electrical tolerances on the critical parameters demonstrated that as a result of the effect of temperature and aging of the resistance on the circuit, the parameters vary by ± 8 percent. According to the experimental curve obtained (see Figure 3) the drift $\Delta R_i/R_{i\ rated} = \pm 8$ percent causes deviation of the amplification coefficient $\Delta K = \pm 15$ percent which contradicts the technical specifications according to which this deviation must not exceed ± 10 percent.

The results of the boundary tests can be widely used for calculating the reliability: with their help it is possible to calculate the electric tolerances and gradual failures and to construct the mathematical models.

Example

Let us consider how by using the boundary tests it is possible to calculate the tolerances on the electric parameters of the circuit as a result of their drift under the effect of temperature and aging.

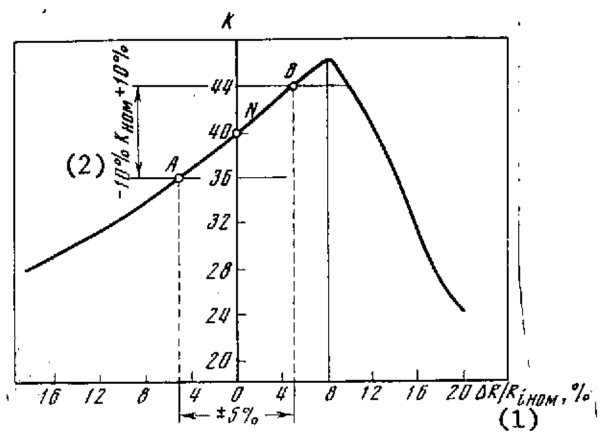

Figure 3. Amplification coefficient as a function of the resistance drift (the fitness reserve for drift of the resistanc equal to ± 5 percent).

Key: 1. $R_{i\ rated}$, % 2. K_{rated}

The output parameter of the circuit is represented in the form of the expansion in a Taylor series

$$y = y_0 + \frac{\partial f}{\partial x_1}\Delta x_1 + \frac{\partial f}{\partial x_2}\Delta x_2 + \dots + \frac{\partial f}{\partial x_n}\Delta x_n$$
$$(n = 1, 2, 3, \dots),$$

where x_i are the investigated input parameters of the circuit.

The tolerance on the output parameter of the circuit will be expressed by the formula

$$\Delta y = \frac{\partial f}{\partial x_1}\Delta x_1 + \frac{\partial f}{\partial x_2}\Delta x_2 + \dots + \frac{\partial f}{\partial x_3}\Delta x_3.$$

The partial derivatives df/dx_i ($i = 1, 2, \dots, n$) are defined from the system of n linear equations

$$\begin{aligned}
\Delta y_1 &= \frac{\partial f}{\partial x_1}\Delta x_{11} + \frac{\partial f}{\partial x_2}\Delta x_{12} + \dots + \frac{\partial f}{\partial x_n}\Delta x_{1n}, \\
\Delta y_2 &= \frac{\partial f}{\partial x_1}\Delta x_{21} + \frac{\partial f}{\partial x_2}\Delta x_{22} + \dots + \frac{\partial f}{\partial x_n}\Delta x_{2n}, \\
&\dots\dots\dots\dots\dots\dots\dots\dots\dots \\
\Delta y_n &= \frac{\partial f}{\partial x_1}\Delta x_{n1} + \frac{\partial f}{\partial x_2}\Delta x_{n2} + \dots + \frac{\partial f}{\partial x_n}\Delta x_{nn}.
\end{aligned}$$

The values of Δy_i and Δx_i have been obtained by the method of boundary tests.

For an amplifier (see Figure 1) the following partial derivatives were found by the results of the boundary tests:

$$\frac{\partial f}{\partial R2} = 0{,}3 \cdot 10^{-3}; \quad \frac{\partial f}{\partial R3} = 0{,}35 \cdot 10^{-2};$$
$$\frac{\partial f}{\partial R5} = -0{,}35; \quad \frac{\partial f}{\partial R7} = 0{,}0226.$$

Consideration of the temperature effects when calculating the electrical tolerances of the circuit reduces to the determination of the maximum possible drift of the output parameter as a result of variation of the parameters of the elements in the temperature range given by the technical specifications in which this circuit must operate. For linear variations of the parameters of the circuit elements under the effect of temperature the magnitude of the deviation Δx_i of the parameter from its rated value $x_{i\ \mathrm{rated}}$ is:

$$\Delta x_i = x_{i\,\text{ном}}\alpha_T \Delta T,$$
(1)

Key: 1. $x_{i\ \mathrm{rated}}$

where α_T is the temperature coefficient; ΔT is the deviation of the temperature from rated.

The equation of the temperature error has the form

$$(\Delta y)_T = \left(\sum_{i=1}^{n} \frac{\partial f}{\partial x_i} x_{i\text{ном}} \alpha_T \right) \Delta T.$$

For operation of the instrument during its operation time the circuit elements change their parameters as a result of aging. The operating conditions (electric loads) and external environment (temperature, moisture) have a significant effect on the aging rate.

The tolerances on the parameters of the elements are calculated in the following way:

$$\Delta x_i = x_{i\text{ном}} \alpha_t \Delta t,$$

where α_i is the aging coefficient; t is the time of continuous operation of the product given by the technical specifications.

The formula for calculating the tolerance on the output parameter has the form

$$(\Delta y)_t = \sum_{i=1}^{n} \frac{\partial f}{\partial x_i} x_{i\text{ном}} \alpha_t \Delta t.$$

Example

For resistors of the MLT type the temperature coefficient per 1° C is $\pm 0.7 \cdot 10^{-3}$ in the temperature range from +25° C to the limiting operating temperature (+120° C) and $\pm 1.2 \cdot 10^{-3}$ in the temperature range from -60 to +25° C.

According to the technical specifications for the product in which the amplifier is used (see Figure 1), the temperature is given by the range from -10 to +50° C.

The calculation of the tolerance on the output parameter is defined by the formula

$$\underset{(1)}{\left(\frac{\Delta K}{K_{\text{ном}}} \right)_T} = \frac{1}{K_{\text{ном}}} \left(\sum_{i=1}^{n} \frac{\partial f}{\partial R_i} R_{i\text{ном}} \right) \alpha_T \Delta T \quad (i = 2,3,5,7) \; (2)$$

Key: 1. K_{rated} 2. $R_{i \text{ rated}}$

We obtain: $K/K_{\text{rated}} = \pm 4.6$ percent.

The time of continuous operation of the product is 2,000 hours. During this period (according to the reference data) the MLT type resistor changes its value by ±4 percent. Thus, the tolerance for aging calculated by the formula

$$\left(\frac{\Delta K}{K_{\text{ном}}}\right)_i = \frac{1}{K_{\text{ном}}}\left(\sum_{i=1}^{n} \frac{\partial f}{\partial R_i} R_{i\,\text{ном}}\right)\frac{\alpha_i t}{100},$$

will be

$$\Delta K/K_{\text{ном}} = \pm 10{,}6\,\%.$$

Thus, the total tolerance on the temperature and aging is $\pm$15.2 percent. According to the technical specifications the tolerance will be $\pm$10 percent. Consequently, the schematic of the amplifier does not correspond to the technical requirements on the product by the results of the preliminary tests.

The boundary tests on the mockups are one of the experimental methods of investigating reliability which permits evaluation of the reliability of the developed product in the drawing stage. This offers the possibility of the needed improvement of the product to improve its reliability. The method of boundary tests permits consideration of the effect of the simultaneous drift of the circuit parameters on its operation. By varying the input parameters by amounts corresponding to the drifts as a result of the temperature, aging and other disturbing factors it is possible to simulate any disturbing effect on the circuit, performing experiments under normal conditions.

N74-33994

UDC 621.396

MONITORING THE PRESENCE OF FOREIGN BODIES IN THE EQUIPMENT

[by A. V. Breslavets, N. I. Bavykin]

[Text]A study of the methods of monitoring the presence of foreign bodies in radio electronic equipment is made. Descriptions follow of the structural design under the operating principle of the device for detecting foreign bodies weighing to 0.0026 grams. There is 1 illustration.

A reduction in the labor consumption when manufacturing the equipment, improving the quality and the operating reliability are provided not only by the quality of the structural development, the reliability of the electrical elements making up the product, the introduction of progressive and highly stable technological manufacturing processes but also the quality and objectivity of performing the testing and control operations.

For quality control of electronic equipment a great deal of attention is given to the discovery and elimination of foreign bodies. They include pieces of the mounting conductors, insulation tape, tubes, splatters of solder, shavings, and so on.

The presence of a foreign body in a closed instrument can lead to the disturbance of its fitness during operation as a result of mechanical damage by this body of the functional nodes or the damage to the electric circuit. Therefore, the detection and removal of foreign bodies are realized in various stages of readiness of the instrument and especially after the final installation.

Recently a great deal of attention has been given to the development and introduction of new methods and means of control.

The widespread methods of detecting foreign bodies in instruments after final installation are visual and audio. In the visual method, a section-by-section inspection of the installation by the naked eye or through a magnifying glass with three-seven-fold magnification is performed. Listening is done in special "silence chambers." The presence of foreign objects is established by ear on collision of them with the case of the instrument. Here, the instrument is suspended on elastic threads or it is locked and rotated in the hands.

The mentioned techniques have a number of significant deficiencies:

The dependence of the quality of the control operation on the subjective factors -- the keenness of vision and hearing of the operator;

Low output capacity and labor consumption of the operation causing severe fatigue of the operator;

Low sensitivity since the objects weighing less than 0.5 grams are not perceived even by experienced controllers (operators);

Impossibility of control in parts of the instrument which are difficult to view;

Necessity for having a special technological "quiet room" insulated by soundproof materials.

At the present time at a number of enterprises a device has been developed, manufactured and introduced for the detection of foreign bodies of metallic and nonmetallic nature weighing to 0.0026 grams in devices closed by a case. The foreign bodies of less weight can be detected by a device with a probability not exceeding 50 percent.

The device (see the figure) is a welded bed 1, on which a sliding rectangular frame 2 made of steel tubing is fastened on the halfaxes. As the drive an ac 380 volt motor is used which turns the moving frame in the vertical plane with a speed of 30 rpm. Inside the moving frame on vacuum rubber stretch bands there is a flat frame 4 10 mm thick with holes for attaching the interchangeable attachments in which the instruments to be checked out are fastened. The pin 5 is connected to the flat frame which on rotation of the frame 2 relative to the bed 1 slides over a stationary cam 3 creating periodic oscillations of the suspended frame 4.

When the frame moves the foreign bodies are knocked against the case of the instrument which is recorded by a sensor emitting the corresponding signal. The sensor is a piezoceramic disc made of TsTS-19 lead zirconate-titanate.

The amplitude E of the alternating electric voltage of the sensor is proportional to the deformation of the element $\Delta\ell$ which, in turn, is proportional to the pressure created by the falling object:

$$E = g\Delta\ell,$$

where $g = 4\pi d/\varepsilon$ is the piezoconstant with respect to deformation; d is the piezoelectric modulus which depends on the form of the deformation; ε is dielectric constant.

The sensitivity of the piezoelectric converters in the reception mode is determined by the ratio d/ε (the absolute sensitivity) for the ratio $d/\sqrt{\varepsilon}$ (the specific sensitivity).

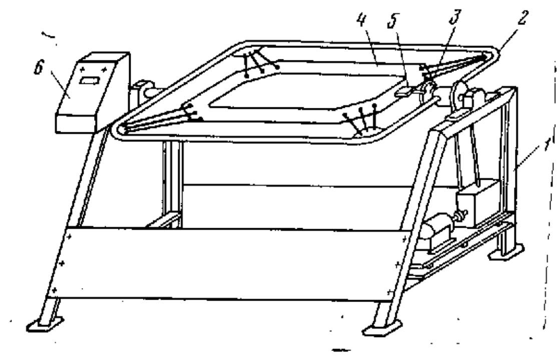

General view of the device for detecting foreign bodies in equipment. 1 -- bed; 2 -- moving frame; 3 -- cam; 4 -- suspended frame; 5 -- pin; 6 -- control unit.

It is possible to increase the sensitivity by applying higher quality materials. Out of all the industrial piezoceramics lead zirconate-titanate has the greatest sensitivity and has stability of its physical parameters.

The disc of the sensor is inserted in a rubber shock absorber which presses it against the case of the instrument. In the same case with the sensor is the piezoelectric signal amplifier. In order to insure reliable mounting connection of the piezoceramic disc with the amplifier on both sides of the disc a layer of copper is applied galvanically.

The signal from the amplifier through the connecting cable and the spring-loaded disc current pickups goes to the control unit 6 with a light signal. In order to prevent false response of the circuit, the signal is included on arrival of no less than 3 signals of a defined level from the amplifier of the sensor. On the front panel of the control unit a "reject" light comes on signaling the presence of a foreign body in the instrument. The control unit has a operation duration regulator. The maximum operating time of the device is 5 minutes.

The device is simple to manufacture and maintain, and its application increases the objectivity and productivity of the control operations.

The technical specifications of the device are as follows:

Admissible weight of the checked out instruments to 35 kg;

Maximum size of the checked out instruments 600 × 600 mm;

Overall dimensions of the device 1480 × 1120 × 1125 mm;

Minimum weight of the detectable objects 0,0026 grams;

Maximum continuous operating time 5 minutes;

Rotation rate of the moving frame 30 rpm.

N74-33995

UDC 621.382.3:629.7.018

OPTIMAL REGIME AND CONDITIONING TIME OF TRANSISTORS FOR EQUIPMENT WITH INCREASED RELIABILITY

[by A. V. Breslavets, V. N. Grigor'yev, E. I. Kuzyuta, E. M. Yampol'skaya]

[Text] It is shown that an economically justified choice of regime and conditioning time for transistors for equipment of increased reliability is impossible without analyzing the stabilization time of the transistor parameters. The optimal regime and conditioning time are well founded. A method is presented for evaluating the optimal conditioning time by the technical-economic indexes. There are 4 illustrations and 4 references.

Modern production of radioelectronic equipment is characterized by the creation of systems capable of performing various operations with respect to assembly, accumulation and processing of a large volume of information, transmitting it to a great distance, realization of automatic control, regulation and monitoring of the processes and objects as a whole. This expansion of the functional goals of a piece of equipment gives rise to continuous growth of its complexity and, as a consequence, an increase in the number of elements in it.

The sudden failure of even one element considering the increasing volume of the programs executed by the equipment can lead to failure of the entire system, interruption of expensive experiments or failure to fulfill the stated goals. Under modern conditions the "price" of failure of the equipment increases immeasurably and, consequently, it is necessary to use all measures to prevent the possibility of the occurrence of failures. This is why, along with the problems of constructing optimal electronic circuits there is the problem of increasing the reliability of the semiconductor devices which has become most widespread in the equipment for various purposes.

One of the important methods of increasing the reliability of semiconductor devices is, as is known, the technological conditioning of these instruments. The technological conditioning at the manufacturing plants of semiconductor instruments is carried out in order to cut down the breakin time in the failure density curve. The conditioning regime and duration in each special case are determined usually experimentally. Technological conditioning frequently stabilizes the parameters of the products, but it cannot guarantee their final establishment. As an example we have experimental data obtained at the consumer enterprise for checking out various types of low-power transistors. In Figure 1 we have the variation with time of the mean relative value of the amplification coefficient k for several lots (n = 100-200 pieces in each lot) of various types of transistors.

The coefficient k is defined for increased temperature in the static regime every 20 hours of continuous operation under a constant electric load. The operating regime of the transistors is established in accordance with the requirements of the technical specifications for them. After each 100 hours of continuous operation the transistors were switched off and held in the disconnected state for 200 hours.

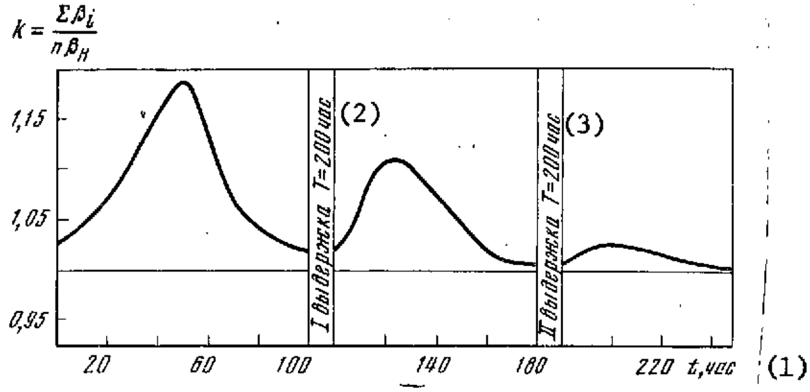

Figure 1. Variation of the mean relative value of the amplification coefficient of transistors $k = \Sigma\beta_i/n\beta_H$ as a function of the operating time in the static mode.

Key: 1. hours
2. first holding T = 200 hours
3. second holding T = 200 hours

The graph (see Figure 1) visually proves the necessity for conditioning the transistors before installing them.

The economically justified selection of the regime and conditioning time is impossible without analyzing the parameter stabilization period of the semiconductor devices.

The exponential law of the probability distribution of failfree operation widely used in reliability theory cannot be acceptable for analyzing the conditioning process. The existing opinion that conditioning promotes accelerated aging of radioelements is, in our opinion, erroneous since the aging period of the product usually comes appreciably later than the expiration of their guaranteed service life. Accordingly, the approach to the analysis of the training process from the point of view of aging seems to us inexpedient (this especially pertains to semiconductor devices, the reserves of which are very high).

The reliability of the elements during conditioning frequently is described by Weibull's law. According to this law the failure intensity decreases monotonically with time from infinity to zero which sometimes agrees with the initial operating period of the elements in a flawlessly manufactured piece of equipment. However, Weibull's law does not take into account the basic operating period of the instrument during which the failure intensity of the radio elements remains in practice constant. It is not always possible to assume that for $t \to 0$ the failure intensity will approach infinity.

Therefore, in the given case it is expedient to find other laws which would more precisely describe the variation of the parameters of the semiconductor devices during the process of their electronic conditioning.

The dependence of the intensity of the parametric failures on time (without considering the aging period at the end of the guaranteed service life) is well approximated by the hyperbolic cotangent:

$$\lambda(t) = \lambda_y \operatorname{cth} \alpha (t_H + t), \tag{1}$$

where λ_y is the steady-state value of the failure intensity at the end of the conditioning period; α is the failure probability after conditioning; t_H is the time during which the maximum failure intensity is observed.

The probability of failfree operation in this case is determined by the formula

$$P(t) = e^{-\int_0^t \lambda(t)\,dt} = \left[\frac{\operatorname{sh} \alpha t_H}{\operatorname{sh} \alpha (t_H + t)}\right]^{\frac{\lambda_y}{\alpha}}. \tag{2}$$

The exponential distribution law ($\lambda = \lambda_y$ = const) can be considered as a special case of expression (2) for $\alpha t_H > 1$. By using expression (2) for the case $\alpha t >> 1 - \alpha t_H$, that is, for the prolonged operating time, we obtain

$$P(t) \approx (1 - e^{-2\alpha t_H})^{\frac{\lambda_y}{\alpha}} e^{-\lambda_y t}. \tag{3}$$

The mean operating time after conditioning can be calculated by the approximate formula

$$\overset{(1)}{T_{cp}} \approx \frac{1}{\lambda_y} (1 - e^{-2\alpha t_H})^{\frac{\lambda_y}{\alpha}}. \tag{4}$$

Key: 1. T_{mean}

In order to select the optimal regime and the time of conditioning of the transistors, the "cotangent hyperbolic" failure distribution law was used.

Let us consider the statistical data obtained during conditioning of series-manufactured low-power transistors over a period of a number of years.

In Figures 2 and 3 we have the failure intensity distribution graphs of one type of transistor and the moving curves 1 for various conditioning regimes. Let us note that the drift of the amplification coefficient β (as the most correlated parameter) beyond the limits of the given levels ($\beta_{min} < \beta < \beta_{max}$) measured at increased temperature is taken as the failure criterion of the transistors.

Figure 2 represents the failure intensity of the transistors during conditioning in the static regime under normal conditions. From the graph it is obvious that the experimental curve 1 and the approximating curve 2 have good coincidence.

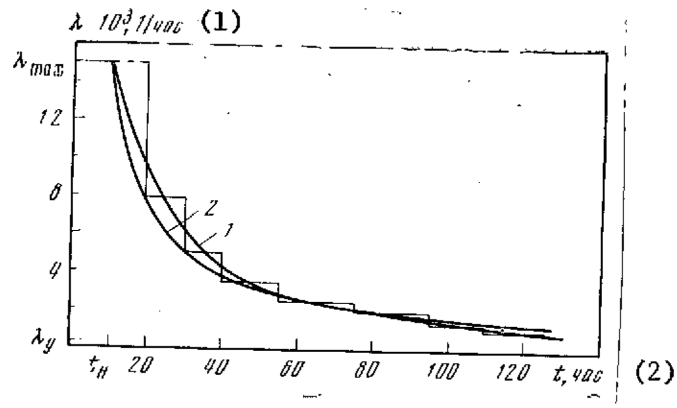

Figure 2. Variation of the failure intensity $\lambda(t)$ for conditioning transistors in the static mode under normal conditions.

Key: 1. 1/hour 2. hours

If we consider that the conditioning of the transistors lasts to a time of $\lambda(t) = 1.1\ \lambda_y$, then from equation (1) we find the conditioning time t = 1,070 hours (the following values are taken as the initial data: $\lambda_y = 0.25 \cdot 10^{-3}$, $t_H = 10$, $\alpha = 15 \cdot 10^{-4}$). The mean operating time of the transistors according to (4) will be 3,600 hours with a probability of failfree operation P = 0.98, the value of which is calculated from equation (3).

For Figure 3 which depicts the function $\lambda(t)$ during conditioning of transistors in the dynamic regime with simultaneous effect of increased temperatures (+70° C), no such experimental and approximating [according to the law (1)] curves are observed. The experimental curve 1 decreases significantly more rapidly than the approximating theoretical curve 2. This is explained by the fact that the process of stabilization of the transistor parameters takes place more intensely than in the preceding case as a result of the conditioning

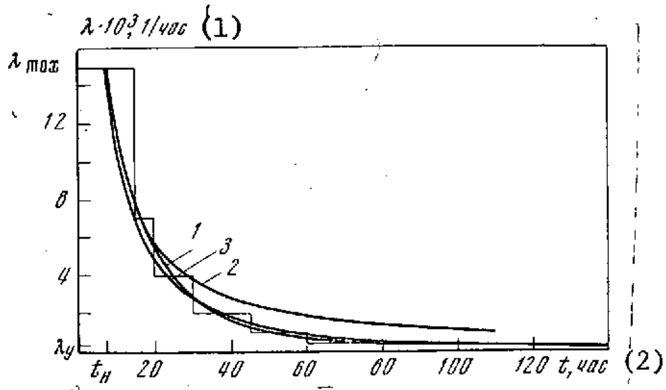

Figure 3. Variation of the failure intensity λ(t) during conditioning of the transistors in the dynamic regime with simultaneous effect from increased temperature.

Key: 1. 1/hour 2. hours

regimes becoming more rigid. The necessity is arising for the introduction of the rigidity factor into expression (1) which will characterize the acceleration of the conditioning process with time.

This empirical coefficient was found

$$\varepsilon^* = \frac{3t + (T - 20°\,C)}{t^{3/2} + (T - 20°\,C)},$$

where T is the temperature at which the conditioning took place; t is time.

Now equation (1) is acquiring the following form:

$$\lambda(t) = \lambda_y \frac{3t + (T - 20°\,C)}{t^{3/2} + (T - 20°\,C)} \operatorname{cth}[\alpha(t_н + t)]. \qquad (5)$$

Equation (5) well approximates the experimental function λ(t) for training the transistors in the dynamic regime at increased temperature (see Figure 3, curve 3).

If we take the condition $\lambda(t) = 1.1\ \lambda_y$ as the criterion for limiting the conditioning time, then according to (5) the conditioning time will be a total of 125 hours. The mean operating time in this case increases to 5,600 hours with a probability of 0.998.

The optimal regime and duration of conditioning can also be estimated beginning with the economic arguments [3]. Let us introduce the following notation: C_1 is the cost of one product; C_{cond} is the cost of one hour of conditioning;

$C_{failfree}$ is the effect from the failfree operation of the product for the time t_0 after conditioning; C_0 is the loss from a failure during the time t_0.

The magnitude of the mean coefficient as a function of the operation of n products will be [4]

$$C = C'_{failfree} - C'_1 - C_{cond} - C'_0; \tag{6}$$

here $C'_{failfree} = C_{failfree}\, np(\tau)\ p_\tau(t_0)$ is the total effect from failfree operation of the elements; $C'_1 = nC_1$ is the cost of n products; $C'_{cond} = n\tau C_{cond}$ is the cost of conditioning the transistors in n products; $C'_0 = C_0 np(\tau)q_\tau(t_0)$ is the loss from failure of the products where $p(\tau)$ is the probability of failfree operation of the products during conditioning lasting τ; $p_\tau(t_0)$ is the probability of failfree operations after conditioning; $q_\tau(t_0)$ is the probability of failure in the time t_0:

$$p(\tau) = \exp\left[-\int_0^\tau \lambda(t)\,dt\right], \tag{7}$$

$$p_\tau(t_0) = \exp\left[-\int_0^{\tau+t_0} \lambda(t)\,dt\right], \tag{8}$$

$$q_\tau(t_0) = 1 - p_\tau(t_0). \tag{9}$$

Considering the values of the terms in the right-hand side of equation (6), the mean effect during operation and maintenance of the products can be expressed by the equation

$$C = np(\tau)p_\tau(t_0)\,C_{\text{б.о}} - nC_1 - n\tau C_{\text{тр}} - np(\tau)\,q_\tau(t_0)\,C_0. \tag{10}$$

(1)

Key: 1. C_{cond}

In order to determine the optimal duration of conditioning for which the maximum C will occur, it is necessary to differentiate equation (10) with respect to τ and equate the derivative $dC/d\tau$ to zero [4]:

$$C_{\text{б.о}}\frac{dp(\tau)}{d\tau}p_\tau(t_0) + C_{\text{б.о}}\,p(t)\frac{dp_\tau(t_0)}{d\tau} - C_0\frac{dp(\tau)}{d\tau}q_\tau(t_0) - C_0 p(\tau)\frac{dq_\tau(t_0)}{d\tau} - C_{\text{тр}} = 0. \tag{11}$$

(1) (2)

Key: 1. $C_{failfree}$ 2. C_{cond}

From equations (7)-(9) we find

$$\frac{dp(\tau)}{d\tau} = -\lambda(\tau)\,p(\tau), \tag{12}$$

$$\frac{dp_\tau(t_0)}{d\tau} = -[\lambda(\tau+t_0) - \lambda(\tau)]\,p_\tau(t_0), \tag{13}$$

$$\frac{dq_\tau(t_0)}{d\tau} = [\lambda(\tau+t_0) - \lambda(\tau)]\,p_\tau(t_0). \tag{14}$$

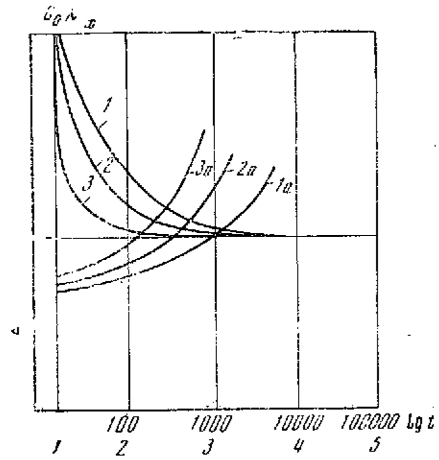

Figure 4. Graphs for determining the optimal conditioning time.

Substituting (12)-(14) in expression (11), after simple transformations we obtain the final equation for determining the optimal conditioning time τ for the given t_0:

$$C_0\lambda(\tau) = (C_{\text{б.в}} + C_0)\,\lambda(\tau+t_0)\,p_\tau(t_0) + \frac{C_{\text{тр}}}{p(\tau)}. \tag{15}$$

This equation is solved graphically [4].

In Figure 4 the graphs are constructed which depict the left-hand side of equation (15) as a function of time (curves 1, 2 and 3, respectively, for the following conditioning regimes: static at normal temperature, static at increased temperature, dynamic at increased temperature) and the right-hand side (denoted by x) of equation (15) as a function of time (curves 1a, 2a and 3a respectively).

The optimal conditioning time is found by the points of intersection of the curves 1 and 1a, 2 and 2a, 3 and 3a.

As is obvious from the graphs (see Figure 4), the optimal conditioning time occurs in the case of the dynamic regime at increased temperature (intersection of curves 3 and 3a) since it is the least, and the means expended on insuring this type of conditioning are effectively paid for by an increase in the service life of the transistors and an increase in the probability of their failfree operation.

Conclusions

1. The failure intensity of the transistors as a function of time (without considering the aging period) is approximated well by the hyperbolic cotangent. Therefore, this reliability law can be used when analyzing the stabilization period of the transistor parameters during their conditioning. The making the training regime more rigid is characterized by accelerating the process of stabilizing the parameters which must be considered by introduction of the rigidity coefficient ε^* which depends on time into the expression for $\lambda(t)$.

2. The technological conditioning partially stabilizes the semiconductor devices; however, as experience shows, it does not guarantee final establishment of their parameters. A study of the processes of stabilizing the transistor parameters at the consumer enterprise shows that in order to construct highly reliable equipment based on semiconducting devices, an inseparable element of the technological process must be conditioning of the transistors in the dynamic regime under the effect of increased temperature as the most effective and economically justifiable form of stabilizing the product parameters.

BIBLIOGRAPHY

1. Dlin, A. M., STATISTICHESKIY KONTROL' I ANALIZ NADEZHNOSTI MASSOVYKH IZDELIY RADIOELEKTRONNOY PROMYSHLENNOSTI (Statistical Monitoring and Analysis of the Reliability of Mass-Produced Products in the Radioelectronic Industry), Moscow, Sovetskoye radio, 1960.

2. Kozeletskiy, E. I., Shevtsov, G. A., "A Reliability Law of Electronic Equipment," NADEZHNOST' I KONTROL' KACHESTVA (PRILOZHENIYE K ZHURNALU STANDARTY I KACHESTVO) (Reliability and Quality Control (Appendix to the Standards and Quality Journal)), No 9, 1970.

3. Kulakov, N. N., Zagoruyko, A. O., METODY OTSENKI POVYSHENIYA NADEZHNOSTI TEKHNICHESKIKH IZDELIY PO TEKHNIKO-EKONOMICHESKIM POKAZATELYAM (Methods of Estimating the Increase in Reliability of Technical Products by the Technical-Economic Indexes), Novosibirsk, Nauka, 1969.

4. Chuyev, Yu. V., et al., OSNOVY ISSLEDOVANIYA OPERATSIY V VOYENNOY TEKHNIKE (Fundamentals of Operations Research in Military Engineering), Moscow, Sovetskoye radio, 1965.

N74-33996

UDC 62-50:629.17

HOLOGRAPHY AND THE CONTROL OF SELF-PROPELLED VEHICLES

[by V. I. Yeroshin, G. P. Novikov, V. M. Busargin, T. I. Kurmanaliyev]

[Text] A study was made of the possibility of applying the principles of holography and optical data processing in the control of self-propelled space vehicles. Various methods of controlling space vehicles are described, 1) by the results of comparing the image with the standard hologram; 2 by the holographic images transmitted over the moon-earth communications channels; 3) on the basis of using autotelevision cameras with a three-dimensional screen. Procedures are presented for obtaining the standard holograms (by the models of the lunar surface, different photographs of a single section of the lunar surface and holography from an artificial moon satellite). The structural organization of the microprogrammed automaton controlling the movement of the space vehicle is also presented. The discussed methods of controlling space vehicles using the principles of holography are opening up prospects for building a vehicle with a self-organizing information system. There are 26 illustrations and 18 references.

The results of the mastery of outerspace at the present time make it possible to formulate some of the special problems and evaluate the prospects of the methodology of controlling research space vehicles.

As is known, the Soviet program for the study and mastery of outerspace provides primarily for the use of automatic devices. This area has obtained predominant significance in the study of the moon and the planets of the solar system in which the broadest application of automated self-propelled space vehicles (ASS) is proposed. These vehicle "steps" along the path of the future penetration of man into the secrets of the cosmology and morphology of the earth and solar system as a whole.

The problem of optimal control of the ASS is one of the urgent problems of modern space engineering. Its solution is connected with significant difficulties, the primary ones of which are the complexity of the operative situation and the reliability of evaluating the actual situation during movement of the ASS and the ineffectiveness of remote control of the vehicle by commands from earth as a result of the significant delays during the radio-transmission process at great distances.

In order to find an approach to resolving the above-indicated difficulties we have analyzed the activity of the operators with respect to controlling the Lunokhod-1 lunar vehicle delivered to the surface of the moon in the vicinity of the Sea of Rains by the Luna-17 automated station.

In this paper, on the basis of analyzing the published scientific data, in addition to classification and discussion of new data in the field of mastering outerspace the authors have stated their goal as follows:

1) To find a model of the future ASS on the basis of analyzing the process of the control and evaluation of the latest achievements in cybernetic and quantum electronics;

2) Investigation of certain specific problems in the realization of self-control and increased dynamic nature of remote control of the ASS.

1. Analysis of the Process of Controlling the Lunokhod-1 Self-Propelled Vehicle

Let us consider the component parts of the process of controlling the vehicle by command from the earth and let us explain those elements of it which impose rigid requirements on the personal qualities of the operators. The operator activity of the crew (the commander, the driver, the navigator, the onboard engineer and the operator of the sharply directional antenna) for controlling Lunokhod-1 can be divided into three basic elements:

1) The reception of information about the characteristics of the movement of the target;

2) The comprehension of this information by the operator and generation of decisions;

3) Manipulation of the servomechanisms (the levers, handles, knobs and toggle switches) to implement the decisions made.

The information received by the operator is connected with the peculiarities of the control of the Lunokhod-1. These peculiarities are the following:

1) The control of the self-propelled vehicle is remote from the ground using two television cameras required for operation of the ground crew and four telephotometers to scan the right and left hemispheres of the lunar surface;

2) Not all of the successive changes in the lunar landscape which take place during forward motion of the vehicle are visible upon the screen at the control station, but they appear in 20 second intervals.

3) The sun is very bright on the moon, there is no atmosphere which disperses the light and softens the shadows. Therefore, even successive frames of the same lunar panorama appear to be dissimilar;

4) The pattern of the scattered light from the lunar surface is found to be very complicated; therefore some of the slopes of the craters are so brightly illuminated that their edges are not to be seen.

By comparing the image of a section of the lunar surface on the television screen with the instrument readings, the operator evaluates the distance to an obstacle, deciphers its shape and determines the dimensions. It is especially difficult to recognize fissures, various depressions and some craters.

It is easy to imagine that the Lunokhod [moon vehicle] driver can far from always intervene in time in the course of the vehicle even when using the start-stop mode of control.

Thus, the control of the Lunokhod by command from the earth imposes strict requirements on the operator qualities of the man. The extraordinary emotional tension has a negative effect on the operator's performance. In addition, the operator is obligated to perform his control function with a reliability of one, that is, not only fail-free, but also error-free. Indeed, the fate of many years of work by a large collective of designers, industrial workers and scientists is in the hands of this crew.

The progress made in the field of cybernetics, information theory and quantum electronics permits us to create space vehicles capable of executing not only highly complex control and regulation functions but also automatically to react to a variety of changes in the external conditions. Such a vehicle must have a self-organizing information system which can analyze and sort the most important observations and make decisions both with regard to the nature of further movement over the surface of the planet and transmission of information to the earth depending on importance, distance from the earth, available energy reserves and a number of other factors.

In this paper the problems of the ASS control have been investigated and analyzed on the basis of monitoring the surrounding situation by the methods and means of holographic engineering.

It must be noted that in classical photography only the intensity of the light wave is recorded, and the phase shifts created by the subject are irreversibly lost. By using the means of ordinary photography and also the television and display screens for which the two-dimensional representation of the real situation is characteristic, the observer must resort to the subjective understanding of the recorded scene in order to comprehend what is depicted on it. Holography permits simultaneous recording of both the amplitude and phase information contained in the scattered wave and, consequently, it offers the possibility of "seeing" the object in all the detail, including the volumetric outlines, the effects of parallax and depth of field. Thus, the image of the observed object in this case differs not at all from the object itself.

Of course, in this experiment the goal was not stated of investigating all the problems which arise in connection with using the principles of holography to control self-propelled vehicles. However, some of the methods of organizing control investigated here can be useful when constructing the ASS in the near future.

Before proceeding to the problems of using holography to control the ASS, let us discuss a brief description of the specific processes of holography and optical information processing.

II. General Principles of Holography

1. Holographic Method of Recording and Obtaining an Image

As is known, the visual perception of surrounding objects includes several successive operations:

The light wave is reflected from the object and carries information about it into the surrounding space;

The pupil of the eye cuts out "pieces" of the wave front, and the collecting lens — crystalline lens — creates an image on the retina which as a result of the photochemical processes arouses an image of the object in the human brain via the nervous system.

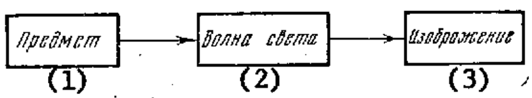

Figure 1

Key: 1. object 3. image
2. light wave

The propagation of light from the objects to the pupil is autonomous. The wave taken from the object does not depend on the object any more and is propagated further in accordance with the diffraction law. In the classical system of image storage or transmission, the object of observation is not the light wave itself, but the image obtained from the wave by means of a lens. The schematic diagram of the traditional optical image system can be represented as shown in Figure 1.

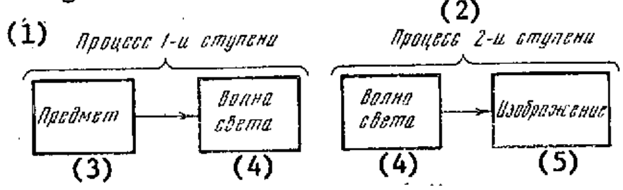

Figure 2

Key: 1. first step process 4. light wave
2. second step process 5. image
3. object

The holographic method is separated into two steps: first, the structure of the light wave itself is recorded ("imprinted"), and then the image is reproduced and obtained. The schematic of a holographic depiction system can be represented by two autonomous processes (Figure 2).

The traditional scheme for obtaining the image is characterized by the fact that the photorecorder records only the mean wave intensity at the focal plane of the lens, and the information about the phases of the scattered wave is completely lost. Therefore, this scheme provides for collecting only part of the information. The representation of the real picture is found to be incomplete. A consequence of this deficiency is impossibility of reproducing the three-dimensional image of the object and instability of the entire process with respect to defocusing the image. Although during defocusing the information about the object does not disappear, in reality as a result of the indicated deficiency it slips away from the observer. During the holographic process these deficiencies are completely eliminated.

Symbolically, this process can be represented as follows. In the first step the wave taken from the object "freezes," that is, the propagation process is interrupted, and the instantaneous structure of the wave propagation is recorded. In the second step the wave is "unfrozen" and propagated farther.

If we place the pupil on the paths of this wave, we see the object as it was at the time the wave was frozen.

Thus, the holographic method of observation solves the problem of obtaining a complete stable image having visual characteristics which are inherent to the natural process of observing an object including the three-dimensional relief, the effects of parallax and depth of field. The image received from the hologram is characterized by properties which are absolutely not part of the ordinary stereophotographic images. If the observer changes position when investigating the holographic image, the perspective of the image also changes as if the observer were looking at the natural objects. If the object in the front view is located in front of any other objects, then the observer can by turning his head see beyond the screening object and see something that was initially hidden from his eyes, that is, the image possibilities and the qualitative reliability of reproduction of the landscape by holographic methods are essentially higher than for ordinary photographic techniques.

2. Conditions of the Holographic Observation Technique

Let us briefly consider the basic realizations of the holographic method of observation.

1. The light source illuminating the object must be monochromatic and coherent. As is known, lasers have such properties. They were irreplaceable sources of radiation for holography. The operating principle and detailed description of the properties and peculiarities of lasers are discussed in a number of special books [1, 2, 3].

2. The space (transverse) and time (longitudinal) coherence of the light source must be such that clear and stable interference patterns will be insured.

The space coherence of the radiation characterizes the capacity for interference of the light waves emitted by various parts of the source and at different angles. It is caused by the fact that the lasers usually emit a light beam with complicated structure in a form of characteristic spots. The spatial coherence is felt in the quality of the hologram. In order to improve it, usually in the structural designs of lasers special devices are provided.

The time coherence defines the capacity of the light waves emitted by the source at various points in times to interfere with each other. The time coherence can quantitatively be characterized by a segment of the path $\Delta\ell$ traveled by the light during the time interval Δt within the limits of which the radiation preserves the coherent properties. Here, the coherence length $\Delta\ell = c\Delta t$ where c is the speed of light.

The time coherence depends on the width of the spectral line emitted by the light source. The more monochromatic the line, the higher the radiation coherence: $\Delta\ell = \lambda^2/\Delta\lambda$ where $\Delta\lambda$ is the width of the spectral line.

The coherence length of the source defines the possible depth of the holographically scene. It is necessary that the difference in the path between any light beams encountered on a hologram not exceed the coherence length. For lasers, depending on the width of the structural line, the coherence length varies from hundreds of meters to units of centimeters.

Thus, when selecting a laser for holography of one object or another, the requirements on the space and time coherence noted above must be taken into account.

3. During exposure the object must be strictly stationary with respect to the entire optical system.

The satisfaction of the investigated conditions insures stationarity of the illuminating and the reflected light wave and at the same time obtaining a stable interference pattern -- the hologram of the image of the object.

3. Holography System

At the present time holograms are obtained by various methods. We shall consider one of them. Let us assume that the object is illuminated by beams of coherent light. Part of the reflected beams are incident on the entrance pupil of the optical system. At any point in the plane of the pupil, the light wave is a function of the distribution of the amplitudes a and phases C of the coherent light

$$\dot{u}(x, y) = a(x, y)\, e^{i\Phi(x, y)}.$$

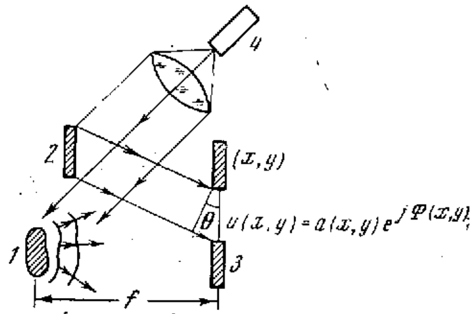

Figure 3. Scheme for obtaining a hologram (θ is the angle at which the reference beam is incident on the photographic plate)
1 -- object; 2 -- mirror forming the reference beam; 3 -- hologram; 4 -- laser

If the photographic plate is put in the plane of the pupil and it is exposed, the film records only the mean square intensity of the light wave reflected from the object -- the object beam. The information about the phases in this case is completely lost.

In order to print the phase information it is necessary to aim a so-called reference light beam coherent with the object beam at the photographic plate at some angle. In this case, in the plane of the photographic plate an interference pattern is created -- the hologram -- bearing both the amplitude and phase information. The system for obtaining the hologram is presented in Figure 3.

As to the appearance of the photographic plate, the first step is made in the above-described holographic process as with respect to "freezing" the light wave.

In order to reproduce the wave, the hologram is illuminated by the same reference beam of the coherent light source (Figure 4).

During reproduction the second step of the holographic process is realized with respect to "unfreezing" the light wave.

The light passing through the hologram can be divided into three components. The first component maintains the direction of the beam; the second component is propagated at an angle of 2θ; the third component is aimed normal to the plane of the hologram. This last component also contains the reproduced wave of interest to us. It can be sent for processing to the optical system or observed by eye.

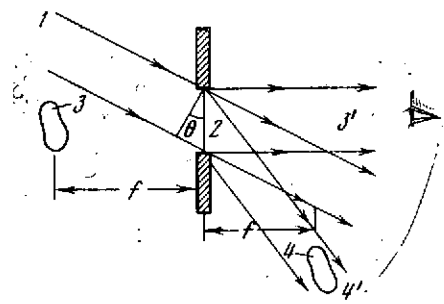

Figure 4. System for wave reproduction.
1 -- reference beam; 2 -- hologram; 3 -- imaginary image formed at the distance f beyond the hologram and visible in the direction normal to the hologram (the beam 3'); 4 -- the actual image formed at the distance f in front of the hologram by the secondary beams which form the angle 2θ with the normal to the hologram (beam 4')

III. Principles of Analog Optical Data Processing and Pattern Recognition

In parallel with holography, in recent years analog optical methods of data processing have been successfully developed which are characterized by significant advantages by comparison with the electrical methods of processing analog data.

The basis for optical processing is not the time principle,but the space principle. The optical processor forms the input signals which are a function of the coordinates x and y and not time. The information in the optical processor is represented in the form of patterns (images, figures). Transparent optical media -- transparencies, filters -- are used as the information carriers.

The transparency of the transparency varies in accordance with the exposed pattern. During the reproduction process this transparency placed upon the path of the coherent light beam correspondingly simulates the amplitude and phase of the light signal passing through it.

The processing of the data in the analog optical system takes place with the speed of light in parallel, that is, it is realized by the projection (superposition) of the individual patterns (input signals) on each other. The result of this superposition is represented in the form of a superposition pattern in the image plane (the output signal).

The relations between the input and output signal, that is, the amplitude distribution of the light emission in the focal planes of the coherent optical system are defined by the spatial (two-dimensional) Fourier transformations analogous to the time (one-dimensional) Fourier transformations in the fields of electronics and radioengineering. This means that if the transparency containing a recording of the initial information is placed in the focal plane of the lens, then the light pattern on the other side of the lens at a distance equal to the focal length will have the form of a two-dimensional spectral image which is a Fourier spectrum of the information recorded on the transparency (the Fourier image).

Thus, the complex distribution of the intensity occurring in the rear focal plane of the lens is determined by transformation of the Fourier function (pattern) given in the forward focal plane of the lens.

By using selective optical elements it is possible to perform the operations of filtration and synthesis of the optical systems analogously to how this is done by using electrical filters on the electrical signals.

The relatively simple optical spatial filters can perform various functions. They can be used to implement optical pattern recognition systems, to isolate the useful signal against a background of noise, and so on.

The holographic equipment essentially simplifies the realization of the pattern recognition optical systems. The recording of the coherent light wave in the form of the Fourier hologram permits us to obtain photographic transparencies which can be used as the matched optical filters in optical pattern recognition systems.

The recognitioning of patterns in this case is usually realized by comparing the spatial frequency spectra of the standard hologram of the test image and the holograms of the analyzed image. In particular, the recognition of patterns by the matched optical spatial filtration can be successfully used in navigation systems for spacecraft, autonomous self-propelled vehicles designed to investigate paths and when processing and analyzing images transmitted from spacecraft.

1. Fourier Transformation Using an Optical Lens

Each two-dimensional image can be expanded in the two-dimensional spectrum of the spatial frequencies. This operation is equivalent to representing the image in the form of a set of sinusoidal diffraction gratings of various periods and orientations [4] analogously to how in radioengineering during expansion of the signal in the spectrum it is represented in the form of a set of sinusoidal oscillations of different frequencies.

The operation of the expansion of an image in the spectrum of the spatial frequencies is realized usually by means of a lens (Figure 5).

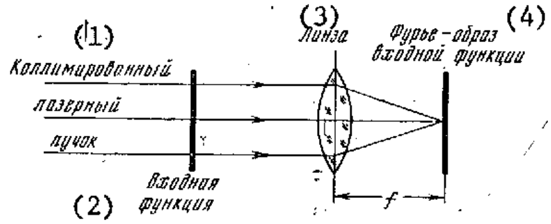

Figure 5. Schematic of the Fourier transformation using an optical lens

Key: 1. columnated laser beam
2. input function
3. lens
4. Fourier transform of the input function

If the two-dimensional image (input function) is placed in the forward focal plane of the optical lens, then according to the Huygens principle, each point of the aperture of the input plane can be considered as the secondary source of the coherent light. After integration over the aperture of the input plane, the mathematical expression of the image obtained in the rear focal plane of the lens is a Fourier transform [5]. The image itself can be represented in the form of the spectrum of spatial frequencies. On rotation of the image at the lens input around the optical axis or variation of its configuration, the rotation or variation of the spatial distribution of the frequency spectrum at the lens output in the Fourier transformed plane will be duplicated. This capacity of the simple optical lens is to realize a two-dimensional Fourier transformation with the speed of light is the main advantage of optical processes by comparison with traditional electrical processors.

2. Optical Matched Filtration

The schematic image of the simplest optical filter is presented in Figure 6.

The Fourier transform is realized by means of lens 1. In the transformation plane the Fourier transform of the object is obtained. By using the lens 2, the frequency spectrum on the plane of the transform is retransformed into the plane of the image. By placing ordinary optical filters in the transformation plane (which is simultaneously the filtration plane), it is possible to change the frequency spectrum in the transformation plane and at the same time transmit certain parts of the spatial spectrum of the object for formation of the image. By using special filters for which a recording of the spectral attributes of the objects is made in advance, it is possible to realize the procedure of image selection and recognition of these objects.

However, the investigated schematic for spatial filtration of the image has the significant deficiency. The filter entering into it and manufactured by ordinary optical methods contains only partial information about the object. The phase information is lost during recording. Therefore, the light signal passing through this filter contains spurious components which are superposed on the recognized image and complicate the interpretation of the results.

The application of the holographic procedure for obtaining a matched spatial filter eliminates this deficiency. In this case the phase information about

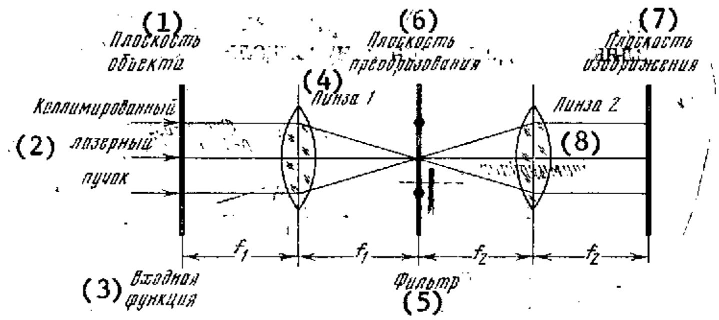

Figure 6. Schematic of an optical filter

Key: 1. plane of the object
2. collimated laser beam
3. input function
4. lens 1
5. filter
6. transformation plane
7. image plane
8. lens 2

the object is retained, and the noise level is reduced sharply. The schematic for obtaining the holographic matched filter of spatial frequencies is presented in Figure 7.

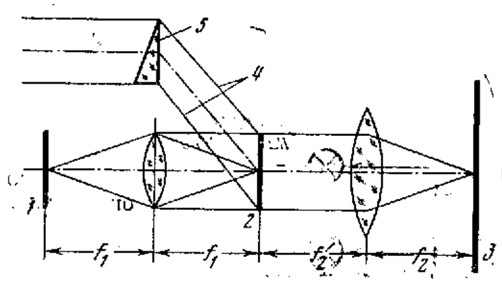

Figure 7. Schematic for obtaining a holographic filter and pattern recognition.
1 -- object plane; 2 -- hologram-filter; 3 -- recognition plane; 4 -- coherent light beam; 5 -- optical wedge.

In plane 2, just as in the preceding case, the Fourier transform of the initial object placed in the plane 1 is formed. However, an additional coherent background participates in this scheme when forming the Fourier transform. As a result of interference in the plane 2 the holographic diffraction grating is formed, the so-called Fourier hologram which "imprints" the spatial spectral image of the initial object. Inasmuch as the hologram "absorbs" information about both the amplitude and phase of the wave pattern, the degree of informative similarity (matching) of the filter obtained in this way to the initial object is very high. This fact significantly simplifies the pattern recognition procedure using holographic matched filters.

3. Pattern Recognition

The problem of recognizing a segment of the surface on the path of movement of an automatic self-propelled vehicle belongs to the area of pattern recognition. It is possible to solve the stated problem by means of the above-described coherent-optical matched filtration.

Actually, having a library of standard holographic filters (a set of surface images) onboard the self-propelled vehicle, it is possible by means of an optical operator to determine the given pattern. The block diagram of the optical processing system for the investigated case is presented in Figure 8. The signal f(x,y) at the system input which is the distribution of the intensity of the light reflected from the object can comprise N individual patterns S_1, S_2,..., S_N. Out of the set of N patterns by means of an optical operator it is necessary to determine a given pattern. The identification process can be carried out if the input signal is applied to the set of N standard holograms (spatial filters) on each of which one of the possible patterns appearing at the system input on movement of the self-propelled craft is recorded.

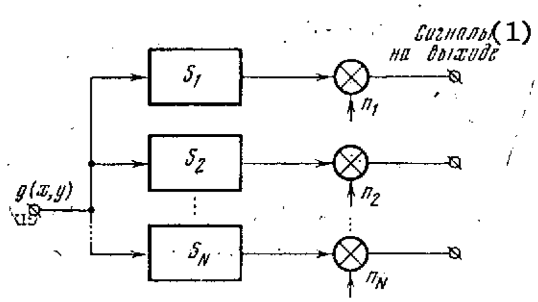

Figure 8. Block diagram of the system for recognizing sections in the terrain(S_1, S_2,..., S_N -- transfer functions of the standard holograms of the patterns; n_1, n_2, ..., n_N-- normalization of the output signal (response) of each channel on performance of the filtration operation)

Key: 1. signals at the output

The recognition of the sections of the planet surface is carried out on the basis of comparing the standard holograms with the image in the field of view of the scanner. Here, situations can arise where the recognized section occupies greater area than the area of the section recorded on the standard hologram. In addition, the recognized sections can have a different content with respect to those which are stored in the library of standard holograms. Therefore, when performing the filtration operation between the initial pattern (section) and the standard pattern the noise signal arises, the intensity of which can be significant. For recognition of a segment of the terrain in the presence of noise it is possible to use special methods of step by step optical processing.

Now let us consider certain methods of controlling the optical self-propelled equipment using the principles of holography and optical data processing.

IV. Control of an Automated Self-Propelled Vehicle by the Results of Comparing the Image with Its Hologram

This method permits formation of the control commands directly onboard the ASS, and ground operations can be reduced to a minimum.

The essence of the method consists in comparing the image (the diapositive) as a section of the lunar landscape (hereafter the movement of the ASS over the lunar surface will be considered) with its hologram. In order to implement the method first standard holograms must be obtained with a recording of the required morphologic peculiarities of the relief. It is possible to obtain the holograms by three procedures:

1) Holographic recording of the model of the lunar surface under ground conditions;

2) Recording the hologram by a set of photographs of a single section of the lunar surface taken under natural conditions in the corresponding direction;

3) Holographic recording of the required section of the surface from an artificial satellite of the moon.

1. Obtaining Holograms by Holographic Recording of a Model of the Lunar Surface

In order to manufacture a model of the lunar surface under ground conditions it is necessary to discover the basic characteristics of the lunar landscape of the proposed spacecraft landing area. By lunar panoramas obtained by the Luna-9, Luna-13, Luna-16 and Lunokhod-1 stations and also the American Lunar Orbiter, Ranger, Surveyor and other stations it is possible to isolate the most characteristic types of formations. The results of studying the Lunar panoramas [6] transmitted by the Luna-9 station are presented in Figure 9.

The optical examination of the landscape and obtaining the holograms of models of the surface sections are illustrated schematically by Figure 10.

It is possible to scan sections of the lunar surface and obtain holograms of these sections by means of a device (Figure 11) constructed by the television camera system of the Luna-9 station.

The selection of the magnitude of the vertical viewing angle (Figure 12) of the scanner is determined by the possibility of surveying and recognition of a quite large part of the surface.

In order to obtain the holograms of sections of the lunar surface located both in direct proximity to the ASS and at a significant distance from it, it is necessary to define the field of view (see Figure 12) of the scanner. For purposes of convenience of execution of the various operations with respect to maneuvering the ASS, the dimensions AB and AC are supposedly selected equal to 2 and 20 m respectively. It is natural that the quality of the holograms of sections of the near zone will be better than the far zone inasmuch as the intensity of the laser beam reflected from the far zones and fixed on the hologram will be less than from the near zones.

It is necessary also to point out that if the spacecraft completes a landing on an uneven surface, then the field of view of the delivered ASS will be limited by the protrusions of the relief. In order to increase the field of view, various periscopic devices can be used (Figure 13).

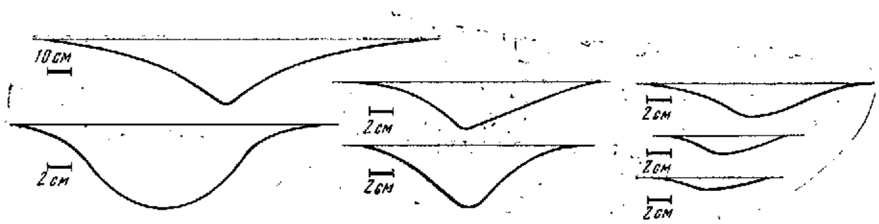

Figure 9. Dimensions and shapes of holes and small craters.

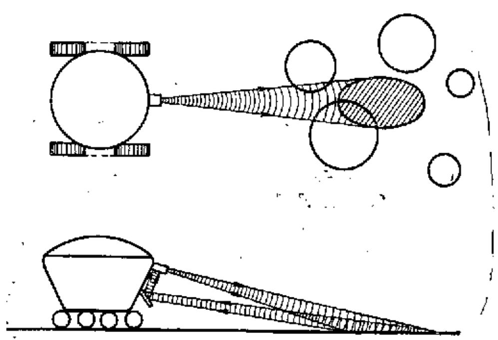

Figure 10. Schematic for optical examination of the landscape by the ASS

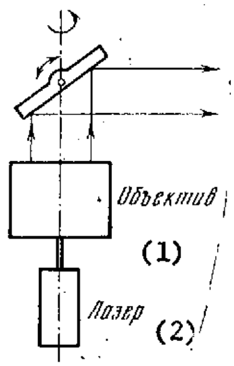

Figure 11. Schematic of the scanner

Key: 1. objective lens
2. laser

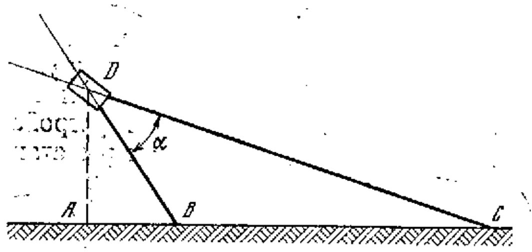

Figure 12. Determination of the field of view of the scanner.

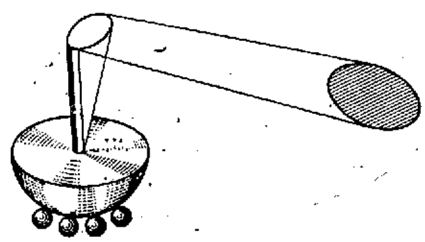

Figure 13. Periscope for scanning the terrain around the ASS.

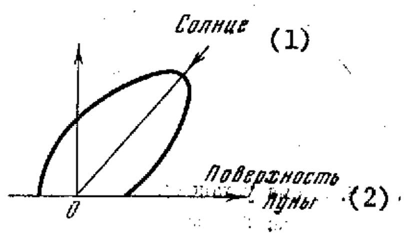

Key: 1. sun
2. surface of the moon

Figure 14. Indicatrix of the scattering of light by the lunar surface.

Obviously, the scattering indicatrix for the laser emission-reflected from the moon has no significant differences from the characteristics presented in Figure 14.

2. Obtaining Holograms by the Photographs of a Single Section of the Lunar Surface

This procedure is based on the capacity of the hologram for reproducing the image when illuminating a small section of it. By observing this section it is possible to see the image of the object as it was obtained when examining in the given direction. The image will appear two-dimensional since when observing through a small hole the eye does not distinguish a three-dimensional image from a two-dimensional one. Therefore, it is possible to replace each segment of the ordinary hologram of an object by a small hologram (microhologram) of its two-dimensional photograph taken in natural lines in the corresponding direction. Thus, it is possible to compile a mosaic hologram which on reproduction gives the three-dimensional image of the object.

The deficiency of this procedure consists in the necessity for having photographs of the sections of the lunar surface taken in different directions. By panoramas of the lunar surface obtained by various space stations it is difficult to obtain the required photographs of the sections with the images of the corresponding holes and craters.

Obviously, the best solution in this case will be to obtain photographs by models of the lunar surface under terrestrial conditions. After obtaining the required photographs it is possible to manufacture a mosaic hologram by the system presented in Figure 15.

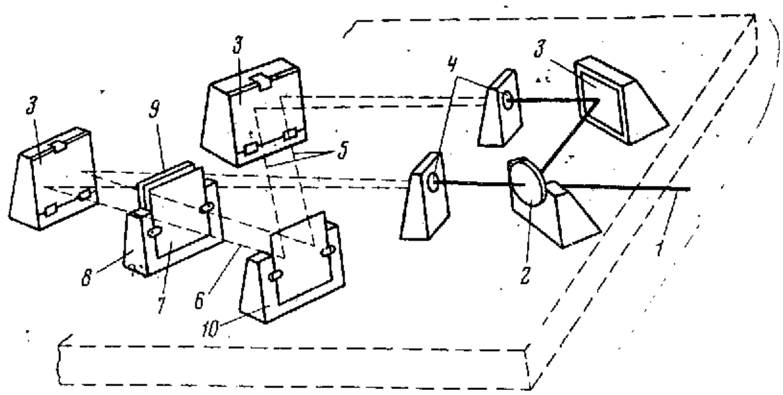

Figure 15. Schematic of the device for obtaining holograms.
1 -- laser beam; 2 -- splitter (semitransparent mirror)
3 -- reflecting mirror; 4 -- short focal length lenses;
5 -- reference beam; 6 -- object beam; 7 -- photograph (positive slide) of the object; 8 -- device for the photograph montage and the dispersion unit; 9 -- dispersion unit;
10 -- setup for the hologram montage

Figure 16. Curves for the diapositive as a function of the exposure of the high and low contrast film

Key: 1. high contrast film
2. low contrast film

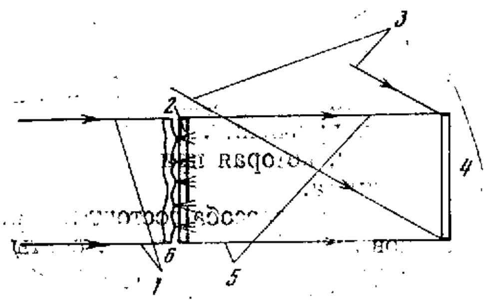

Figure 17. Use of scattered light to record holograms. 1 -- from the radiation source; 2 -- diapositive; 3 -- reference beam; 4 -- hologram; 5 -- object beam; 6 -- dispersion unit.

By installing various diapositives of an object at the location of the object 7 in the system, various microholograms are obtained. Then it is necessary only correctly to combine the microholograms into a single mosaic hologram which on reproduction gives a three-dimensional image. However, in the case where the object is, for example, a diapositive with quite blunt structure (and we can include a diapositive with a recording of the sections of the moon with holes and craters here), there will be noticeable regions on the hologram for which the exposure turns out to be much greater or much less than the value corresponding to the linear section of the curve t (E) (Figure 16).

The linear relation between the amplitude coefficient of transmission and the magnitude of the exposure is described by the expression [7]

$$t_n = t_b + \beta (E - E_b),$$

where t_b is the shift of the transmission coefficient in the region of the linear section of the curve t(E); β is the slope of the curve at the operating point; E is the exposure to which the film is subjected; E_b is the displacement exposure.

Considering that E = JT where J is the intensity of the incident light, T is the duration of the exposure, and the complex field amplitude where the exposure $u = \sqrt{J}$, the curve t(E) in the linear section can be approximated by the expression

$$t_n = t_b + \beta T |\Delta u|^2,$$

where Δu is the small variation of the complex amplitude.

From the curve (see Figure 16) it is obvious that the linear relation for the quadratic law (characteristic for t_n) is satisfied only in a bounded interval.

As a result of nonlinearity it is possible to expect some distortion of the image contrast. The problem of the dynamic range of the light sensitive material can be solved using the method proposed in [8]. As is demonstrated in Figure 15, the diapositive 7 is lighted through the dispersion unit 9. Since this unit disperses the light in a broad range of directions, the light from each small section of the diapositive (Figure 17) is incident on all points of the hologram.

Thus, in this case we shall not have sections with very large or very small exposures which in one way or another would be obtained on direct illumination of the diapositive.

3. Obtaining Holograms by the Method of Holographic Recording of Sections of the Lunar Surface from an Artificial Lunar Satellite

The procedure can be used to obtain holograms of sections of the moon and also other heavenly bodies which have not been investigated or for which there are no detailed maps.

Inasmuch as the first method of controlling the ASS is constructed on the principle of comparing the optical images, in the investigated method for obtaining holograms it is necessary to solve the problems of stationarity of the holographically recorded scene and maximum similarity of the holograms obtained of them to the optical images on movement of the ASS over the surface.

The schematic of the system for obtaining holograms of the surface is presented in Figure 18.

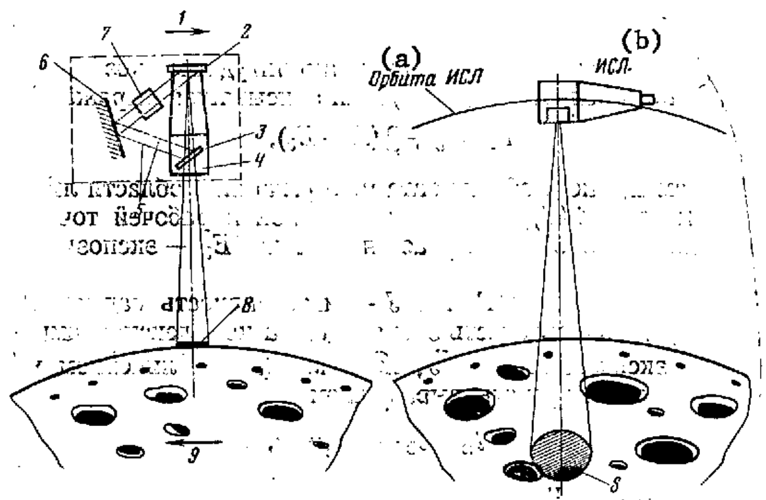

Figure 18. Schematic of the system for obtaining holograms of the lunar surface.
1 -- flight direction of the artificial lunar satellite;
2 -- holograpm; 3 -- semitransparent mirror; 4 -- objective of the dispersing unit; 5 -- reference beam; 6 -- reflecting mirror; 7 -- delay element of the reference beam; 8 -- section of the surface with an area S recorded on the hologram; 9 -- apparent direction of movement of the object
Key: a. orbit of the artificial lunar satellite
b. artificial lunar satellite

The obtaining of a hologram is a two step process of recording and reproducing the image in which it is not the image of the object itself that is recorded, but the interference pattern of the waves scattered by it. Thus, the hologram is sensitive to the phase of the incident wave which is defined both by the shape of the object and its displacement at the time of taking the hologram. The effect of the movement of the object (we shall provisionally consider that the lunar surface is moving) on the reproduced image in the general case differs from the effect of movement on the ordinary photographic systems. In order to record a given point of an object on the corresponding region of the hologram it is necessary that the pattern obtained as a result of interference of the waves scattered from the point and the reference wave above this region remain essentially stationary during the exposure. The movement of the object which causes displacement of the pattern leads to a decrease in contrast of the recorded image and intensity of the reproduced wave.

Let us analyze the effect of displacement of the object in the example of a point object which is illuminated by a collimated beam. This case is depicted schematically in Figure 19.

The magnitude of displacement of the object which leads to displacement of the pattern on the hologram by one band (a phase shift of 2π radians) is defined by the expression

$$l=\left|\frac{\lambda}{\cos\beta-\cos(\beta-\alpha)}\right|,$$

where λ is the wavelength of the illuminating beam.

In the case where the object is displaced perpendicular to the illuminating beam ($\beta = \pm\pi/2$), the above-presented equality reduces to the expression

$$l=\left|\frac{\lambda}{\sin\alpha}\right|.$$

When the object moves parallel to the illuminating beam ($\beta = 0$) we have the following equality:

$$l=\left|\frac{\lambda}{1-\cos\alpha}\right|$$

and the investigated magnitude of the displacement satisfies the inequality

$$l\leqslant\left|\frac{\lambda}{\sin\alpha}\right| \quad \text{for} \quad |\alpha|=\pi/2.$$

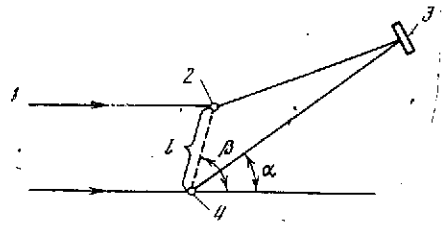

Figure 19. Effect of the movement of a point object illuminated by a collimated beam on the reproduced image(α is the angle between the straight line connecting the point and its image on the hologram and the direction of the illuminating beam; β is the angle between the direction of movement of the point and the direction of the illuminating beam; ℓ is the magnitude of the displacement during the exposure time). 1 -- illuminating beam; 2 -- final position of the object; 3 -- hologram; 4 -- initial position of the object.

The presented expressions permit evaluation of the admissible displacements of the object under various conditions. In order to decrease the phenomenon of blurring of the image, it is necessary to increase the orbital altitude of the artificial lunar satellite to hundreds of kilometers. However, the perspective of the holographic image will be insignificant as a result of smallness of the amplitude of the hologram by comparison with the distance to the moon. Desiring to obtain a holographic image with good perspective, it is necessary to put the artificial lunar satellite in a selenocentric elliptical orbit with a perigee as low as possible (5-15 km). However, under these conditions it is necessary to use a pulse laser with pulse duration from tens to hundreds of nanoseconds. Then the exposure time will be so small that the movement of the artificial lunar satellite will in practice have no effect on the quality of the hologram.

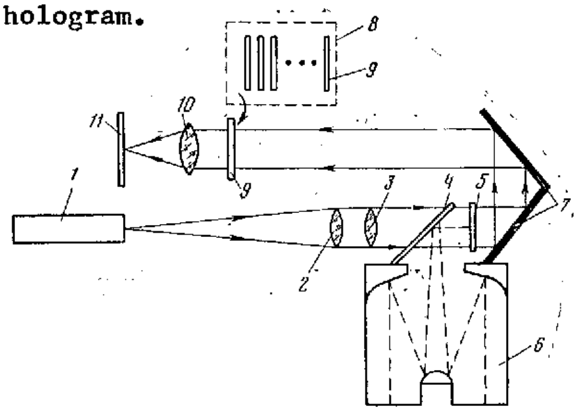

Figure 20. Block diagram of the recognition device.
1 -- laser; 2 -- collimator lens; 3 -- focusing lens;
4 -- movable mirror; 5 -- light sensitive material;;
6 -- objective lens of the scanner; 7 -- reflecting mirrors;
8 -- hologram storage unit (memory); 9 -- hologram;
10 -- focusing lens; 11 -- recognition plane

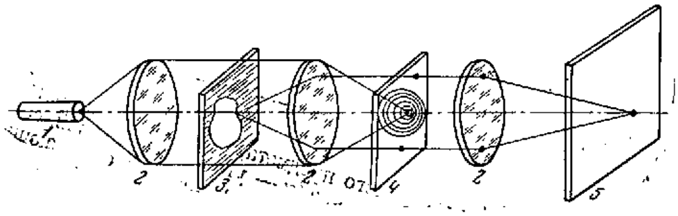

Figure 21. Schematic representation of the target recognition system.
1 -- laser; 2 -- focusing lens; 3 -- diapositive (hologram); 4 -- standard hologram; 5 -- recognition plane

After preparing holograms with recordings of the required sections of the surface they are placed in the pattern recognition device, the block diagram of which is presented in Figure 20.

In recording the panorama of the terrain (section) in the field of view of the objective, the moving mirror 4 is set at the position shown in Figure 20. In this way an image of the section is recorded on the light sensitive material. For recognition the movable mirror 4 is tilted, and the laser beam illumating the image recorded on the light sensitive material 5 converts it to a combination of signals with different spatial frequencies which, on being reflected from the system of mirrors 7, is aimed at the hologram 9. The spatial frequencies of interest to us corresponding to the image of the terrain panorama pass through the hologram almost without attenuation at the same time as other frequencies corresponding to other elements of the input optical image are strongly attenuated by the hologram. The signals corresponding to the image of the given section of the surface insure the occurrence in the recognition plane of a bright light spot, and the other signals form background noise. The schematic representation of the recognition system for the sections of the surface [9] is presented in Figure 21.

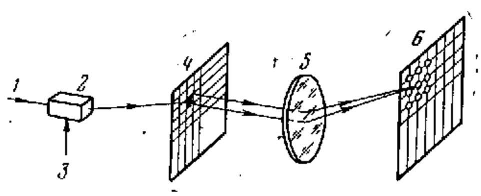

Figure 22. Schematic of the organization of the hologram storage.
1 -- laser beam reflected from the mirrors 7 (see Figure 20); 2 -- deflecting system; 3 -- control signal of the deflection system; 4 -- matrix of the microholograms 5 -- focusing lens; 6 -- recognition plane

In the recognition plane the image is reproduced which appears in the form of a light point located at a distance from the optical axis of the system. The position of the light point in the recognition plane corresponds to the position of the recognized target in the field of view of the objective lens. It is obvious that the recognition of the target can take place if the optical image does not overlap the hologram or is not rotated with respect to it.

The precision of the recognition is effected by the difference in the dimensions of the optical image and the hologram. However, by using the corresponding optical system it is possible to insure recognition here when the dimensions of the compared images differ by ten times.

The investigated method of recognizing the targets, the most effective from the point of view of creating partially or completely autonomous ASS permits storage in its memory (the hologram module) of a large number of different situations which can be encountered on the path of the ASS. In this case all the information of the program storage module can be recorded in the form of a microhologram matrix (Figure 22) on a photographic plate.

The deflection system 2 provides 10^4 different output positions of the beam with a searching speed on the order of 1 microsecond [10]. This means that it is possible to place 10^4 microholograms on the hologram 4 with the required images recorded. Let us note that the hologram storage module 8 (see Figure 20) can be used as a device for storing the microhologram matrices. However, it is necessary to consider that the dimensions of the microholograms will depend not only on the resolution limit of the light sensitive material in accordance with the Rayleigh criterion but also the possibility of filtering the spatial frequency for recognition of the target.

As the recognition plane 6 it is possible to use the photodiode matrix, the number of photodiodes of which is equal to the number of microholograms located on the hologram 4. The corresponding microhologram is addressed by a laser beam and in the case of recognition will be illuminated by one of the photodiodes of the matrix 6.

The output signals of the photodiodes are used to shape the control instructions by means of the controlling microhologram automaton investigated below.

4. Control of the Self-Propelled Vehicle

After considering the problem of target recognition, it is necessary then to solve the following problems:

1) Optimal selection of the standard hologram from the storage module 8 (see Figure 20);

2) Shaping the self-propelled vehicle control instructions.

The first problem is connected with decreasing the selection of standard holograms. Obviously, the selection of the sorting criteria must be based on analyzing the information of an entire set of holograms and the possibility of movement of the ASS over the surface.

In order to solve the problem of formation of the control commands it is necessary to place defined attributes in correspondence to each hologram (microhologram). For example, let us consider turning of the ASS by a given angle, movement with the velocity V following the former (previously selected) course, movement in the opposite direction (reverse), measurement of different parameters, performance of the physical-chemical analysis of a section of the lunar surface, transmission of the information gathered as a result of the studies to the ground, transmission of a decision to select the method of advance made onboard the ASS, and so on.

In solving the problem of creating the semiautonomous ASS, it is necessary to program the general purposeful behavior of the vehicle in its systems, that is, establish in what way it must move and what information it must gather. The operations program of such a vehicle is limited and is designed for a defined number of situations. Therefore, at defined points in time the operator must switch the programs from the ground or simply remotely control the automaton.

Selecting the Hologram Sorting Criterion

Considering the extraordinariness of the situation in which the ASS finds itself on planets hundreds of thousands of kilometers from the earth, it is necessary first of all to estimate the possibility of movement. The criterion of some possibility of forward motion can be a standard hologram recording signs (in particular, the characteristic features of the lunar surface) which the ASS is in no position to surmount. Such signs can be craters or deep slopes, holes and various protrusions and large lunar rocks. The discovery of these signs must be made by the method of comparing the standard hologram and the panorama before the ASS.

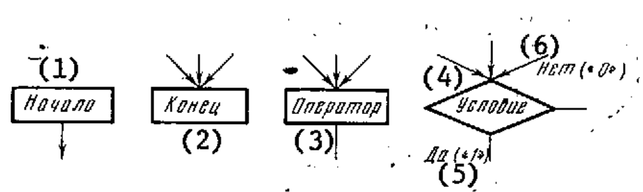

Figure 23. Types of apexes of the graph of a microprogrammed automaton.

Key: 1. begin
2. end
3. operator
4. condition
5. yes
6. no

Shaping the Control Commands

In performing the operations of examining the surface and discovering the similarity, it is necessary to shape the commands for the required nature of movement of the ASS. Above all it is necessary to examine this surface in the direct proximity of the ASS (for example, at a distance of no more than 2 meters). If for the comparison no similarity is detected (that is, there is no indicated type of crater directly in front of the vehicle), it is necessary to proceed to the hologram with the recording of a protrusion (bank, rock) over which it is also impossible to move. On making the comparisons, when there is convergence, signals are generated for the formation of the commands. The algorithm for processing the control commands can be considered as a controlling microprogrammed automaton, the law of operation of which will be determined not only by the condition of the surface and the nature of possible movements of the ASS but also the general purpose.

The procedure for performing the operations in such an automaton are represented in the form of the approximate connected graph containing apexes of four types: initial, final, operator and provisional (Figure 23).

Based on the formulated criteria for the control of ASS, let us write the operation of the microprogram automaton in the form of the algorithm flow chart presented in Figure 24.

In the presented chart for the algorithm the following are indicated:

α and β -- the angles of turning of the scanner in the right-hand and left-hand halfplanes respectively relative to the selected direction of movement of the ASS;

$(\alpha + 1)$and$(\beta + 1)$ -- increments on the initial angles of turn of the scanning device selected within the limits of the viewing angle of the objective;

γ and z -- angles of turn of the periscope in the right-hand and left-hand halfplanes respectively;

$(\gamma +1)$ and $(z + 1)$ -- increments on the initial angles of turn of the periscope.

The holograms with a recording of the crater a distance of more than 5 meters from the ASS were selected beginning with the fact that on the first examination of the surface (recognition of a crater at a distance of no more than 2 meters from the ASS), the zone of from two to five meters will be examined.

When analyzing the situation for the possibility of movement ahead, a periscope can be used which examines sections of the surface inaccessible to the scanner as a result of its limited viewing angles.

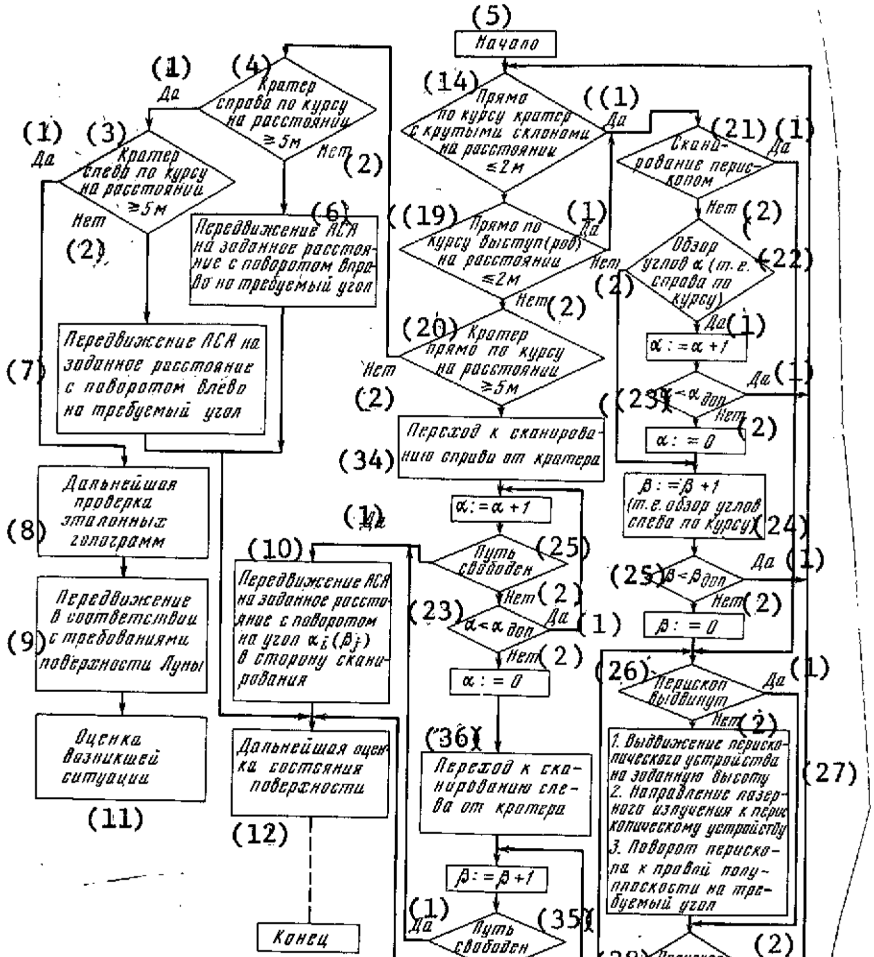
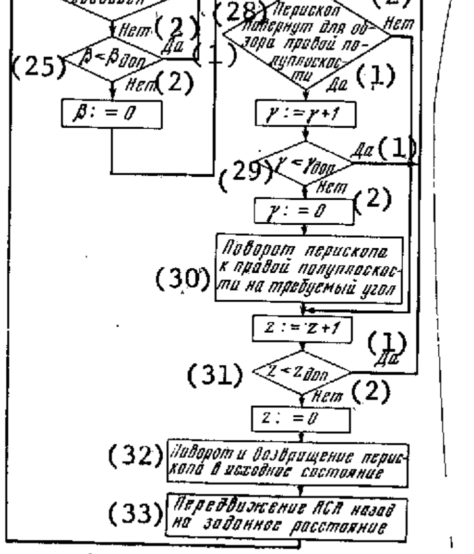

Key:
1. yes
2. no
3. crater to the left of the heading at a distance $\geq$ 5 meters
4. crater to the right of the heading at a distance $\geq$ 5 meters
5. begin
6. movement of the ASS a given distance with turning to the right by the required angle
7. movement of the ASS a given distance with turning to the left by the required angle
8. further checking of the standard holograms
9. movement in accordance with the requirements of the lunar surface
10. movement of the ASS a given distance with turning by an angle α_i (β_j) in the scanning direction

Figure 24. Flow chart for the algorithm of the operation of the microprogram automaton controlling the movement of an automatic self-propelled vehicle

Key: continued for Figure 24

11. evaluating the situation which has arisen
12. further evaluation of the condition of the surface
13. end
14. straight ahead along the heading is a crater with deep slopes at a distance of $\leq$ 2 meters
15. straight ahead along the heading there is a protrusion (a trench) at a distance of $\leq$2 meters
20. There is a crater straight ahead along the heading at a distance of $\geq$5 meters
21. periscope scanning
22. scanning of the angle α (that is, to the right of the heading)
23. $\alpha < \alpha_{admissible}$
24. $\beta := \beta + 1$ (that is, the scanning of angles to the left of the heading)
25. $\beta < \beta_{admissible}$
26. periscope extended
27. 1. extension of the periscope to the given height
    2. direction of laser emission to the periscope
    3. turning the periscope toward the right-hand halfplane by the required angle
28. periscope turned to view the right-hand halfplane
29. $\gamma < \gamma_{admissible}$
30. turning the periscope to the right-hand halfplane by the required angle
31. $z < z_{admissible}$
32. turning and returning the periscope to the initial position
33. movement of the ASS in reverse a given distance
34. conversion to scanning to the right of the crater
35. path clear
36. conversion to scanning to the left of the crater

A restriction is also introduced on the angle the periscope can be turned both in the right-hand halfplane (the angle γ) and in the left-hand halfplane (the angle z) inasmuch as there is no necessity for examining the sections that the ASS has already traveled over. If the movement ahead (both with turning and without it) is impossible as a result of certain causes, the vehicle can go into reverse without examining the terrain.

When a circular field of view is necessary it is easy to introduce corrections in the given flow chart of the algorithm or introduce a supplementary one, combining it with the general one.

In the flow chart for the algorithm, of course, far from all the situations have been taken into account which can be encountered on the path of the ASS. The degree of completeness of the flow chart for the microprogram automaton will depend on the general purpose of the ASS, the landing site, the proposed route, the area of investigation and also the problems solved directly onboard the ASS.

V. Control of the Automatic Self-Propelled Vehicle by Holographic Images Transmitted over the Moon-Earth Communications Channels

This method permits significant simplification of the mission of the operators in evaluating the actual lunar panoramas occurring along the path traveled by the Lunokhod. When solving this class of problems connected with the proposed method, the authors have given special attention to the possibility of transmitting holograms over the moon-earth television communications channel. The difficulty consists in the necessity of transmitting lunar panoramas, the holograms of which (just as the holograms of three-dimensional objects with a large viewing angle) are characterized by high spatial frequencies (on the order of 1,000 lines/mm). The implementation of the given method permits:

1) Transmission of the holograms over a two-dimensional or one-dimensional channel and reproduction of the volumetric (three-dimensional) image on the receiving side, inasmuch as the information will be transmitted not only about the light intensity distribution but also the direction of the light beams which will contain the reproduced wave front;

2) Transmission of very high contrast on the target as a result of uniform energy distribution of the light front over the light formation surface with a holographic method of recording the data. It was pointed out above that as a result of bright illumination on the moon (during the lunar days), the slopes of certain craters are entirely unnoticeable. Actually, the photographic emulsions do not transmit the contrast greater than 10^2 whereas the holographic methods permit transmission of a contrast of 10^5-10^8, that is, in practice all the brightness gradients detected in nature;

3) Performance of operations with the spectra of the spatial frequency in order to convert the images by comparing them (and also parts of them) with the standards and removal of the unnecessary parts of the image since the image on the hologram is encoded in the form of a superposition of spatial frequencies.

Before considering the specific method of transmitting the holograms, let us discuss some problems connected with selecting the frequency band for transmitting the holograms. Let us indicate the fact that it is clearly sufficient to transmit only the information which is perceived by the viewing apparatus. Its carrying capacity is limited, and it opens the possibility of transmitting holograms with a limited frequency band. By comparing the image which we observe on television or in the movies, it is possible to establish that the latter transmits much more information. Correspondingly, the quality of the movie image turns out to be better since the movie frames have an information capacity almost 20 times greater than the television frame. Nevertheless, the television on a frequency band of 6.5 megahertz not only exists, but it is widespread.

It is known that the inertia of ~~a~~an eye is about 0.2 seconds and it would be sufficient to transmit 5 frames per second although, of course, the eye would notice the presence of flickering. It is obvious that the volumetric information can be recorded if for each element in the recording plane, along with the brightness the magnitude of the distance between the corresponding points on the surface of the object and the recording plane is recorded.

The number of levels distinguishable by the eye for large details usually does not exceed 200. Stereoscopic television systems are limited by much lower discrimination of levels, in particular, the levels of such systems does not exceed 15. In order to transmit holograms while maintaining the same quality of the image for each plane as in an ordinary system, the frequency bands must be doubled since it is necessary to transmit the brightness coordinates (analogous to the transmission in two-dimensional television) and an additional brightness coordinate. Considering that the hologram contains a significant amount of redundant information and using certain means of reducing the frequency band, it is possible to introduce the frequency band on which the hologram is transmitted into the frames of a standard broadcast system.

Let us note that the recording of holograms on the receiving end encounters a number of difficulties. Up to now there is no satisfactory device which replaces the receiving tube in the holographic system. It is also necessary to have a high quality spatial frequency converter and to solve the problems of increasing the sensitivity of the system and improving the signal/noise ratio.

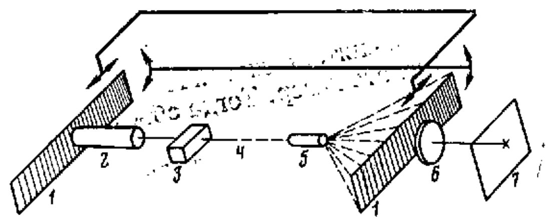

Figure 25. Schematic of the hologram transmission using variable-period gratings.
1 -- grating with variable period; 2 -- photomultiplier;
3 -- upper frequency filter; 4 -- communications channel;
5 -- light source (photodiode); 6 -- objective lens;
7 -- photorecording surface (hologram)

One of the possible approaches to the problem of transmitting holograms is presented in [11]. It is based on the principle of modulation analysis of the spectrum of the spatial frequencies of the hologram using a grating with variable period and orientations. The results of the analysis in the form of signals are transmitted over the communications channel, and on the receiving end the inverse stroboscopic conversion of the transmitted signal by means of the grating (analogous to the first one) to the initial spatial frequencies and then synthesis of the initial hologram from them by storage in the high-resolution photorecording medium takes place. The schematic of the hologram transmission is presented in Figure 25.

In the plane of the holographic interference pattern bounded by the entrance aperture, there is a one-dimensional grating 1, the spatial frequency of the lines of which varies periodically in time within the limits of the spatial frequency band of the hologram, and the orientation varies by a small angle after each period of variation of the spatial frequency.

An essential advantage of the investigated procedure is the fact that the required gratings with high spatial frequencies at the present time are obtained holographically as a result of the interference of two cylindrical wave fronts [12].

The time frequency band ΔF transmitted over the communications channel is defined by the spatial frequency band of the hologram Δf and the speed of displacement of the gratings V:

$$\Delta F = V\Delta f.$$

If we use the band of a standard television channel ΔF = 6.5 megahertz, then for Δf = 1000 lines/mm, the displacement rate of the gratings must be 6.5 m/sec.

It must be noted that on introducing quantization with respect to orientation of the gratings it is also possible to decrease the information redundancy in the holograms and at the same time accelerate the transmission.

A deficiency of the investigated hologram transmission system is the necessity for synchronizing the movement of the gratings, low speed and also the restriction in the transmission of the high spatial frequencies as a result of the presence in the receiving end of the objective lens 6 which depicts the grating on the photographic plate 7. In incoherent light the best objective lenses have a resolution on the order of several hundreds per millimeter. Obviously, the second restriction can be removed if we use a laser as the modulation light source 5 then the objective lens can be excluded in general.

VI. Control of the Automatic Self-Propelled Vehicle on the Basis of Using Phototelevision Cameras with a Three-Dimensional Screen

The essence of the given method consists in recording the holographic image of a section of the lunar surface on a three-dimensional screen of a television camera (Figure 26) with later transmission of it to the digital computer memory where it is processed by previously compiled algorithms and the control commands for the ASS are generated.

The primary difficulty in implementing this method consists in the absence of of cathode ray tubes of the television cameras with a three-dimensional screen. With the appearance of these cathode ray tubes, the possibility is opened up for effective control of the ASS. In this case the image of the hologram taken on movement of the ASS (or at the times of the halts when using the continuous-emission laser) is recorded directly at the times of reproduction on the three-dimensional screen.

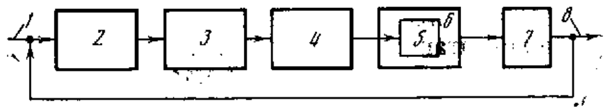

Figure 26. Structural diagram of the control of the automatic self-propelled vehicle.
1 — input image; 2 — scanner objective; 3 — hologram; 4 — phototelevision camera with three-dimensional screen; 5 — memory; 6 — digital computer; 7 — ASS; 8 — heading period

Inasmuch as the holographic image has high redundancy, on transmission of it to the digital computer memory it is necessary to use means of reducing the information, for example, fast Fourier transformation or Adamara transformation. The method can turn out to be the most effective when constructing completely autonomous information devices,in the control systems of which adaptable and logical circuits are used which determine the most efficient trajectory of motion.

Conclusions

The proposed methods of controlling self-propelled vehicles using the principles of holography are opening up prospects for the creation of devices with a self-organizing information system. This type of equipment will make it possible to perform a comprehensive study of the lunar surface and the planets and select the most important observations. It will be possible to make decisions regarding the nature of the data to be transmitted to the ground. These decisions must be made depending on the importance of the transmitted information, the distance to the earth, the available energy supply and a number of other important parameters.

The further development of operations in the field of creating self-propelled vehicles will permit clearer determination of the effectiveness of the control techniques not only proposed in this paper but also in a number of others, and evaluation of the efficiency of performing the base experiment beginning with the expected results, considering the expenditures arising from its statement.

Although the given paper basically is of a descriptive nature and does not contain comprehensive theoretical grounds (only those are presented which in the authors' opinion permit explanation of the essence of the discussed material), it, nevertheless, permits the definition of a class of control problems requiring solution when creating self-propelled automatic vehicles.

BIBLIOGRAPHY

1. Shavlov, A., et al., OPTICHESKIYE KVANTOVYYE GENERATORY (Lasers) Translated from the English, Moscow, IL, 1962.

2. Mikaelyan, A. L., et al., OPTICHESKIYE GENERATORY NA TVERDOM TELE (Solid State Lasers), Moscow, Sovetskoye radio, 1967.

3. Mashkevich, V. S., KINETICHESKAYA TEORIYA LAZEROV (Kinetic Theory of Lasers), Moscow, Nauka, 1971.

4. Landsberg, G. S., OPTIKA (Optics), Moscow, Gostekhizdat, 1957.

5. Soroko, L. M., OSNOVY GOLOGRAFII I KOGERENTNOY OPTIKI (Fundamentals of Holography and Coherent Optics), Moscow, Nauka, 1971.

6. PERVYYE PANORAMY LUNNOY POVERKHNOSTI (First Panoramas of the Lunar Surface), I, Moscow, Nauka, 1967.

7. Marechal, "Optical Filtering by Double Diffraction," OPTICAL PROCESSING INFORMATION, Massachusetts Institute of Technology Press, 1963.

8. Leith, E. N., Upatnieks, Z.,"Wavefront Reconstruction with Diffused Illumination and Three-Dimensional Objects," J OF THE OPTICAL SOCIETY OF AMERICA, Vol 54, No 11, 1964.

9. Holeman, J. M., Welch, J. D., "Space Navigation by Special Filtering of Landmarks," SPACE AERONAUTICS, Vol 47, No 6, 1967.

10. Langdon, R. M., "A High Capacity Holographic Memory," MARCONI REVIEW, Vol 33, No 177, 1970.

11. Fridman, G. Kh., Tsvetov, Ye. P., Los' V. F, Galushchenko, V. V., "New Method of Transmitting Holograms over a Communications Channel," TEKHNIKA KINO I TELEVIDENIYA (Movie and Television Engineering), No 9, 1971.

12. Fridman, G. Kh., Tsvetov, Ye. P., Los' V. F., Galushchenko, V. V., "Interference Method of Optical Pattern Recognition," VOPROSY RADIOELEKTRONIKI SERIYA OBSHCHETEKHNICHESKAYA (Problems of Radioelectronics, General Engineering Series), No 12, 1970.

13. Ostrovskiy, Yu. I., GOLOGRAFIYA (Holography), Leningrad, Nauka, 1970.

14. Lovental', S., Bel'vo, I., PROSTRANSTVENNAYA FIL'TRATSIYA I GOLOGRAFIYA -- NOVOYE V KOGERENTNOY OPTIKE (Spatial Filtration and Holography -- What's New in Coherent Optics), Moscow, Energiya, 1970.

15. Mareshal', A., Franson, M., STRUKTURA OPTICHESKOGO IZOBRAZHENIYA (Structure of an Optical Image), Translated from the French, Moscow, Mir, 1964.

16. O'Neil, E., VVEDENIYE V STATISTICHESKUYU OPTIKU (Introduction to Statistical Optics), Translated from the English, Moscow, Mir, 1966.

17. Soroko, A. M., "Holography and Interference Data Processing," USPEKHI FIZICHESKIKH NAUK (Progress in the Physical Sciences), Vol 90, No 1, 1966.

18. Lugt, A. V., "Signal Detection by Complex Spatial Filtering," JEEE TRANS. OF INFORMATION THEORY, JT-10, No 2, 1964.

- End -